

Aus der Klinischen Kooperationseinheit Dermatoonkologie des Deutschen
Krebsforschungszentrums (DKFZ) an der Klinik für Dermatologie, Venerologie
und Allergologie der Medizinischen Fakultät Mannheim
(Direktor: Prof. Dr. med. Jochen Utikal)

**Role of tumor-derived extracellular vesicles in immunosuppression
in malignant melanoma patients**

Inauguraldissertation
zur Erlangung des Doctor scientiarum humanarum (Dr. sc. hum.)
der
Medizinischen Fakultät Mannheim
der Ruprecht-Karls-Universität
zu
Heidelberg

vorgelegt von
Xiaoying Hu

aus
Henan, China
2019

Dekan: Prof. Dr. med. Sergij Goerd
Referent: Prof. Dr. Jochen Utikal

*Dedicated to my parents and my family
for their constant love and support*

PUBLICATIONS

Fleming V*, **Hu X***, Weller C, Weber R, Riester Z, Hüser L, Sun Q, Nagibin V, Kirschning C, Bronte V, Utikal J, Altevogt P, Umansky V. Melanoma extracellular vesicles induce immunosuppressive myeloid cells by PD-L1 upregulation via TLR4 signaling (submitted, ***equally contributed**).

Groth C, **Hu X**, Weber R, Fleming V, Altevogt P, Utikal J, Umansky V. (2019). Immunosuppression mediated by myeloid-derived suppressor cells (MDSCs) during tumor progression. **Br J Cancer**, 120(1):16-25. Doi: 10.1038/s41416-018-0333-1.

Huber V, Vallacchi V, Fleming V, **Hu X**, Cova A, Dugo M, Shahaj M, Sulsenti R, Vergani E et al. (2018). miRNAs delivered by tumor extracellular vesicles induce myeloid suppressor cells in melanoma patients and predict resistance to immunotherapy. **J Clin Invest**, 128(12):5505-5516. Doi: 10.1172/JCI98060.

Umansky V, Adema GJ, Baran J, Brandau S, Van Ginderachter JA, **Hu X**, Jablonska J, Mojsilovic S, Papadaki HA, Pico de Coaña Y, Santegoets KCM, Santibanez JF, Serre K, Si Y, Sieminska I, Velegraki M, Fridlender ZG. (2018). Interactions among myeloid regulatory cells in cancer. **Cancer Immunol Immunother**, Doi: 10.1007/s00262-018-2200-6.

Weber R, Fleming V, **Hu X**, Nagibin V, Groth C, Altevogt P, Utikal J, Umansky V. (2018). Myeloid-derived suppressor cells hinder the anti-cancer activity of immune checkpoint inhibitors. **Front. Immunol**, 11;9:1310. Doi: 10.3389/fimmu.2018.01310.

Fleming V, **Hu X**, Weber R, Nagibin V, Groth C, Altevogt P, Utikal J, Umansky V. (2018). Targeting myeloid-derived suppressor cells to bypass tumor-induced immunosuppression. *Front. Immunol*, 2;9:398. doi: 10.3389/fimmu.2018.00398.

Umansky V, Blattner C, Fleming V, **Hu X**, Gebhardt C, Altevogt P, Utikal J. (2017). Myeloid-derived suppressor cells and tumor escape from immune surveillance. *Semin Immunopathol*, 39(3):295-305. Doi: 10.1007/s00281-016-0597-6.

CONFERENCE AND WORKSHOPS PRESENTATIONS

Oral Presentation

- 11/2018 1st European Symposium on Myeloid Regulatory Cells in Health and Disease in Essen, Germany
- 04/2017 Mye-EUNITER: Myeloid Derived Suppressor Cells: Analysis and Clinical Monitoring of Myeloid Regulatory Cells in Brno, Czech Republic

Poster Presentation

- 11/2018 DKFZ PhD poster session, Heidelberg, Germany
- 07/2018 DKFZ PhD Retreat, Weil der Stadt, Germany
- 05/2018 CIMT – The association for cancer immunotherapy in Mainz, Germany
- 04/2018 Mye-EUNITER: Myeloid Derived Suppressor Cells: Identification and Implications in Human Diseases in Kreta, Greece
- 11/2017 Hallmarks of skin cancer in Heidelberg, Germany
- 03/2017 Mye-EUNITER: Myeloid Derived Suppressor Cells: Analysis and Clinical Monitoring of Myeloid Regulatory Cells in Brno, Czech Republic
- 05/2016 CIMT – The association for cancer immunotherapy in Mainz, Germany

Table of Contents

PUBLICATIONS	I
CONFERENCE AND WORKSHOPS PRESENTATIONS.....	III
LIST OF FIGURES	VIII
ABBREVIATIONS	X
1 INTRODUCTION	1
1.1 The immune system	1
1.1.1 The innate immune system.....	1
1.1.2 The adaptive immune system.....	8
1.2 Tumor immunology	10
1.2.1 Tumor immunoediting.....	12
1.3 Myeloid-derived suppressor cells (MDSCs).....	14
1.3.1 Expansion, activation and recruitment of MDSCs	14
1.3.2 Immunosuppressive activity mediated by MDSCs	15
1.4 Monocytes.....	18
1.4.1 The role of monocytes in innate immunity.....	18
1.4.2 Regulation of monocyte death and survival	19
1.5 Malignant melanoma	20
1.5.1 Melanoma treatment.....	20
1.6 Extracellular vesicle.....	21
1.6.1 Tumor-derived extracellular vesicles.....	24
1.6.2 Role of tumor-derived EVs in immune regulation.....	25
1.6.3 Clinical application of EVs.....	25
2 AIM OF THE PROJECT	27

3 MATERIAL AND METHODS	28
3.1 Material.....	28
3.1.1 Cell lines.....	28
3.1.2 Cell culture products.....	28
3.1.3 Cell culture media.....	28
3.1.4 Kits.....	29
3.1.5 Antibodies	30
3.1.6 Primers for mRNA.....	31
3.1.7 shRNA.....	32
3.1.8 Chemicals and biological reagents.....	32
3.1.9 Solutions	33
3.1.10 Routine laboratory material.....	35
3.1.11 Laboratory equipment.....	36
3.1.12 Software for data analysis	37
3.2 Methods.....	38
3.2.1 Cell culture	38
3.2.2 Counting of cells.....	38
3.2.3 Isolation of EVs from melanoma cell line	38
3.2.4 Isolation of EVs from plasma of melanoma patients.....	39
3.2.5 Quantification of purified EVs	41
3.2.6 Biochemical methods.....	41
3.2.7 Statistical analysis.....	50
4 RESULTS.....	51
4.1 Characterization of EVs	51
4.1.1 Characterization of EV from melanoma cell lines.....	51

4.1.2	Characterization of EV from plasma of melanoma patients	53
4.2	Effect of HT-144 EV on CD14 ⁺ monocytes.....	54
4.3	HT-144 EVs protect CD14 ⁺ monocytes from spontaneous apoptosis ..	56
4.4	CD14 ⁺ monocytes show immunosuppressive activity upon HT-144 EV treatment.....	58
4.5	HT-144 EVs upregulate PD-L1 on CD14 ⁺ monocytes	60
4.6	The involvement of NF- κ B activation in PD-L1 upregulation.....	62
4.7	The upregulation of PD-L1 via TLR signaling	63
4.8	Melanoma cells release EVs carrying HSP86	64
4.9	HSP86 knockdown results in the impairment of PD-L1 upregulation...	65
4.10	Functional inhibition of CD8 ⁺ T cells by HSP86 ⁺ melanoma EVs.....	67
4.11	Circulating EVs from melanoma patients upregulate PD-L1 and show anti-apoptotic effect on monocytes.....	68
4.12	HSP86 expression and monocyte modulation by EVs from melanoma patients undergoing anti-PD-1 therapy	69
4.13	Effects of EVs from melanoma patients undergoing anti-PD-1 therapy	72
4.14	PD-L1 expression on circulating monocytes predicts the response to anti-PD-1 immunotherapy.....	73
4.14.1	Clinical characteristics of melanoma patients.....	73
4.14.2	PD-L1 expression on circulating monocytes is associated with anti-PD-1 response.....	75
5	DISCUSSION	77
5.1	EVs from melanoma cell lines and plasma of patients show typical EV characterization.....	77
5.2	Melanoma EVs promote survival and migration ability of monocytes .	79
5.3	The change of phenotype and induction of immunosuppressive activity of monocytes by tumor-derived EVs	80

5.4	PD-L1 upregulation on monocytes by tumor-derived EVs is dependent on Toll-like receptor signaling pathway	81
5.5	Inflammatory pathway is induced in circulation monocytes by tumor-derived EV	82
5.6	HSP86 as major player on EVs from melanoma cell lines and patients for PD-L1 upregulation and immunosuppression	83
5.7	EVs from plasma of responders and non-responders undergoing anti-PD1 treatment show different activity on monocytes	84
5.8	PD-L1 on monocytes as potential predictive marker for responsiveness of anti-PD1 therapy in melanoma patients	85
5.9	Conclusion	86
6	SUMMARY	87
7	ZUSAMMENFASSUNG	89
8	REFERENCES	91
9	CURRICULUM VITAE	104
10	ACKNOWLEDGEMENTS	105

LIST OF FIGURES

Figure 1: TLR signal transduction pathways.	5
Figure 2: The three E's of cancer immunoediting.....	11
Figure 3: Main mechanisms of immunosuppression mediated by myeloid-derived suppressor cells (MDSCs)	17
Figure 4: Signaling networks, regulating the life span of monocytes and macrophages.....	19
Figure 5. Extracellular vesicles: biogenesis and interaction with target cells.....	23
Figure 6: Isolation of EVs from melanoma cell lines	39
Figure 7: Isolation of EVs from plasma melanoma patients.	40
Figure 8: In vitro transmigration assay.....	48
Figure 9: Scheme of study design	49
Figure 10: Representative dot plot showing the gating strategy of latex bead-conjugated EVs	53
Figure 11: Characteristic of HT-144 EV	52
Figure 12: Characteristic of EVs isolated from plasma of melanoma patients.....	54
Figure 13: HT-144 EVs induce cytokine gene expression and migration activity of monocytes	55
Figure 14: Effect of HT-144-EV on the apoptosis of primary monocytes.....	57
Figure 15: Gating strategy of T cell proliferation assay.	58
Figure 16: HT-144 EV treated monocytes inhibit CD8 ⁺ T cell proliferation and modulate IFN- γ production.	59
Figure 17: PD-L1 expression on monocytes upon the treatment of melanoma EV.	61
Figure 19: Involvement of TLR in the upregulation of PD-L1 on CD14 ⁺ monocytes	63
Figure 20: Expression of HSP86 and PD-L1 on EVs from melanoma cell lines.	65
Figure 21: HSP86 is required for PD-L1 upregulation.	66

Figure 22: HSP86 on HT-144 EV play a crucial role in acquiring the immunosuppressive activity by monocytes	68
Figure 23: Effects of EV from plasma of melanoma patients on normal monocytes.	69
Figure 24: HSP86 expression on EVs and their capacity to stimulate immunosuppressive activity on monocytes.	71
Figure 25: PD-L1 and HLA-DR expression on monocytes upon the treatment of responder and non-responder EVs.....	72
Figure 26: Gating strategy of PD-L1 on classical monocytes	75

ABBREVIATIONS

A	
Alix	ALG-2-interacting protein X
APAF1	Apoptotic protease activating factor 1
APC	Antigen-presenting cells
AP-1	activator protein-1
AP	Adaptor protein
ARG-1	Arginase-1
B	
BAX	Bcl-2-associated X protein
BAK	Bcl-2 homologous antagonist/killer
BAD	BCL2-antagonist of cell death
BCA	Bicinchoninic acid assay
Bcl-XI	B-cell lymphoma-extra-large
BID	BH3 interacting-domain death agonist
B-RAF	B-Rapidly accelerated fibrosarcoma
BSA	Bovine serum albumin
BTLA	B- and T-lymphocyte attenuator
C	
CCL	Chemokine (C-C motif) ligands
CCR	C-C chemokine receptor
CD	Cluster of differentiation
CDK	Cyclin-dependent kinase
c-FLIP	cellular FLICE-inhibitory protein
CFSE	Carboxyfluorescein diacetate succinimidyl ester
CIN	chromosomal instability
CLR	C-type lectine receptors
COX	cyclooxygenase
CTL	Cytotoxic T lymphocyte
CTLA-4	Cytotoxic T lymphocyte-associated antigen 4
CXCL	C-X-C motif chemokine
Cy	Cyanin

D	
DAMP	damage-associated molecular pattern
DC	dendritic cell
DMSO	Dimethyl sulfoxide
DNA	Deoxyribonucleic acid
DMEM	Dulbecco's Modified Eagle's Medium
E	
EDTA	Ethylene diamine-tetra-acetic acid
EGF	Epidermal growth factor
EGFRvIII	Epidermal growth factor receptor variant III
Et al.	Et alteri
ERK	Extracellular signal-regulated kinases
ESCRT	Endosomal sorting complex required for transport
EV	Extracellular vesicles
F	
FACS	Fluorescence activated cell sorting
FADD	Fas-associated protein with death domain
FAK	focal adhesion kinase
FasL	Fas ligand
FBS	Fetal bovine serum
FITC	Fluorescein-isothiocyanat
FMO	Fluorescent minus one
FSC	Forward scatter
G	
g	G-force
GM-CSF	Granulocyte-macrophage colony-stimulating factor
G-CSF	Granulocyte colony-stimulating factor
H	
HER-2	Human epidermal growth factor receptor 2
HIF	Hypoxia-inducible factor
HLA-DR	Human leucocyte antigen-DR
HMGB-1	high mobility group box 1
HSP	Heat-shock proteins

HRP	horseradish peroxidase
I	
ICOS	inducible costimulatory molecule
IDO	indoleamine 2 3-dioxygenase
IFN	Interferon
IGF1R	Insulin like growth factor 1 receptor
IKK	I κ B kinase
IL	Interleukin
IL-1R	IL-1 receptor
ILV	Intraluminal vesicle
IMC	Immature myeloid cells
Inos	Inducible nitric oxide synthase
IncARSR	lncRNA Activated in RCC with Sunitinib Resistance
IRAK	IL-1R associated kinase
IRF	Interferon response factor
ITIM	immunoreceptor tyrosine based inhibitory motif
ITSM	immunoreceptor tyrosine-based switch motif
J	
JAKs	Janus kinase
K	
kDa	Kilo Dalton
L	
LAG	Lymphocyte-activation gene
LPS	Lipopolysaccharides
M	
MACS	Magnetic-activated cell sorting
MAPK	Mitogen-activated protein kinase
Mcl	Myeloid leukemia cell differentiation protein
MCA	Methylcholanthrene
MCP	Monocyte chemoattractant protein
M-CSF	Macrophage colony-stimulating factor
MDSC	Myeloid-derived suppressor cell
MEK	MAPK/Erk kinase
MFI	Median fluorescence intensity

MHC	Major histocompatibility complex
MIN	microsatellite instability
min	Minutes
miRNA	Micro RNA
MM	Malignant Melanoma
MMP	Matrix metalloproteinases
MVB	Multivesicular bodies
MyD88	Myeloid differentiation primary response 88
M Φ	macrophage
N	
ncRNA	noncoding RNA
NF- κ B	Nuclear factor 'k-light-chain-enhancer' of activated B-cells
NFI	Neurofibromatosis type 1
NIN	nucleotide-excision repair instability
NK	Natural killer
NLR	Nucleotide-binding oligomerization domain-like receptor
NO	Nitric oxide
NOD	Nucleotide-binding oligomerization domain
NRAS	Neuroblastoma RAS Viral Oncogene Homolog
NTA	Nanoparticle tracking analysis
P	
PAMP	pathogen-associated molecular pattern
PBS	Phosphate buffer saline
PBMC	peripheral blood mononuclear cell
PCR	Polymerase chain reaction
PD-1	Programmed cell death protein I
PDCD6IP	Programmed cell death 6 interacting protein
PD-L1	Programmed death-ligand 1
PE	Phycoerythrin
PGE2	prostaglandin E2
PFS	Progression-free survival
PH	potential hydrogen
PMN	Polymorphonuclear
PRR	Pathogen Recognition Receptors

PVDF	Polyvinylidenfluorid
R	
Ras	Rat sarcoma
RB	Retinoblastoma protein
RFXAP	Regulatory factor X-associated protein
RIG-I	Retinoic-acid-inducible gene I
RIPK1	Receptor-interacting serine/threonine-protein kinase 1
RLR	Retinoic-acid-inducible gene I (RIG-I)-like receptors
RNA	Ribonucleic acid
ROS	Reactive oxygen species
rpm	Rounds per minute
RPMI	Roswell Park Memorial Institute medium
RT	Room temperature
S	
s	Seconds
SCF	Stem cell factor
SDS-PAGE	Sodium dodecyl sulfate polyacrylamide gel electrophoresis
SHP	Src homology region 2 domain-containing phosphatases
SMAD	Mothers against decapentaplegic homolog
SSC	Side scatter
STAT	Signal transducer and activator of transcription proteins
T	
TAA	Tumor associated antigen
TAK1	Transforming growth factor β -activated kinase
TBK1	Tank-binding kinase 1
TBS	Tris-buffered saline
TERT	Telomerase reverse transcriptase
TGF	Transforming growth factor
TIM	T-cell immunoglobulin and mucin-domain containing-3
TIR	Toll/interleukin-1 receptor
TLR	Toll-like receptors
TME	Tumor microenvironment
TNF	Tumor necrosis factor

TRAF	TNF receptor associated factor
Treg	Regulator CD4 ⁺ T cells
TRAIL	TNF-related apoptosis-inducing ligand
TRIF	TIR-domain-containing adapter-inducing interferon- β
TRAM	TRIF-related adaptor molecule
TSG101	Tumor susceptibility gene protein 101
T-VEC	Talimogen laherparepvec
TERT	Telomerase reverse transcriptase
V	
VEGF	Vascular endothelial growth factor
VISTA	V-domain Ig suppressor of T cell activation

1 INTRODUCTION

1.1 The immune system

The primary task of the immune system is to protect human bodies from different foreign pathogens like bacteria, viruses, fungi and parasites. Organs of the immune system are located throughout the body. The key organs are thymus and bone marrow, which belong to the primary organs where immature lymphocyte developed. Tissues like spleen, lymph nodes, tonsils, Peyer's patches, and mucosa-associated lymphoid tissue belong to the secondary lymphatic organs where mature naïve lymphocytes are maintained and activated by antigen. The cells of the immune system rely on a distinct set of receptors to distinguish between self and non-self or altered self-structures on cells. Conceptually, the host immune system is divided into the innate immune system, which reacts rapidly and non-specifically when it encounters a pathogen, and adaptive immune system, which react slower but is specific for non-self-antigens (Murphy et al., 2009).

1.1.1 The innate immune system

The innate immune system serves as the first line of defense with the epithelial barrier and can also stimulate adaptive immune responses. It consists of a variety of cells and soluble molecules that cells secrete. The cells involved in the innate immune system include basophils, dendritic cells (DCs), eosinophils, Langerhans cells, mast cells, monocytes and macrophages, neutrophils and natural killer (NK) cells. The soluble factors that contribute to innate immunity include the soluble

proteins lysozyme, interferon, and complement (Galley and Webster, 1996; Merle et al., 2015; Van Der Vaart et al., 2012).

The innate immune response relies on the recognition of pathogen-associated molecular patterns (PAMPs) through germline-encoded receptor called pattern recognition receptors (PRRs). When phagocytic cells like neutrophils, macrophages or DCs, recognize PAMPs via complementary PRRs, the PAMP bearing structure will be phagocytosed and a range of cytokines or chemokines will be secreted (Croce, 2008; Murphy et al., 2009). The cytokines and chemokines released by macrophages in response to bacterial constituents initiate the process known as inflammation. The activation of complement on the bacterial cell surface by invading bacteria can also lead to the phagocytosis and local inflammation (Murphy et al., 2009). In addition, NK cells are important effector cells for the innate immune system. They can recognize stressed cells in the absence of self MHC (major histocompatibility complex, called HLA in human) and antibodies, which allow them to react much faster than other immune cells (Anfossi et al., 2006). The cytotoxicity of NK cells is regulated by a balance between activating and inhibitory signals (Mandal and Viswanathan, 2015). Other important cells of the innate immune system are monocytes that will be discussed comprehensively in Chapter 1.4.

1.1.1.1 Pathogen recognition receptors (PRRs) and pathogen-associated molecular patterns (PAMPs)

PRRs are receptors which are predominantly expressed on immune cells and can recognize a broad spectrum of common molecular motifs known as pathogen- or damage-associated molecular patterns (PAMPs and DAMPs) (Murphy et al., 2009; Tang D et al., 2012). PRRs of the innate immunity differ from that of the adaptive

immunity. The PRRs are categorized into four families: Toll-like receptors (TLRs), Nucleotide-binding oligomerization domain-like receptors (NLRs), C type lectin receptors (CLRs) or RIG-1 like receptors (RLRs) (Mogensen, 2009). Among those four families, TLRs are the best characterized. PAMPs are usually specific to micro-organism, e.g. single- or double-stranded RNA (recognized by TLR3, 7 and 8), bacterial liposaccharide (LPS, recognized by TLR2 and 4), flagellin (recognized by TLR5) or dsDNA and unmethylated CpG DNA fragments (recognized by TLR9) (Kawai and Akira, 2011; Kawasaki and Kawai, 2014; Tang D et al., 2012). Ligation of PRR-PAMP triggers proinflammatory and antimicrobial responses by activating intracellular signaling pathways, e.g. kinases, adapter molecules and transcription factors like nuclear factor- κ B (NF- κ B), activator protein-1 (AP-1), and IFN regulators factors (IRFs) (Tang D et al., 2012).

1.1.1.2 Toll like receptors

TLRs are characterized by a Toll/IL-1 receptor (TIR) homology domain in the cytoplasmic region and a leucine-rich repeat domain extracellularly (Medzhitov, 2001). They are expressed differently in a variety of cells, including monocytes, DCs as well as non-immune cells like vascular endothelial cell, adipocytes, cardiac myocytes and intestinal epithelial cells. There are 10 different human TLRs (12 in mice) (O'Neill et al., 2013). TLR3, TLR7, TLR9 are nucleic-acid receptors that are expressed intracellularly whereas other TLRs are expressed on the cell surface (Kawasaki and Kawai, 2014; O'Neill et al., 2013).

After recognizing their corresponding PAMPs, specific signaling cascades will be initiated via individual TLRs based on the recruitment of a single or a specific combination of TIR-domain-containing adaptor protein like MyD88, TIRAP, TRIF or

TRAM (Kawai and Akira, 2011). TLR signaling is divided into two distinct signaling pathways, the MyD88-dependent and TRIF-dependent pathway. All TLRs (except TLR3) signal through the MyD88-dependent pathway (shaded in blue in Fig. 1). Mitogen-activated protein kinase as well as NF- κ B control the induction of proinflammatory cytokines and chemokines as well as the upregulation of co-stimulatory molecules on DCs (Lawrence, 2009; Sen and Baltimore, 2013). Moreover, the TRIF-dependent pathway (shaded in red in Fig. 1) can induce the activation of IRF3 followed by the production of type I interferons. Late-phase NF- κ B can also be activated via TRIF-dependent pathway. Production of inflammatory cytokines requires the activation of both late and early phase NF- κ B (Kawai and Akira, 2010).

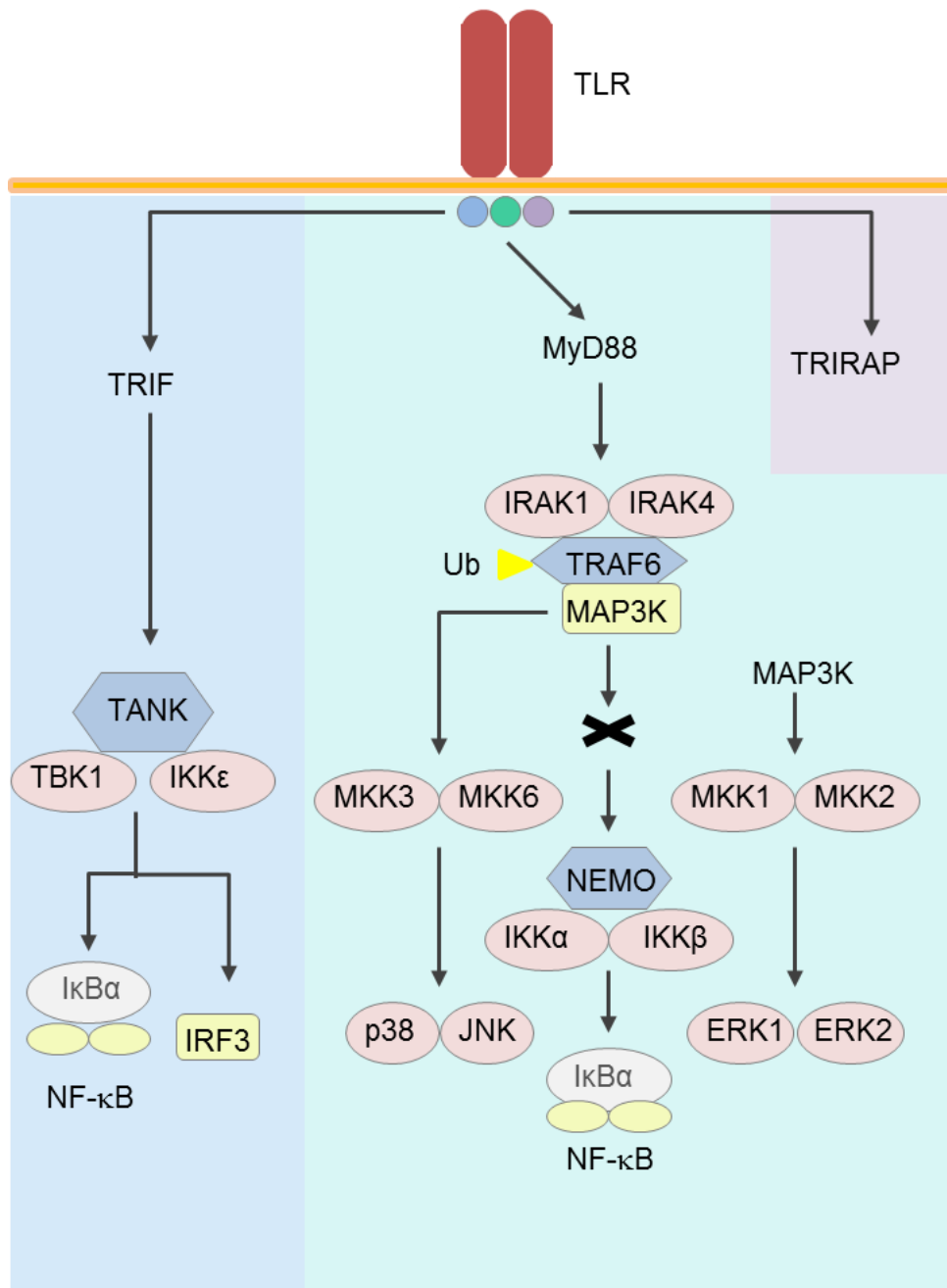


Figure 1: TLR signal transduction pathways. Two distinct signaling pathways, the MyD88-dependent and TRIF-dependent pathway are grouped based on their use of the TLR adaptors. TIRAP conducts the signal from TLR4 to MyD88, and TRAM mediates the signal from TLR4 to TRIF. The TRIF/TBK1 signaling complex phosphorylates IRF3 and lead to the production of Interferon type I. Myddosome is formed upon TLR engagement and IRAK1 will be activated during its formation. IRAK1 activation induces TRAF6 activation following K63-linked polyubiquitination on TRAF6 and TAK1. IKK complex-NF-κB and MAPKs (mitogen-activated protein kinases) will be activated upon TAK1 activation. Figure was adapted from Barton et al., 2003.

1.1.1.3 Heat shock proteins

Heat shock proteins (HSPs) are highly conserved molecules that are constitutively present or can be induced upon exposure to a variety of environmental stress conditions, including heat shock, oxidative stress, nutritional deficiencies, ultraviolet irradiation, viral or bacterial infection, inflammation and chemicals (Ciocca and Calderwood, 2005; Colaco et al., 2013). Tumor microenvironment is characterized by hypoxia, low pH, altered metabolism and high demand of new blood vesicle formation (Reynolds et al., 1996). Therefore, various HSPs are shown to be highly expressed in tumor cells or tissues, such as HSP27 in gastric cancer (Baba et al., 2013), HSP70 in breast and oral cancer (Kaur et al., 1998; Patricia et al., 2000), HSP90 α in breast and endometrial cancer (Komatsu, 1996; Yano et al., 1999). Besides, HSPs can be actively released by tumor cells into the extracellular milieu directly or via extracellular vesicles (Liu et al., 2015; Reddy et al., 2018; Vicencio et al., 2015). Cells undergoing necrotic lysis can also secrete HSPs in an autocrine, paracrine, or endocrine manner, in response to cytotoxic T lymphocytes (CTL), NK cells, or viral infections (Colaco et al., 2013).

HSPs are categorized into several families based on their molecular weight including the small heat shock protein families, Hsp40, Hsp60, Hsp70, Hsp90, Hsp100 (Prohaszka, 2003; Wu et al., 2017). HSPs are also called molecular chaperones, which ubiquitous chaperone nascent polypeptides so to stabilize newly synthesized or improperly folded protein (Saibil, 2013). It has been shown that some heat shock proteins, e.g. Hsp70, Hsp90, gp96 and calreticulin, could serve as important adjuvants in the stimulation of immune response based on their ability to bind not only whole proteins but also peptides (Srivastava et al., 1994). Within last decades, more HSPs are shown to have both stimulatory and regulatory roles in innate and adaptive immune responses (Prohaszka, 2003).

1.1.1.4 HSP90 family

As one of the most abundant proteins in cells, HSP90 family accounts for 1–2% of all cellular proteins in most cells under non-stress conditions (Chen et al., 2006). Many oncogenes are client proteins of HSP90, including (i) tyrosine-kinase receptors like HER2, mutant EGFR, c-KIT, VEGFR and IGF1R, (ii) signal-transduction proteins like NRAS, mutant BRAF, BCR–ABL, AKT and IKK, (iii) transcription factors like HIF1 α and mutant P53, (iv) cell-cycle regulatory proteins like CDK4, CDK6, PMYT1, cyclin D and mutant RB, (v) anti-apoptotic proteins like APAF1, survivin, RIPK1, BCL2 or other proteins like hTERT, FAK1, MMP2 (matrix metalloproteinases) (Garcia-Carbonero et al., 2013).

Expression pattern of HSP90 was determined in a large cohort of melanoma patients. Higher HSP90 expression was shown in melanoma tissues compared to nevi and was associated with disease progression (Liu and Zhang, 2008). Moreover, Mbofung et al. (Mbofung et al., 2017) found that T-cell-mediated killing of patient-derived human melanoma cells was enhanced *in vitro* by the application of HSP90 inhibitor ganetespib that was also observed to be potentiated in the responses to anti-CTLA4 and anti-PD1 therapy in mouse model. Nowadays, promising effects in clinical trials have been shown with the application of HSP90 inhibitors (Eroglu et al., 2018; Garcia-Carbonero et al., 2013; Mbofung et al., 2017; Trepel et al., 2010). 17-Demethoxygeldanamycin (17-AAG), a geldanamycin derivative, is a natural product that binds to HSP90 and inhibits its activity. In 2011 in the frame of phase II clinical trial, 17-AAG was applied together with trastuzumab (anti-HER2 antibody) in HER2-positive breast cancer patients with metastasis who were previously resistant to trastuzumab (Modi et al., 2011). Those findings provide proof for HSP90 to serve as a therapeutic target in the treatment of cancer.

1.1.2 The adaptive immune system

As mentioned above, pathogens can activate the innate immune response and then work together to stimulate the adaptive immune system. The major task for the adaptive immune system is to fight long-lasting infections and to create immunological memory that leads to protective immunity on a second encounter with the same pathogen (Goldszmid and Trinchieri, 2012; Murphy et al., 2009). The adaptive immune system is comprised by T cells and B cells which are responsible for T-cell-mediated immune responses and antibody responses respectively. Unlike B lymphocytes, which can recognize extracellular pathogens and secrete antibodies for systemic response, T cells can only recognize intracellular pathogens and act at short range (Bonilla and Oettgen, 2010; Kumar et al., 2018). T cells are activated by the recognition of peptide: MHC complexes displayed on the surface of antigen presenting cells (APCs) like DCs (Bonilla and Oettgen, 2010; Murphy et al., 2009).

1.1.2.1 T cells

T cells can be divided into three subsets: cytotoxic ($CD8^+$ CTL), helper (T_H cells) and regulatory T cells (Tregs). The activation of T cell requires three signals. The first signal which has already mentioned earlier is the requirement of the presence of peptide: MHC. T cell expressing CD4 co-receptor binds to class II MHC proteins, whereas cytotoxic T cells that express CD8 co-receptor binds to class I MHC proteins. Co-stimulatory proteins like B7.1 (CD80) or B7.2 (CD86) and tumor necrosis factor (TNF) families are needed for signal two. Those proteins are typically expressed on activated DCs. The binding of them to other receptors on T cell surface initiate the second signal. The third signal is inflammatory cytokines such as interleukin 12 (IL-12) or type I interferons (type I IFN).

After activation, cytotoxic T cells can directly kill the infected cells either by releasing perforin which then polymerizes in the target cell plasma membrane to form transmembrane channels, or through the binding of Fas ligand on cytotoxic T cell surface to Fas, which is a transmembrane receptor protein on the target cells (Barry and Bleackley, 2002; Murphy et al., 2009). The binding will activate a death-inducing caspase cascade that leads to apoptosis of target cells. Helper T cells can secrete a variety of cytokines and display a broad spectrum of co-stimulatory proteins on their surface to help macrophages to destroy the microbes or activate B cells to make antibodies against the microbes (Oh and Hwang, 2014). On the other hand, similar strategies are used by Tregs to inhibit the function of cytotoxic T cells, helper T cells and DCs to keep homeostasis in human body (Murphy et al., 2009).

1.1.2.2 Negative feedback regulation of T cells

Co-inhibitory receptors, together with the above mentioned co-stimulatory receptors like CD28 and ICOS, maintain homeostasis through a continuous balance between positive and negative signaling. Co-signaling is controlled through either the modulation of cell surface expression or the differential expression patterns of receptor-ligand pairs function (Chen and Flies, 2013). CTLA-4 and PD-1 are the best-studied co-inhibitory receptors.

1.1.2.3 Programmed death-1 receptor/ Programmed death-1 ligand 1

PD-1 (CD279), a type I transmembrane protein, was first identified in 1992 (Ishida et al., 1992). It contains two phosphorylation sites located in an immunoreceptor tyrosine-based inhibitory motif (ITIM) and an immunoreceptor tyrosine-based switch motif (ITSM) of the intracellular tail which is important for the inhibitory function of PD-1 (Blank and Mackensen, 2007; Ishida et al., 1992). The ligands for PD-1 are programmed death ligand-1 (PD-L1, CD274) and programmed death ligand-2 (PD-

L2, CD273) (He et al., 2004). When PD-1 binds to its ligand, intracellular tyrosinases in ITIM and ITSM are phosphorylated and an inhibitory signal is delivered to T cells followed by a decreased proliferation and cytokine production (Keir et al., 2008).

PD-L1 is widely expressed on a variety of APCs, non-hematopoietic cells and non-lymphoid organs like lung, heart, placenta and liver whereas the expression of PD-L2 is restricted to macrophage and DCs (Keir et al., 2008). Regulator of PD-L1 were widely investigated within last ten years. Of note, inflammatory signaling, oncogenic signaling, microRNA, genetic alteration and post-translational regulation are found to be main players for PD-L1 up or down regulation (Sun et al., 2018). Among them, IFN- γ was described to be a strong inducer of PD-L1 acting mainly via the JAK/STAT1/interferon regulatory factor (IRF) 1 pathway in various tumor types, healthy tissues and immune cells (Brown et al., 2003; Dong et al., 2002; Sheikh et al., 2010; Shi, 2018). In addition to IFN- γ , other cytokines like TNF- α , epidermal growth factor (EGF), IL-4, IL-17, IL-27 were also shown to be important players in regulating PD-L1 expression. Furthermore, the ligands of TLR can also induce the expression of PD-L1. For instance, PD-L1 expression could be strongly upregulated via poly(I:C)/TLR3 signaling in neuroblastoma cells and LPS/TLR4 signaling in bladder cancer cells (Boes and Meyer-Wentrup, 2015; Qian et al., 2008; Shi, 2018).

1.2 Tumor immunology

Cancer is characterized by the growing of cells in an abnormal uncontrolled manner induced by mutations in protooncogenes and tumor suppressor genes that control crucial cell functions, particularly growth and survival (Hahn and Weinberg, 2002). These alterations provide antigens that the adaptive immune system can recognize to distinguish the cancer cells from normal cells. In 1957, Burnet and Thomas

formulated the theory of cancer immunosurveillance and proposed that lymphocytes act as sentinels in recognizing and eliminating continuously arising, nascent transformed cells (Burnet, 1957; Dunn et al., 2002). Over the past two decades researchers have shown that the immune surveillance is only a part of the story, and the concept “cancer immunoediting” consisting of three phases (elimination, equilibrium and escape) has been proposed by Schreiber et al. (Mittal et al., 2014; Schreiber et al., 2011) (Fig. 2).

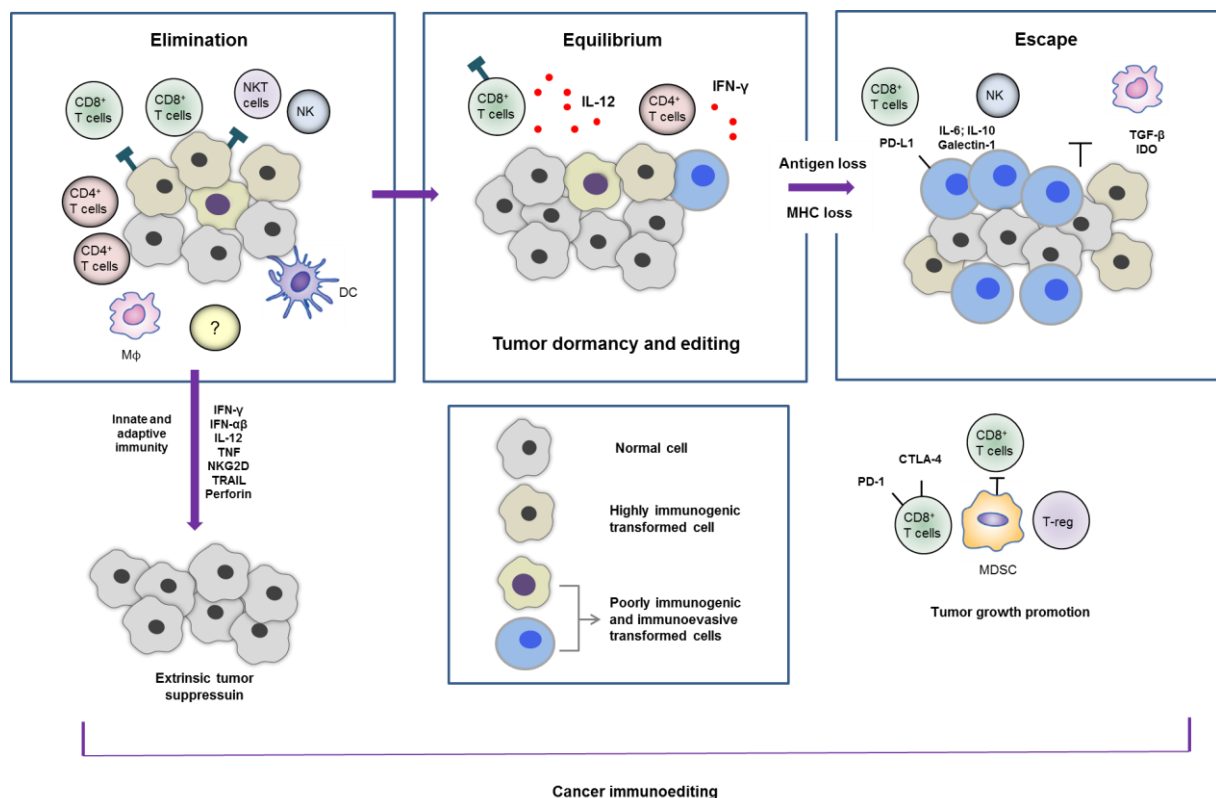


Figure 2: The three E's of cancer immunoediting. Schematic representation of interactions between tumor cells with immune system that are divided into three phases: elimination, equilibrium and escape. Figure was adapted from Schreiber et al., (Schreiber et al., 2011).

1.2.1 Tumor immunoediting

The first phase of immunoediting is the elimination phase. During the proliferation of tumor cells, inflammatory signals will be released, and innate immune cells will be recruited to inflammatory lesions to affect tumor cells. DCs are activated by pro-inflammatory cytokines released by innate immune cells or DAMPs released by dying tumor cells. Those DCs further induce the adaptive anti-tumor immune responses (Dunn et al., 2002, 2006; Schreiber et al., 2011). Various effector molecules are shown to be important for the elimination phase like IFN- γ , perforin, Fas/FasL and TRAIL. If the tumor cells are completely destructed, the immunoediting concept ends at this point.

Equilibrium is a phase when some tumor cell variants co-exist with the effector cells of the immune system in a functional state of dormancy. Genomic instability like nucleotide-excision repair instability (NIN), microsatellite instability (MIN), and chromosomal instability (CIN) has the potential to reduce the immunogenicity of tumor variants (Dunn et al., 2002). Moreover, some of those will display an enhanced capacity to grow in an unlimited immune selecting environment, which enable tumor cell variants eventually resist the host's immunological sieg (Dunn et al., 2004). The balance between the immune system and the developing tumor during the equilibrium phase controls tumor outgrowth. The existence of an equilibrium phase was shown in both mouse and human. Immunocompetent C57BL/6 mice were treated with low dose 3'-methylcholanthrene (MCA) ,and no apparent tumor was detected. However, upon antibody-mediated depletion of IFN- γ and T cells, half of the animals quickly developed tumors at the site of the MCA treatment (Koebel et al., 2007). In patients, circulating, disseminated tumor cells were still detectable in breast cancer patients who were free of clinically detectable tumor 20 years after treatment (Meng et al., 2004). In some cases, the selected tumor cell variants are able to

suppress the anti-tumor immune response which further result in the outgrowth of clinically apparent cancers. At this point, cancer immunoediting enters the escape phase.

Many mechanisms are shown to mediate the escape phase, including loss of antigenicity, immunogenicity or immunosuppressive microenvironment. As mentioned earlier, genetic alterations can lead to reduced antigenicity of tumor variants through loss of tumor antigen expression. This can arise due to : (i) absence of strong tumor antigens, (ii) loss of MHC class I, class I-like, or co-stimulatory molecules, or (iii) loss of antigen processing function (Schreiber et al., 2011). tumor cells could escape also via the induction of resistance or survival by activating pro-oncogenic transcription factors like STAT3 or the upregulation of anti-apoptotic molecule BCL-2 (Catlett-Falcone et al., 1999; Schreiber et al., 2011). Moreover, tumors, which retain sufficient antigenicity for immune recognition can escape elimination due to the loss of immunogenicity. Upregulation of the immunoinhibitory molecule PD-L1 on malignant cells and surrounding stroma cells, or negative regulatory markers that are expressed on the tumor-infiltrating lymphocytes (e.g. PD-1, LAG-3, TIM-3, VISTA, CD244, CD160, and BTLA) are the main driving forces of the immunogenicity reduction (Beatty and Gladney, 2015; Dunn et al., 2002; Schreiber et al., 2011). Of note, the development of an immunosuppression within the tumor microenvironment may also facilitate the escape phase. Immunosuppressive microenvironment is comprised of regulatory immune cells and soluble factors such as vascular endothelial growth factor (VEGF), TGF- β , galectin, or indoleamine 2,3-dioxygenase (IDO). Myeloid-derived suppressor cells (MDSCs) were shown to be crucial in inhibiting host-protective antitumor responses (Kumar et al., 2016; Umansky et al., 2016).

1.3 Myeloid-derived suppressor cells (MDSCs)

In the past few decades, accumulating evidence has demonstrated that MDSCs belong to the major regulators of the immune system in various diseases, especially in cancer (Condamine et al., 2015; Dolcetti et al., 2008; Hanahan and Coussens, 2012; Medzhitov et al., 2011; Umansky et al., 2014). Therefore, targeting MDSC becomes an important strategy of cancer immunotherapy. MDSCs represent a heterogeneous population of myeloid cells and can be identified by various markers in human and mouse. Polymorphonuclear (PMN)- and monocytic (M)-MDSC are two major subsets defined in tumor-bearing mice as $CD11b^+Ly6G^+Ly6C^{lo/-}$ and $CD11b^+Ly6G^-Ly6C^{hi}$ respectively. In human peripheral blood mononuclear cells (PBMC), PMN-MDSC are characterized as $CD11b^+HLA-DR^{-/lo}CD14^-CD15^+$ or $CD11b^+CD14^-CD66b^+$ and M-MDSC as $CD11b^+HLA-DR^{-/lo}CD14^+CD15^-$. Early-stage MDSCs (e-MDSC) are defined as Lin^- (including CD3, CD14, CD15, CD19, CD56) $HLA-DR^-CD33^+$ cells, however the mouse equivalent is still not identified (Bronte et al., 2016;). Under various pathological conditions like cancer, chronic inflammation and infection and autoimmune diseases, myeloid-cell progenitors will differentiate into MDSCs (instead of the maturation into DCs, macrophages or granulocytes) and will acquire immunosuppressive function (Gabrilovich and Nagaraj, 2009; Parker et al., 2015).

1.3.1 Expansion, activation and recruitment of MDSCs

Numerous inflammatory factors produced in the tumor microenvironment by tumor cells and immune cells or fibroblasts are involved in the expansion and activation of MDSC, including prostaglandin E2 (PGE2), cyclooxygenase 2 (COX-2), growth factors like VEGF, granulocyte-macrophage colony-stimulating factor (GM-CSF), granulocyte colony-stimulating factor (G-CSF), macrophage colony-stimulating factor

(M-CSF), stem cell factor (SCF), TGF- β , tumor necrosis factor (TNF)- α , S100A9 and/or S100A8, cytokines like IL-1 β , IL-6, and IL-10 as well as TLR ligands (Gabrilovich and Nagaraj, 2009; Marvel and Gabrilovich, 2015; Parker et al., 2015; Ugel et al., 2015; Wesolowski et al., 2013).

MDSCs are shown to be accumulated in tumor tissues of mice and patients with melanoma, prostate, lung, breast, gastric, ovarian and colorectal cancer (Adah et al., 2016; Coosemans et al., 2016; Du Four et al., 2015; Gebhardt et al., 2015; Idorn et al., 2014; Limagne et al., 2016; Su et al., 2017; Zoglmeier et al., 2011). Chemokines and C-C motif chemokine receptors are the main driver for the migration of MDSCs to tumor tissue. For instance, C-C motif chemokine ligand (CCL) 2 and its receptors C-C chemokine receptor type (CCR) 2, CCR-4, and CCR-5 have been described to play a pivotal role for both M-MDSC and PMN-MDSC migration (Chun et al., 2015; Lesokhin et al., 2012; Umansky et al., 2017). Furthermore, there are evidence showing that the interaction of CCR5 and its ligands CCL3, CCL4, CCL5 (Schlecker et al., 2012; Tang et al., 2015; Umansky et al., 2017), other chemokines like CXCR-CXCL12 (Obermajer et al., 2011), CXCR2-CXCL1 (Wang et al., 2017), CXCR2-CXCL2 (Zhang et al., 2017) and CCL15 (Inamoto et al., 2016; Itatani et al., 2013) are of great importance in the recruitment and expansion of MDSCs.

1.3.2 Immunosuppressive activity mediated by MDSCs

MDSC-induced immunosuppression is mediated by a variety of mechanisms. Based on previous publication in mouse and human, main mechanisms could be summarized as follows (Groth et al., 2018; Fig. 3): a) induction of immunosuppressive cells like M2 macrophages and Tregs by IL-10 and IFN- γ , b) impaired homing of effector T lymphocytes especially CD8⁺ T cells via downregulation of the cell adhesion molecule L-selectin, CD162 and CD44, c)

production of reactive oxygen species (ROS) and nitric oxide (NO), which can induce the expression of immunosuppressive molecule like Cox-2, hypoxia-inducible factor 1-alpha (HIF-1 α) and arginase 1 (ARG1), d)depletion of metabolites critical for T cell functions such as L-arginine, e) activation of ectoenzymes CD39 and CD73, mainly in a HIF-1 α -dependent manner, which regulate adenosine metabolism, and f) expression of negative immune checkpoint molecules like PD-L1. Through those mechanisms, activated MDSC can suppress the function of various cells in both innate immune system like NK cells (Elkabets et al., 2010) and adaptive immune system like T cells (Bronte et al., 2016; Ghansah, 2012) and B cells (Li et al., 2014). In tumor microenvironment, MDSC can promote tumor invasion and metastasis by the secretion of different soluble factors such as MMPs, proangiogenic factors like VEGF, TGF- β , DAMPs etc. (Meyer et al., 2011; Talmadge and Gabrilovich, 2013). VEGF can stimulate tumor neovascularization, whereas MMPs (especially MMP9) facilitate invasion and metastasis (Umansky et al., 2016). The expansion of MDSCs can be promoted by DAMPs such as S100A8/A9, leading to an influx of inflammatory molecules within the tumor microenvironment (Parker et al., 2015).

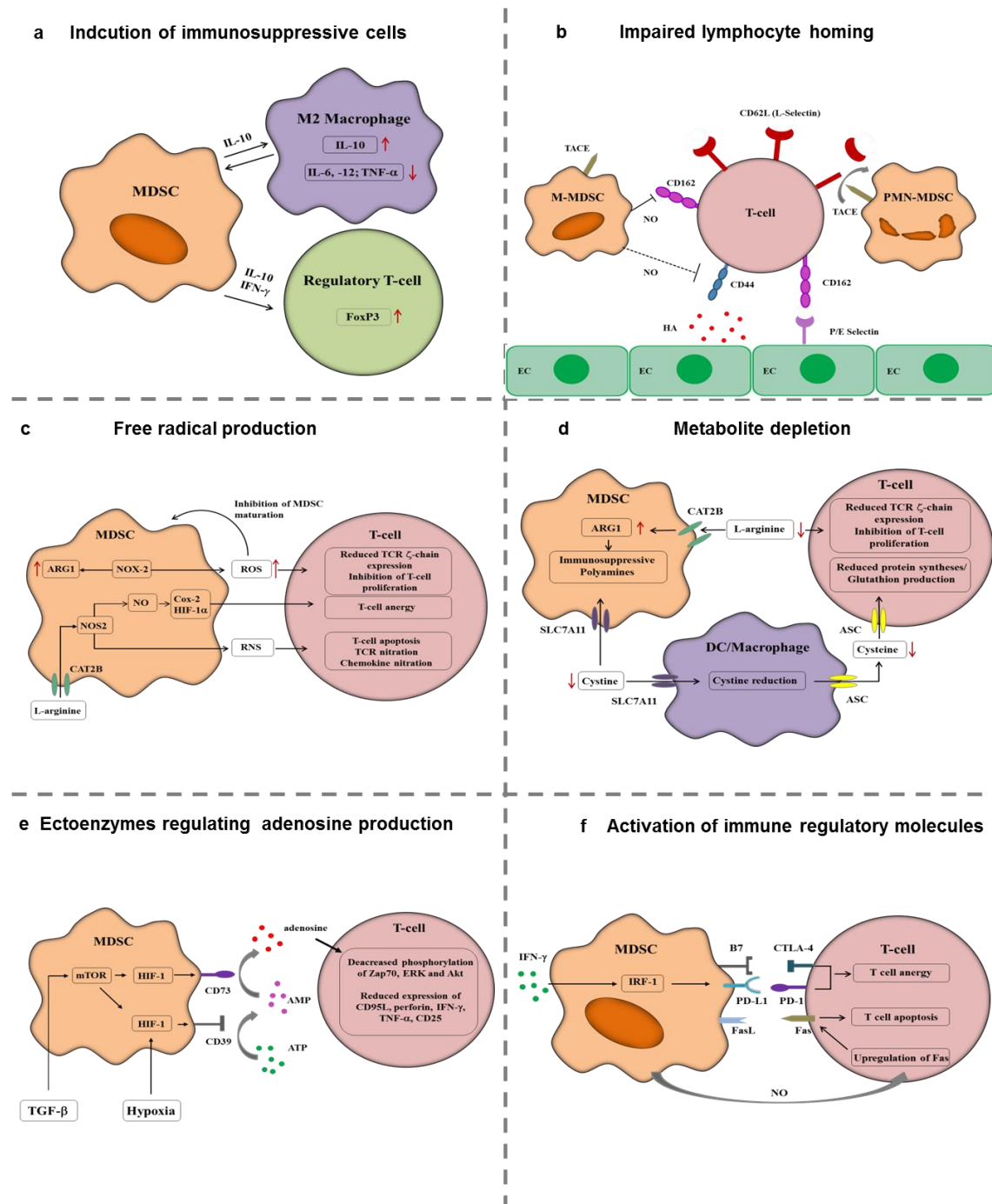


Figure 3: Main mechanisms of immunosuppression mediated by myeloid-derived suppressor cells (MDSCs). a) induction of immunosuppressive cells, b) impairment of the recruitment of effector lymphocytes, especially CD8⁺ T cells, c) production of ROS and NO d) depletion of metabolites critical for T cell functions such as L-arginine, e) generation of ectoenzymes CD39 and CD73, f) expression of negative immune checkpoint molecules like PD-L1. The figures was adapted from Groth et al., 2018.

1.4 Monocytes

Monocytes are generated in the bone marrow from hematopoietic progenitor cells and play a critical role in pathogen challenge and homeostasis. Under normal condition, monocytes circulate in the bloodstream only for few days before undergoing spontaneous apoptosis (Fahy et al., 1999). Under pathological conditions such as infection, inflammation or cancer, monocytes can be rapidly recruited to tissues where they differentiate into macrophages, DCs or MDSCs who have a longer life span (Parihar et al., 2013). In human, circulating monocytes are divided into three subgroups based on their phenotype and function (Gordon and Taylor, 2005; Ziegler-Heitbrock, 2015). The classical monocytes (approx. 90–95%) are defined as CD14⁺⁺CD16⁻ cells, whereas the intermediate and non-classical monocytes are CD14⁺⁺CD16⁺ and CD14⁺ CD16⁺⁺ respectively (Ziegler-Heitbrock et al., 2010).

1.4.1 The role of monocytes in innate immunity

A complex network of survival and death signals are involved in controlling monocyte life span. Monocytes and macrophages express a broad range of TLRs (Hawn and Underhill, 2005). In response to PAMPs or DAMPs, monocytes produce various pro-inflammatory cytokines like IL-1 β , TNF- α via TLR signaling (Goyal et al., 2002). However, when inflammation occurs, anti-inflammatory cytokines like TGF- β , IL-10, IL-13, IL-4 and PGE2 will also be produced by classical monocytes to counteract ongoing inflammation (Yang et al., 2014). As a result of respiratory burst, an activation of monocytes causes a massive generation of ROS. Elevated monocyte chemoattractant protein-1 (MCP-1/CCL2) production is also known to be a crucial characteristic of monocyte activation (Parihar et al., 2010).

1.4.2 Regulation of monocyte death and survival

A complex network of survival and death signals controls the life span of monocytes (Fig. 4). The initiation of monocyte apoptosis is regulated by intrinsic (also called the mitochondrial pathway) and extrinsic pathways. Some factors like Fas receptors, TNF receptor, caspases, BAX, BID, BAK, or BAD are known to promote apoptosis while others play crucial role in inhibiting apoptosis. Those negative regulators can be categorized into anti-apoptotic factors such as Bcl-2, Bcl-XL, Mcl-1 and survivin or pro-survival factors like cFLIP, FADD, Akt, and NF- κ B.

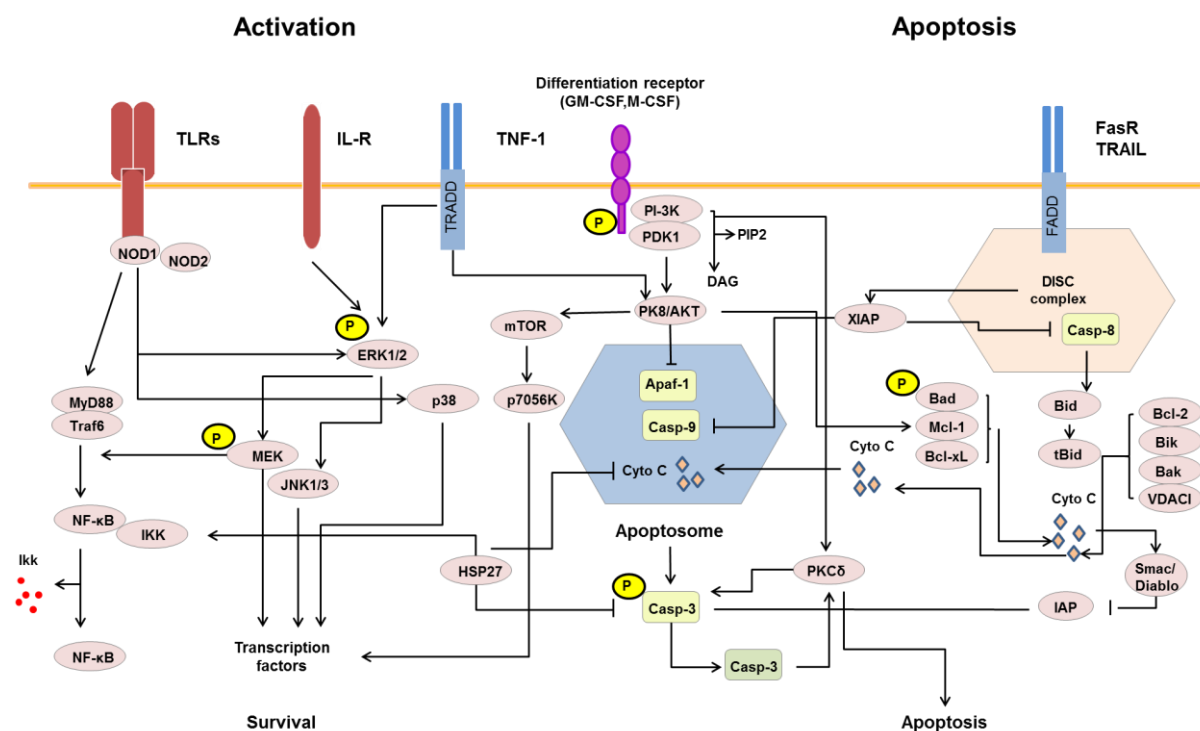


Figure 4: Signaling networks, regulating the life span of monocytes and macrophages.

Figures was adapted from Parihar et al., 2010.

1.5 Malignant melanoma

Melanoma is a deadliest form of skin cancer. Worldwide, 1.7 % of primary malignant cancers (excluding nonmelanoma skin cancer) are newly diagnosed as cutaneous melanoma and account for 0.7 % of all cancer annually (Schadendorf et al., 2018). Melanoma originates from the pigment-producing melanocytes in the skin. In early stages, melanoma is highly localized and can be treated by surgery and adjuvant therapy. However, melanoma rapidly becomes life-threatening once it developed into regional metastases. The preferential sites of metastasis are regional lymph nodes, lung, liver, bone and brain. Since 2011, melanoma treatment has been revolutionized with the approval of tyrosine kinase inhibitors, immune check point inhibitors and talimogene laherparepvec (T-VEC, also known as OncoVEX^{GM-CSF}) (Pol et al., 2016; Schadendorf et al., 2018).

1.5.1 Melanoma treatment

1.5.1.1 Target therapy

A genomic classification of melanoma includes four subtypes: B-Raf, Ras, NF1 and triple wild-type subtypes, since the occurrence and progression of melanoma are closely correlated with those mutations (Akbani et al., 2015). The BRAF, RAS (N/H/K) and NF1 subtypes are observed in more than 90% of cutaneous melanoma patients (Akbani et al., 2015). Those mutations located at different levels of the MAPK/Extracellular signal-regulated kinase (ERK) pathway remain the most frequently drug-target pathway in melanoma. B-Raf and MAPK/Erk kinase (MEK) inhibitors considerably improved the treatment of melanoma but failed in the retention of a durable response and drug resistance.

1.5.1.2 Immunotherapy with immune check point inhibitors

Immunotherapy has transitioned from interferon and interleukin cytokine-based treatment to antibodies against CTLA-4 and PD-1. Notably, the application of anti-CTLA-4 and anti-PD-1 therapy allowed the handling of wide-type B-Raf melanomas and leads to a dramatic improvement in the prognosis and survival of advanced melanoma patients.

Nivolumab or Pembrolizumab, monoclonal antibodies against PD-1, were approved in 2014 and are widely used in the treatment of melanoma, small cell lung cancer, renal cell carcinoma, lymphoma and other cancer types. Patients treated with anti-PD-1 antibodies showed significant clinical benefits and prolonged survival. However, a substantial percentage of patients do not respond to this treatment. Higher mutation load (Hugo et al., 2017) and PD-L1 expression on tumor cells (Iwai et al., 2002; Tumeh et al., 2014) were shown to be associated with better outcomes. However, clinical responses to anti-PD-1 therapy in PD-L1-negative tumors also have been observed (Dutriaux et al., 2014; Powles et al., 2014). Predictive biomarkers for the clinical response and characterization of resistance mechanisms to tumor immunotherapy are necessary to have a better guidance of clinical decision.

1.6 Extracellular vesicle

Extracellular vesicles (EVs) are membraned-bound vesicles with complex cargos including lipids, proteins, DNA, mRNA and noncoding RNA (ncRNA) like miRNA. EVs are classified into exosomes (40-150 nm), microvesicles (MVs, 200-500 nm) and apoptotic bodies (1-2 μm) based on their size, origin, biological function and biogenesis pathway (Syn N et al., 2016; Pitt et al., 2016). Exosomes are released by multivesicular bodies (MVBs) through endosome membrane whereas microvesicles

bud directly from the plasma membrane. In addition, cells undergoing apoptosis are dissociated into various sizes of vesicles that are known as apoptotic bodies (Maas et al., 2016; Pitt et al., 2016). The size of EV subsets are overlapping and there is to date no consensus over the specific markers for EV subpopulation. However current purification approaches for EVs are mainly size or density based, which does not allow to talk about a distinct EV subpopulation.

In 2018, a nomenclature recommendation by the International Society for Extracellular Vesicles is offered, which claims that operational terms of EV subtypes should be used, either refer to physical characteristics, biochemical composition or descriptions of conditions or cell of origin (Théry et al., 2018). EVs can be divided into “small EV” (sEV) and “medium/large EV” (m/l EV) based on size with ranges defined < 200nm (small) or > 200nm (large and/or medium) respectively or low, middle, high density EVs with each range defined. On the other hand, the description based on biochemical composition e.g. as CD63⁺/CD81⁺ EVs or Annexin A5-stained EVs, can also be used. Moreover, EVs purified under hypoxia, irradiation, injury, cellular stress or EVs secreted by a specific cell type like podocyte EVs, large oncosomes are acceptable with a clear description (Théry et al., 2018).

Several mechanisms have recently been identified to be essential for EV biogenesis (Fig. 5). The best characterized mechanism is the recruitment of the endosomal sorting complex required for transport (ESCRT) machinery to recognize and sort ubiquitinated proteins into intraluminal vesicles (ILVs) (Antonov and Stulova, 2013; Maas et al., 2017). Accessory proteins are required for proper function of the ESCRT pathway including programmed cell death 6 interacting protein (PDCD6IP; also known as ALIX) and tumor susceptibility gene protein 101 (TSG101) (Maas et al., 2017; Xu et al., 2018; Zaborowski et al., 2015). Pathways that are ESCRT-independent can also occur (e.g., synthesis of ceramide to induce vesicle curvature

and budding) (Antonov and Stulova, 2013; Maas et al., 2017; Van Niel et al., 2018). EVs can be taken up through different mechanisms, including i) the ligand-receptor interaction, ii) a direct release of EV contents (nucleic acids, proteins, lipids) in the extracellular space, iii) Rab GTPases dependent EV-plasma membrane fusion (including RAS- related protein RAB7A, RAB11, RAB27A, RAB27B, and RAB35) or iv) uptake by endocytosis then further fused with endosomal membrane (El Andaloussi et al., 2013; Van Niel et al., 2018).

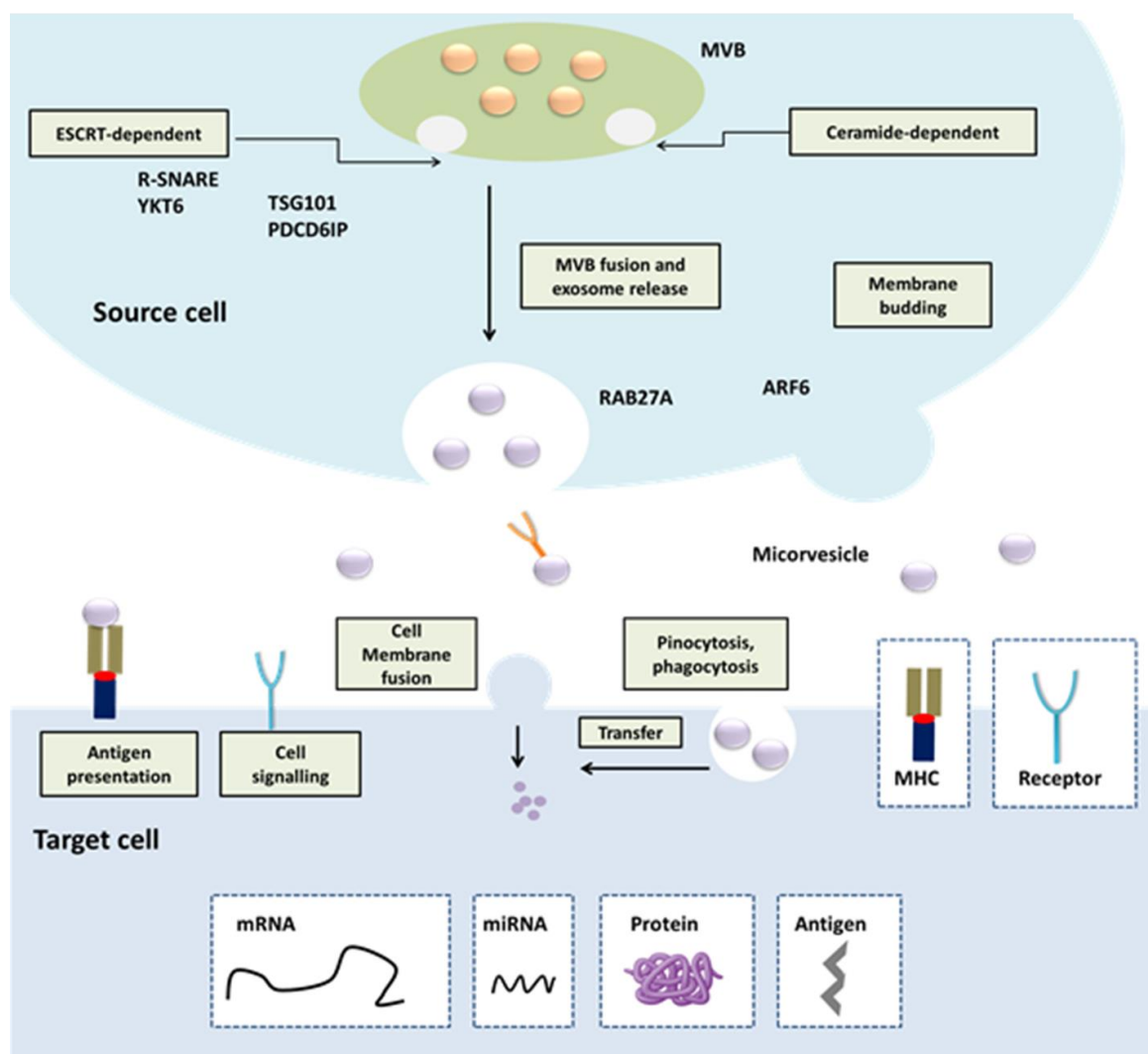


Figure 5. Extracellular vesicles: biogenesis and interaction with target cells. EVs can activate recipient cells via deliver transcription factors, oncogenes, non-coding regulatory RNAs (such as microRNAs) mRNAs into them. This activation can also be mediated by a direct binding of cell surface receptors via protein and lipid ligands. EVs can directly activate cell surface receptors via protein and bioactive lipid ligands, transfer cell surface receptors or

deliver effectors including transcription factors, oncogenes and infectious particles into recipient cells. EVs can also regulate immune response by transfer MHC molecules and antigens and are highly involved in antigen presentation. Figures was adapted from El Andaloussi et al., 2013.

1.6.1 Tumor-derived extracellular vesicles

The crosstalk between cells in tumor microenvironment are mediated by direct cell-cell contact locally or through the secretion of EVs and soluble factors like cytokines, chemokines or growth factors (Gajewski et al., 2013; Ge et al., 2012). The secretion of EVs is particularly active in proliferating cells like cancer cells (Whiteside, 2016). Emerging evidence suggests tumor-derived EVs can promote the progression, invasion and metastasis of cancers by various mechanisms (Théry et al., 2006).

Firstly, oncogenic molecules such as mutated proteins, fusion gene mRNAs, and oncogenic lncRNAs, can be transferred to tumor microenvironment. It was shown that the delivery of epidermal growth factor receptor variant III (EGFRvIII) to EGFRvIII-negative cancer cells by glioblastoma EVs result in the acceleration of cancer growth (Al-Nedawi et al., 2008). In parallel, tumor EVs can promote tumor progression through the interaction with endothelial cells, inducing their proliferation and activating angiogenesis-related gene expression in those cells (Nazarenko et al., 2010; Skog et al., 2012). Tumor self-promoting behavior can also be mediated via the reprogramming of normal fibroblast into myofibroblasts by the uptake of tumor EVs, containing TGF- β 1, or by the enhancement of fibroblast migration, which may further contribute to local invasion and pre-metastatic niche formation (Morello et al., 2013; Sánchez et al., 2015; Webber et al, 2010).

1.6.2 Role of tumor-derived EVs in immune regulation

The role of EVs in immune regulation has also been intensively studied within last decades (Liu et al., 2015; Robbins and Morelli, 2014). Tumor EVs exhibit both anti-tumor and tumor promoting effects via immune activation or suppression. For instance, EVs contain tumor associated antigen (TAA), co-stimulatory molecules or MHC molecules that can be delivered to DCs and activated DCs will stimulate the cytotoxic immune response of tumor-infiltrating T cells (Wolfers et al., 2001). However, most of publications argue that tumor EVs may rather perform immunosuppressive functions by triggering the expansion of immune suppressive cells. Ovarian carcinoma cells secreted EVs, expressing FasL, which can lead to the apoptosis of T lymphocytes and a concomitant loss of TCR ζ -chain in patients (Taylor et al., 2003). Besides, EVs from bladder, breast, colorectal and prostate cancer are also involved in the inhibition of T cells via adenosine production (Clayton et al., 2011). Nasopharyngeal carcinoma EVs were also shown to inhibit T-cell proliferation, Th1 and Th17 differentiation but induce Treg differentiation via the delivery of miRNA (Ye et al., 2014). Tumor EVs can also be internalized by other immune cells. Pancreatic cancer-derived EVs can inhibit the expression of regulatory factor X-associated protein (RFXAP), an important transcription factor for MHC II, through miR-212-3p in DCs and induce immune tolerance (Ding et al., 2015).

1.6.3 Clinical application of EVs

EVs are present in different kind of biological fluids, including blood, urine, ascites, bile, breast milk, synovial, cerebrospinal fluid and so on (Théry et al., 2006). Many studies have shown elevated EV concentration or specific markers associated with tumor EVs in biological fluids of patients with melanoma, ovarian, pancreatic and breast cancer, indicating that EVs may serve as a diagnostic marker (Goedert et al.,

2014; Hood et al., 2011; Melo et al., 2015; Yu et al., 2015). Besides, EVs from renal cell carcinoma were described to incorporate lncRNA, namely lncARSR (lncRNA Activated in RCC with Sunitinib Resistance) that are correlated clinically with poor sunitinib responses (Qu et al., 2016).

2 AIM OF THE PROJECT

MDSCs are known to be a major obstacle for an effective immunotherapy of many cancer types (especially melanoma). The goal of this study was to decipher the role of melanoma-derived EVs in the conversion of circulating CD14⁺ monocytes into immunosuppressive myeloid cells, namely M-MDSCs. The effects of EVs from melanoma cell lines, HT-144 and SK-MEL-28, were tested on purified CD14⁺ monocytes isolated from periphery blood mononuclear cells of healthy donor. The suppressive capability of EV-educated monocytes was investigated by analyzing the expression of the immunosuppressive mediator PD-L1 and the ability of inhibiting CD8⁺ T cell proliferation as well as IFN- γ production. Additionally, we investigated the underlying mechanisms involved in the induction of PD-L1 expression on monocytes. Moreover, the possible ligands carried by tumor EVs leading to the stimulation of PD-L1 expression on monocytes were analyzed. Finally, we tested if the immunosuppressive capacity can be induced on monocytes stimulated by EVs from plasma of advanced melanoma patients.

3 MATERIAL AND METHODS

3.1 Material

3.1.1 Cell lines

Cell line	Source	Cell type	Mutation	Medium
HT-144	ATCC	Melanoma cell line	BRAF V600E	RPMI
SK-MEL-28	ATCC	Melanoma cell line	BRAF V600E	RPMI

3.1.2 Cell culture products

Product	Company	Catalog No.
0.4 % Trypan blue solution	Sigma Aldrich	T8154
B-Mercaptoethanol (50 mM)	Gibco	31350
Bovin serum albumin	Sigma	7030-50G
Dimethylsulfoxid (DMSO)	Merck	109678
Dimethylsulphoxide Hybrid Max (DMSO)	Sigma Aldrich	472301-100ML
DPBS (1x)	Gibco	14190-094
Fetal Bovine Serum	PAN Biotech GmbH	3702-P260718
Bicoll	Merck	L 6715
HEPES Buffer (1M)	Sigma Aldrich	H0887
MACS BSA Stock Solution (10 %)	Miltenyi Biotec	130-091-376
MEM NEAA (100x)	Gibco	11140-035
OptiMEM™	Gibco	31985070
Penicillin/ Streptomycin	PAA	P11-010
RPMI Medium 1640 (1x) + GlutaMAX™	Gibco	61870-010
sodium pyruvate (100 mM)	Gibco	11360-039
UltraPure™ EDTA (0.5M, pH 8.0)	Gibco	15575
X-Vivo 20	Lonza	BE04-448Q

3.1.3 Cell culture media

Name	Composition
Full RPMI Medium	500 ml RPMI Medium 1640 (1x) + GlutaMAX™
	10 % FBS

	1 % P/S
Serum free RPMI Medium	500 ml RPMI Medium 1640 (1x) + GlutaMAX™
	1 % P/S
Full Monocyte Medium	500 ml RPMI Medium 1640 (1x) + GlutaMAX™
	10 % FBS
	1 % P/S
	10 mM HEPES
	1 mM Sodium Pyruvate
	50 µM β-Mercaptoethanol
	1 mM MEM Non-essential amino acids
Monocyte EV-depleted medium	500 ml RPMI Medium 1640 (1x) + GlutaMAX™
	10 % FBS (Ultracentrifuged at 23000 rpm for 16h)
	1 % Penicillin/ Streptomycin
	10 mM HEPES
	1 mM Sodium Pyruvate
	50 µM β-Mercaptoethanol
	1 mM MEM Non-essential amino acids

3.1.4 Kits

Product	Company	Catalog No.
CD14 MicroBeads, human	Miltenyi Biotec	130-050-201
CD8 MicroBeads	Miltenyi Biotec	130-045-201
CellROX® Reagents	Thermo Fisher Scientific	C10422
FoxP3/ Transcription Factor Fixation/ Permeabilisation Concentrate and Diluent	eBioscience	00-5521-00
Human IFN-γ ELISA MAX™ Deluxe	Biolegend	430104
NOS Detection Kit	Cell technologies	NOS200-2
Pierce™ BCA Protein Assay Kit	Thermo Fisher Scientific	23227
Pierce™ LAL Chromogenic Endotoxin Quantitation Kit	Thermo Fisher Scientific	88282
SensiFAST™ SYBR® Lo-ROX Kit	Bioline	BIO-94020

Toxisensor™ Chromogenic LAL Endotoxin Assay	GeneScript	L00350
Venor® GeM Classic Mycoplasma Detection Kit	Minerva	11-1050

3.1.5 Antibodies

Primary Antibodies

Name	Clone	Company	Catalog No.
CD9	MZ3	Biolegend	124802
CD81	5A6	Biolegend	349501
CD63	H5C6	Biolegend	353013
Calreticulin	D3E6	Cell signaling	12238S
GAPDH	FF26A/F9	Biolegend	649202
gp100	HMB45	Dako	MA5-16712
ALIX	3A9	Cell signaling	2171S
Bcl-2	100	Biolegend	648701
Human Phospho-RelA/NF-κB	S536	RnD Systems	MAB72261-SP
Human/Mouse RelA/ NF-κB	D14E12	RnD Systems	MAB50781
CD282 (TLR2) Antibody, Functional Grade	6C2	eBioscience™	16-9021-81
CD284 (TLR4) Antibody, Functional Grade	HTA125	eBioscience™	16-9917-82
Mouse IgG2a κ Isotype Control, Functional Grade	eBM2a	eBioscience™	16-4724-82

Secondary Antibodies

Name	Clone	Company	Catalog No.
Anti-Mouse IgG	Polyclonal	Sigma-Aldrich	A9044-2ML
Anti-Rabbit IgG	Polyclonal	Sigma-Aldrich	A0545-1ML
Anti-Rat	Polyclonal	Sigma-Aldrich	A9037-1ML

Conjugated Antibodies

Name	Fluorochrome	Clone	Company	Catalog No.
CD14	Percp-Cy5.5	MφP9	BD	562692
CD11b	APC	ICRF44	BD	550019
HLA-DR	APC-Cy7	L243	BD	335796
PD-L1	PE-Cy7	MIH1	BD	558017
CD8	Pacific Blue	RPA-T8	BD	558207
Annexin V	PE		BD	556421

3.1.6 Primers for mRNA

Primer	Species	Orientation	Sequence
β-actin	Human	forward	5'-GCCCTGAGGCACTCTTCCA-3'
		reverse	5'-CCAGGGCAGTGATCTCCTTCT3'
IL-1β	Human	forward	5'-TGTAATGAAAGACGGCACACC-3'
		reverse	5'-TCTTCTTTGGGTATTGCTTGG-3'
IL-6	Human	forward	5'-GGTACATCCTCGACGGCATCT-3'
		reverse	5'-GTGCCTCTTTGCTGCTTTCAC-3'
IL-10	Human	forward	5'-CGATTTAGAAAGAAGCCCAA-3'
		reverse	5'-TCAACAGCTAGAAAGCGTGGT-3'
TNFα	Human	forward	5'-GCCAGAGGGCTGATTAGAGA-3'
		reverse	5'-CAGCCTCTTCTCCTTCCTGAT-3'
CCL2	Human	forward	5'-GACCAGGAAAGAATGTGAAAG-3'
		reverse	5'-GCTCTGCCAATTGACTTTCCTT-3'
PD-L1	Human	forward	5'-TATGGTGGTGCCGACTACAA-3'
		reverse	5'-TGGCTCCCAGAATTACCAAG-3'
Bcl-2	Human	forward	5'-TTGTGGCCTTCTTTGAGTTCGGTG-3'
		reverse	5'-GGTGCCGGTTCAGGTA CT CAGTCA-3'
Bcl-XL	Human	forward	5'-CTG AATCGGAGATGGAGACC-3'
		reverse	5'-TGGGATGTCAGGTC ACT GAA-3'
Mcl-1	Human	forward	5'-AGAAAGCTGCATCGA ACCAT-3'
		reverse	5'-CCAGCTCCTACTCCAGCAAC-3'
survivin	Human	forward	5'-CAGATTTGAATCGCGGGACCC-3'
		reverse	5'-CCAAGTCTGGCTCGTTCTCAG-3'

Bax	Human	forward	5'-CCTGTGCACCAAGGTGCCGGAACT-3'
		reverse	5'-CCACCCTGGTCTTGGATCCAGCCC-3'
Caspase3	Human	forward	5'-TCCTGAGATGGGTTTATGT-3'
		reverse	5'-ATGTTTCCCTGAGGTTTGC-3'

3.1.7 shRNA

TRC Number	Gene	Clone ID	Company
TRCN0000001025	HSP90AA1	NM_005348.x-616s1c1	Sigma-Aldrich
TRCN0000001028	HSP90AA1	NM_005348.x-867s1c1	Sigma-Aldrich
TRCN0000207114	shControl		Sigma-Aldrich

3.1.8 Chemicals and biological reagents

Product	Company	Catalog No.
10 % Tween® 20 Solution	BioRad	161-0781
10 x Permeabilization Buffer	eBioscience	00-8333-56
7-AAD	BD	51-68981E
ACK lysis buffer	Gibco	A10492-01
Acrylamide solution	Carl Roth	2267.2
Albumin IgG free	Carl Roth	3737.4
Amiloride,5'- (N, N-Dimethyl)-hydrochloride	Enzo	ALX-550-261-M005
Ammonium persulfate (APS)	Sigma-Aldrich	A-3678
ATX Ponceau S red staining solution	Sigma-Aldrich	09189-IL-F
Carboxyfluorescein succinimidyl ester (CFSE)	Biolegend	423801
Clear PAGE LDS sample buffer (4x)	Invitrogen	MP0007
Glycine	Carl Roth	3908.1
Methanol	Carl Roth	8388
MISSION® shRNA Bacterial stock	Sigma Aldrich	SHCLNG
MISSION® TRC2 pLKO.5-puro Non-mammalian Control Plasmid DNA	Sigma Aldrich	SHC202
Lipofectamine® RNAiMAX	Life Technologies	13778075

Transfection Reagent		
Lipofectamine 2000	Life Technologies	11668030
PageRuler Protein ladder prestained	Thermo Fisher Scientific	26616
Pierce® ECL Western Blotting Substrate	Thermo Fisher Scientific	#32106
Pierce® RIPA Buffer 100 ml	Sigma Aldrich	89900
Powdered milk	Carl Roth	T145.3
Roti-Phenol/ Chloroform/Isoamylalkohol	Carl Roth	A156.1
Rotiphorese Gel 30 (37,5:1)	Carl Roth	3029.1
SDS	Carl Roth	0183.3
SIG10 5α Chemically Competent cells	Sigma Aldrich	CMC
Temed	BioRad	#1610800
TRIS	Carl Roth	0188.3
Trizol ® Reagent	Life Technologies	15596018
Trypan Blue Solution	Sigma Aldrich	T8154
RBC Lysis Buffer (10x)	Biolegend	420301
Dynabeads® Human T-Activator CD3/CD28	Gibco	111.31D
Annexin V Binding Buffer (10X)	BD	556454
NF-κB Activation Inhibitor VI, BOT-64	Sigma Aldrich	113760-29-5

3.1.9 Solutions

Name	Composition
Freezing medium 1	60 % FBS
	40 % X-VIVO 20
Freezing medium 2	75 % FBS
	25 % DMSO
1 x TBS	5 mL 1 M Tris/HCl, pH 8
	15 mL 1 M NaCl
	470 mL ddH ₂ O

Stacking polyacrylamide gel	6 mL ddH ₂ O
	1.35 mL 30 % Acrylamide solution
	2.5 mL 0.5 M Tris/HCl, pH 6.8
	100 µL 10 % SDS
	100 µL 10 % APS
	10 µL TEMED
10 % Separating polyacrylamide gel	21.3 mL ddH ₂ O
	13.3 mL 30 % Acrylamide solution
	5.3 mL 3 M Tris/HCL, pH 8.8
	400 µL 10 % SDS
	133 µL 10 % APS
	TEMED
10 x Running buffer	30 g Tris base
	144 g Glycine
	10 g SDS
	10 L ddH ₂ O
10 x Transfer buffer	121.2 g Tris base
	576 g Glycine
	4 L ddH ₂ O
Blocking buffer for western blot	DPBS
	3 % BSA
	0.05 % Tween-20 in TBS
FACS buffer	DPBS
	2 % FBS
	0.2 % NaN ₃
MACS buffer	DPBS
	1% BSA
	0.5 mM EDTA
NP-40 lysis buffer	50 mM Tris HCl, pH 8.0
	150 mM NaCl
	5 mM EDTA
	10 % NP40
	1 x Protease Inhibitor

3.1.10 Routine laboratory material

Product	Company	Catalog No.
6-well flat bottom with lid	Thermo Fisher Scientific	140675
12-well flat bottom with lid	BD	353043
24-well flat bottom with lid	Greiner bio-one	622160
96-well flat bottom with lid	TPP®	92096
96-well U-bottom with lid	Sigma Aldrich	M9436-100EA
serological pipettes: 5, 10 and 25 mL, sterile	Greiner bio-one	606180; 607180
15 mL conical tubes	Falcon	352096
50 mL conical tubes	Falcon	352070
Amicon® Ultra Centrifugal tube	Merck Millipore	UFC905024
Cellstar Cell culture flask 25 cm ²	Greiner	658170
Cell culture flasks T75	Sigma Aldrich	C7231-120EA
TC dish, 150 Standard	Sarstadt	3903
Cryovial, 2 mL sterile	Sigma Aldrich	V5760-500EA
Filter tips: 20, 200, 1000 µL	Steinbrenner	L1000
Freezing Container, "Mr. Frosty"		
Safe lock tubes: 0.5, 1.5 and 2 mL	Eppendorf	SL-GPS-L10, L250,
Filter tips: 20, 200, 1000 µL	Steinbrenner	L250, L1000
Syringe 1 mL	BD	
Neubauer chamber	Brand	
Needles Sterican®	B. Braun	4657705
Stericup&Steritop 0.22 µM Millipore Express PLUS membrane	Merck Millipore	SCGPU02RE
LeucoSep tubes	Greiner Bio-one	
iBlot Transfer Stack	Thermo Fisher Scientific	IB24002

ThickBlot Filter Paper	BioRad	1703
PVDF membrane	Thermo Fisher Scientific	88520

3.1.11 Laboratory equipment

Device	Name	Provider
Balance	BP 3100P	Sartorius
Cell culture incubator	Hera cell	Heraeus
Centrifuges	BiofugeprimoR	Heraeus
	MEGAFUGE 40R	Heraeus
	Labofuge 400R	Heraeus
Confocal microscope	TCS SP2	Leica
Flow cytometer	FACS Canto II	BD Biosciences
Flow cytometer	FACS Lyric	BD Biosciences
Heating block	Digital Block Heater HX-2	Peqlab
Imaging system	Fusion SL	VilberLourmat
Laminar flow hood	Hera safe	Thermo Electron Cooperation
Magnetic stirrer	RCT basic	IKA Werke
Microplate Reader	Tecan infinite M200	Tecan
Microscope	DMIL	Leica
MACS Magnet and stand		Miltenyi Biotec
N2 tank		
Nanoparticle tracking system	NanoSight NS300	Malvern
Nanodrop Spectrophotometer		
Pipettes	Transferpette® S	Brand
Power supply	PowerPac™ HC High Current	BioRad

Real-Time PCR machine	MX3005 qPCR System	Stratagene
Shaker	Logic shaker	NeoLab
Thermal Cycler	DNA Engine Peltier Thermal Cycler	BioRad
Transfer device	iBlot™ Gel Transfer Device	Thermo Scientific
Ultracentrifugation rotor	Surespin 630	Sorvall
Ultracentrifuge	SorvallDiscovery 90SE	Hitachi
Vortexer	REAX top	Heidolph
	Vortex Genie 2	Scientific Industries
Water bath	DC3	HAAKE, GFL

3.1.12 Software for data analysis

Product	Version	Company
Flow Jo	7.6.1	Tree Star Inc., Ashland, USA
GraphPad PRISM	5	GraphPad Software Inc., San Diego, USA
Image J	1.51d	NIH
Mendeley	1.46	Mendeley
I control 1.10	1.10	TECAN

3.2 Methods

3.2.1 Cell culture

The human melanoma cell lines (HT-144, SK-MEL-28) were cultured in 75 cm² full RPMI media indicated in table 3. All cell lines were cultured in a humidified incubator at 37°C and 5 % CO₂. Cell lines were sub-cultured every 2-4 days as soon as they reached around 70 % confluency. For passaging adherent cells, 3 mL of 1 x Trypsin containing 5 mM EDTA was used and added to the cells. Afterwards, the cells were incubated for 3 - 5 min at 37 °C to allow the cells to detach. The cells were then transferred into pre-warmed medium in Falcon tubes and were centrifuged (1500 rpm, 7 min, RT). After removal of the supernatant, the cells were resuspended in 20 ml of the respective cell culture media for culture (37°C, 5% CO₂).

3.2.2 Counting of cells

When necessary, the respective cell suspension was centrifuged for 7 min at 1500 rpm and pellets were resuspended in an appropriate volume of cell culture medium. Next, 90 µL trypan blue solution was mixed with 10 µL cell suspension for live-dead discrimination. Live cells were counted with a Neubauer counting chamber and the total cell number was calculated using the following formula:

$$\text{Total live cells/mL} = \text{Counted cells/counted squares} \times \text{dilution factor} \times 10 \times 10^4 \text{ cells/mL}$$

3.2.3 Isolation of EVs from melanoma cell line

For EV isolation from conditioned media of human melanoma cell lines, a protocol was established based on the previously described method (Lobb et al., 2015). Cells were expanded and grown to 70% confluency in 75 cm² cell culture dishes. The media was discarded. The cells were washed with PBS then further incubated for 24 hours in serum free media. Next, the media were harvested after 24 hours and centrifuged at 1500 rpm at 4 °C for 7 minutes to remove detached cells. Supernatant

was collected and frozen at -20°C until use. On the day of EV isolation, the frozen supernatant was thawed at 37°C and then filtered through $0.22\ \mu\text{M}$ filters to remove contaminating apoptotic bodies and cell debris. Clarified EV containing media was concentrated by a $100\ \text{kDa}$ size exclusion filtration at $3800\ \text{g}$ for $30\ \text{min}$ at RT using Amicon Ultra Centrifugal Filters which allowed the separation of protein. The concentrated media was collected from the filters, diluted with filtered PBS ($0.22\ \mu\text{M}$ filters), and then ultra-centrifuged for $90\ \text{min}$ at $100,000\ \text{g}$ to pellet EVs. The supernatant was carefully removed, and the pellet was resuspended in $500\ \mu\text{L}$ sterile filtered PBS and stored at -20°C . The method for EV isolation from melanoma cell lines is illustrated schematically in Fig. 6.

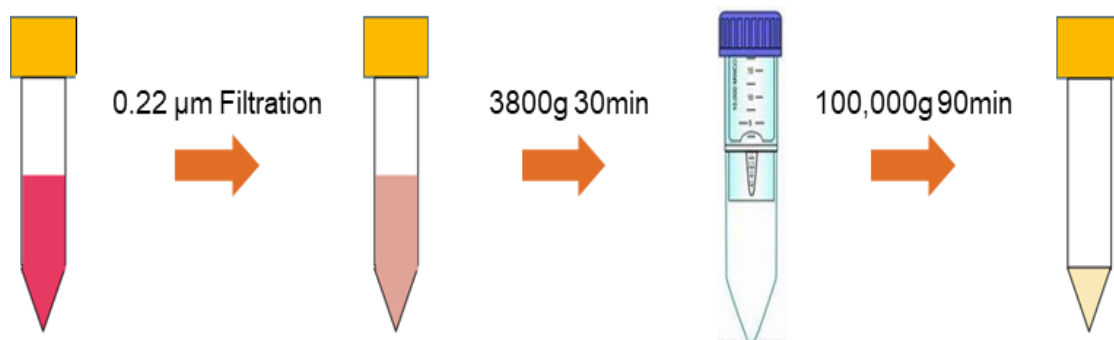


Figure 6: Isolation of EVs from melanoma cell lines. Cell culture media was sterile filtered with $0.22\ \mu\text{M}$ filters followed by ultrafiltration at $3800\ \text{g}$ for $30\ \text{min}$. EVs were pelleted by ultracentrifugation by $100,000\ \text{g}$ at 4°C for $90\ \text{min}$.

3.2.4 Isolation of EVs from plasma of melanoma patients

3.2.4.1 Plasma preparation

Whole blood was obtained from melanoma patients in heparin-coated tubes and proceeded within 2 hours. Density gradient centrifugation at $400\ \text{g}$ for $30\ \text{min}$ using Biocoll (Biochrom, Berlin, Germany) was used for separation of plasma, peripheral blood mononuclear cells (PBMCs) from erythrocytes and others. Isolated PBMCs

were adjusted to 10^7 cells and cryopreserved in RPMI supplemented with 30% human serum and 10% DMSO at -80°C . Plasma was aliquoted to clean tubes and stored at -80°C until use.

3.2.4.2 Isolation of EV from plasma of melanoma patients

For the isolation of EVs from human plasma, 5mL plasma was thawed, diluted with PBS and centrifuged at 2000 g for 10 min to remove platelets and cell debris. The supernatant was taken and filtered through a $0.22\ \mu\text{m}$ Syringe Filter (Merck). Filtered plasma was centrifuged at 10,000 g for 30 min to remove debris and then EVs were pelleted by ultracentrifugation at 100,000 g for 70 min. The pellet was re-suspended in sterile-filtered PBS and frozen at -20°C until use. In some experiments, EVs were depleted from plasma by ultracentrifugation at 100,000 g and used as controls.

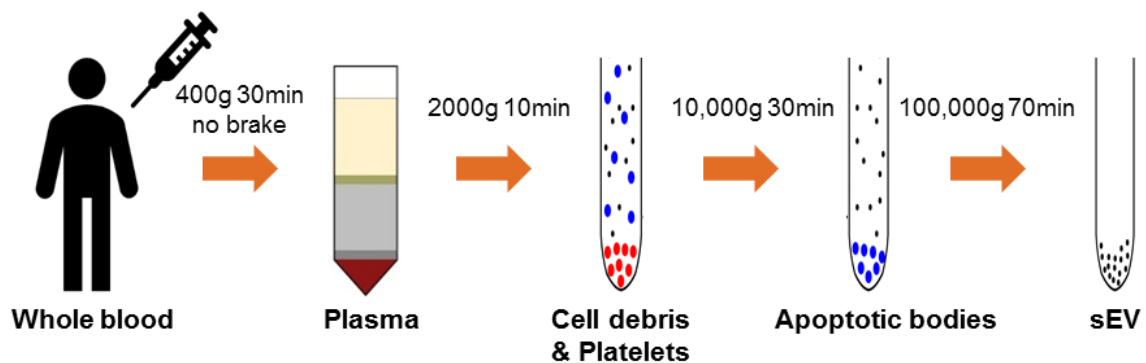


Figure 7: Isolation of EVs from plasma melanoma patients. Whole blood was taken from patients and centrifuged at 400 g for 30 min for the collection of plasma and PBMC. Plasma was further centrifuged at 2000 g for 10 min after freeze-thaw to get rid of platelets. Cell debris, platelets and apoptotic bodies were removed via centrifugation at 2000 g for 10 min and at 10,000 g for 30 min. EVs were pelleted via ultracentrifugation at 100,000 g at 4°C for 90 min.

3.2.5 Quantification of purified EVs

3.2.5.1 Nanoparticle tracking analysis (NTA)

Light scattering technologies, especially nanoparticle tracking analysis is widely used to measure the particle numbers and size distribution profiles. Prior to analysis, EVs were diluted 1:1000 with sterile PBS and then loaded into Malvern NanoSight NS300 device. Videos were recorded five times (60 seconds each) with camera level set between 7 and 10 and detection threshold set at 5. NTA 3.0 software was used to calculate the size and concentration of the particles with corresponding standard error via analysis of recorded video. Temperature was monitored and updated after each run. After each batch of EV, detection chamber was washed with sterile PBS.

3.2.5.2 Protein quantification

To determine the protein concentration of or EVs and cell lysates, Pierce BCA Protein Assay Kit (Thermo Scientific) was used according to the manufacturer's instructions. First, working reagent was prepared by mixing 50 parts of BCA reagent A with 1 part of BCA reagent B. Then, 10 μ L of standards and diluted samples were pipetted out on a 96-well plate and 200 μ L of WR was added to each well. The plate was incubated at 37°C for 30 min followed by the measurement of the absorbance at 562 nm using the microplate reader.

3.2.6 Biochemical methods

3.2.6.1 RNA isolation and cDNA synthesis

Total RNA was isolated from cells using TRIzol according to the manufactures protocol. RNA concentration and quality were measured by TECAN 200 spectrophotometer. Isolated RNA was stored at -80 °C until further downstream

measurement. cDNA was synthesised using the Sensi FAST™ cDNA Synthesis Kit from Bioline (Table 1).

Table 1: Program for cDNA synthesis amplification

Reagent	Volume [μ l]	Step	Temp. [$^{\circ}$ C]	Time [min]	Cycles
Total RNA or mRNA (up to 1 μ g)	n μ l	1	25	10	1
5x TransAmp Buffer	4 μ l	2	42	15	1
Reverse Transcriptase	1 μ l	3	85	5	1
DNase/RNase free-water	Up to 20	4	4	hold	1

3.2.6.2 RT-PCR

To determine the expression levels of mRNA, quantitative real-time PCR (qPCR) was performed using SYBR Green Master Mix (Applied Biosystems, Life technologies) on a Stratagene Mx3005P real-time PCR system. In all experiments, 18s was used as the housekeeping gene and the values were normalized to it. Relative gene expressions were quantified by calculating ($\Delta\Delta$ Ct). Amplification program is shown in Table 2.

Table 2: Program for mRNA amplification

Reagent	Volume	Final concentration	Step	Temp. [$^{\circ}$ C]	Time [s]	Cycles
2x SensiFAST SYBR Lo-ROX Mix	10	1x	1	50	120	1
10 μ M forward primer	0.8	400nM	2	95	10	42
10 μ M reverse primer	0.8	400nM	3	59 – 63	60	42
Template	up to 8.4		4	95	60	1
H ₂ O	as required		5	65	30	1
	20 final volume		6	95	30	1

3.2.6.3 Protein isolation

Cells were cultured in 6-well plates for whole cell protein isolation. On the day for isolation, cells were detached from the well with a cell scraper on ice and washed with PBS at 300 g for 7 min. Pellets were resuspended in 300 μ L NP-40 lysis buffer

with Protease Inhibitor. In order to maintain the phosphorylation of proteins, 1x of phosphorylation inhibitor was added to the lysis buffer. The cells were lysed for 30 min at 4 °C on a shaking platform and afterwards centrifuged at 13,000 g for 15 minutes at 4 °C. The supernatant containing the proteins was transferred to a fresh Eppendorf tube and stored at -20 °C. To determine the protein concentration, method indicated in 3.2.5.2 was used.

3.2.6.4 Western Blot

3.2.6.4.1 SDS-polyacrylamide gel electrophoreses (SDS-PAGE)

In order to analyze the protein expression in whole cell lysates or EVs by Western Blot, proteins were separated according to their molecular weight by discontinuous SDS polyacrylamide gel electrophoresis (SDS-PAGE). Protein was first mixed with LDL-sample buffer supplemented with 5 % β -mercaptoethanol, heated for 5 min at 95°C and then placed on ice. 30 μ g of protein from each sample was loaded on a 10 % SDS gel and separated at 100 V until the leading front runs out of the SDS gel. For determination of the protein size, a protein standard was applied. Electrophoresis for CD9-Western Blots was carried out under non-denaturing conditions with β -mercaptoethanol free loading buffer.

3.2.6.4.2 Protein transfer

After electrophoresis, proteins were transferred on to a Polyvinylidenfluorid (PVDF) membrane and a semi-dry blotting technique was used. Three sheets of waterman papers were soaked with 1 x transfer buffer and put onto the anode of the blotting device. PVDF membrane was first activated with methanol for 1 minutes, rinse with transfer buffer, and then placed on top of the waterman papers. Subsequently, the SDS-gel was equilibrated in transfer buffer and placed above the PVDF membrane, followed by three sheets of waterman papers. The proteins were then transferred

onto the PVDF membrane at 0.6 mA/per blotting stack for 90 min. Afterwards, transfer of proteins to the membrane were routinely checked with Ponceau S staining.

3.2.6.4.3 Protein detection

After transfer, PVDF membrane was blocked for 30 min at room temperature with 3 % BSA in TBS. In parallel, primary antibodies were prepared in TBS-T supplemented with 3 % BSA. The membrane with appropriate dilutions of primary antibody was incubated overnight at 4°C on a shaking platform. Afterwards, the membrane was washed with TBST for three times, and then incubated with appropriate dilution of conjugated secondary antibody at room temperature for 1 h. Before signal development, the membrane was washed again with TBS-T for three times. Pierce® ECL Western Blotting Substrate was used for protein detection and the images were acquired by the Fusion SL detection device.

3.2.6.5 Magnetic-activated cell sorting (MACS)

Human CD14⁺ monocytes and CD8⁺ T cells were purified from the leukocyte concentrates purchased from the German Red Cross Blood Service Baden Württemberg-Hessen according to the manufacturer's protocol (Miltenyi). Briefly, after PBMC isolation, an appropriate number of cells was incubated with magnetic nanoparticles coated with anti-CD14 or anti-CD8 antibody to allow the attachment of cells expressing corresponding antigens to the magnetic nanoparticles. After incubation, the cells were positively selected via columns in magnetic field. The isolated monocytes and T cells fractions were stained with anti-CD14 or anti-CD8 antibodies. The purity was > 90%.

3.2.6.6 Fluorescence-activated cell sorting (FACS) analysis

3.2.6.6.1 Surface staining

1×10^6 cells from culture or primary cells isolated from the peripheral blood were washed and suspended in 100 μ L FACS buffer with Fc-blocking reagent for 10 min at 4 °C. Appropriate fluorochrome-conjugated monoclonal antibodies were added and cells were further incubated for 30 min at 4°C in the dark. When biotinylated antibodies were used, cells were washed with FACS buffer and incubated with conjugated streptavidin for an additional 30 min at 4°C. Afterwards, stained cells were washed twice with 200 μ L FACS buffer by centrifugation at 1500 rpm for 5 min to remove the unbound antibodies and measured with FACS Canto II (BD) using the BD Diva Software V.6.1.1.

3.2.6.6.2 Intracellular staining

For intracellular staining, cells were first stained for surface markers as described above. Afterwards, cells were washed and incubated in 100 μ L of Fixation/Permeabilization solution (1:4 dilution) (eBioscience) for 45 min at 4 °C. Subsequently, fluorescence-labelled antibodies against intracellular antigens was added and washed twice with 200 μ L 1x Perm/Wash buffer (ebioscience). Cells were incubated for 30 min at 4°C in the dark. Then, cells were washed with 1x Perm/Wash buffer, resuspended with 100 μ L of FACS buffer and measured by flow cytometry. Flow Jo software 7.6.1 was used for data analysis.

3.2.6.6.3 EV staining

Since EVs are too small to be detected by BD Canto and BD Lyric flow cytometers, latex beads (4 μ M) were used to couple with EVs for protein detection indirectly. First, latex beads were diluted 1:1000 with PBS and incubated with 50 μ g EVs from each sample for 1 h at room temperature on a shaking platform with the speed of 900

rpm. To stop the coupling reaction, 100 μ L of 1M Glycin/PBS and 100 μ L of 10 % BSA in PBS were added followed by the incubation at room temperature for 30 min on a shaking platform. EV-bead complexes were washed twice with 1 mL FACS buffer for 2 min at 13.000 g and then subjected to staining with appropriated dilution of primary antibody for 1 h at 4 °C in the dark. Afterwards, EV-Bead complexes were washed twice and incubated with secondary antibody diluted with FACS buffer for 60 min at 4°C in the dark followed by two times washing at 13.000 g for 2 min with 1 ml FACS buffer. Flow cytometry analysis was performed for detection of respective protein.

3.2.6.7 T cell proliferation assay

The proliferation rate of CD8⁺ T cells was checked to evaluate the immunosuppressive activity of melanoma-EV educated monocytes. First, CD14⁺ monocytes were isolated as described in 3.2.7 and stimulated with melanoma EVs for 16h. Next day, EVs were washed out twice at 1500 rpm for 5 min at 4 °C. Freshly isolated CD8⁺ T cells were stained with 5 μ M Carboxyfluorescein diacetate succinimidyl ester (CFSE) and added to the plate with or without activation with pre-washed CD3/CD28 Dynabeads. After 72 h incubation, the supernatants were collected for IFN- γ detection, and cells were washed at 1500 rpm for 5 min. Fc-Block reagent and anti-CD8 antibody were added for 20 min at 4 °C in the dark. Flow cytometry analysis was performed after washing and re-suspended in 100 μ L FACS buffer.

3.2.6.8 Enzyme-linked immunosorbent assay (ELISA)

For detection of IFN- γ secretion by CD8⁺ T cells after co-culture with melanoma EV stimulated monocytes, cell supernatant of human CD8⁺ T cells was harvested and measured according to manufacturer's instructions (Biolegend). Briefly, 96-well plate

was coated with Human IFN- γ capture antibody overnight at 4°C followed by 4 times washing of the plate. Non-specific binding was blocked by incubating with assay diluent at RT for 1 hour on a plate shaker. After 4 times washing, pre-diluted (1:10) samples and standards was added and incubated at RT for 2 hours with shaking. Afterwards, the plate was incubated with 100 of diluted detection antibody at RT for 1 hour followed by incubation with 100 μ L of diluted Avidin-HRP solution at RT for 30 minutes. The plate was washed 4 times in between and 5 times afterwards. 100 μ L of freshly mixed TMB substrate solution was added and incubated in the dark for 20 minutes. The reaction was stopped with 100 μ L of stop solution and the absorbance was acquired at 450 nm within 15 min.

3.2.6.9 Transwell migration assay

Cell migration towards a gradient of EV containing serum-free monocyte culture medium was performed in a transwell assay. Briefly, CD14⁺ monocytes were isolated as indicated in 3.2.7 and re-suspended in serum-free monocyte culture media at the concentration of 2.5×10^5 /mL. 750 μ L serum-free monocyte culture medium with EVs of different concentration was added in a 24-well plate. Afterwards, the trans-wells were inserted in 24-well plate and 200 μ L cell suspension was added into each trans-well and incubated at 37 °C for 3 h. Subsequently the medium was removed from each insert and all inserts were wash twice with PBS. The cells on the trans-wells are fixed by formaldehyde (3.7% in PBS) at RT for 2 min followed by two times wash by PBS. 100% methanol was used to permeabilize cells at RT for 20 min. After the permeabilization, the cells were wash twice by PBS and further stained with Giemsa at RT for 15 min in the dark. The transwells were washed again for two times and the non-migrated cells were scraped off with cotton swabs from the top of the inserts. Light microscope was used for counting of the migrated cells.

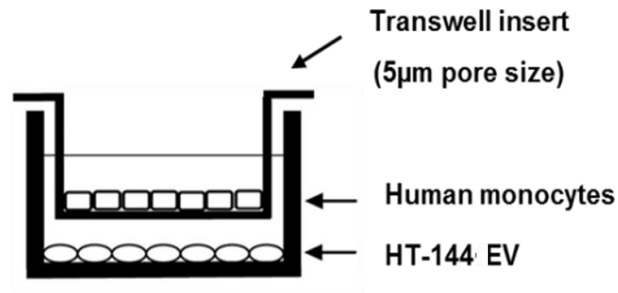


Figure 8: In vitro transmigration assay.

3.2.6.10 Transduction with lentiviral particles

Lentiviral transduction was performed by Qian Sun (DKFZ). Briefly, HEK293T cells were used for lentiviral particle production. Two independent lentiviral shHSP90AA1 constructs (shHSP90AA1-1 TRCN0000001025; shHSP90AA1-2 TRCN0000001028) and a control vector (shControl TRCN0000207114) were purchased from Sigma-Aldrich. For transfection, plasmid containing respective shRNA (11 µg) was incubated with the packaging plasmids VSV-G (5.5 µg) and pCMV-dR 8.91 (8.25 µg) in DMEM and X-treme GENE® (Roche) solution for 30 min. After incubation, they were added to HEK293T producer cells. Supernatant of infected HEK293T cells was discarded after 12h transfection, and then harvested at 24, 36 and 48h. Supernatants were pooled together and filtered with sterile syringe filters (0.22 µM). 0.5 mL of filtered supernatant were added to a 6-well plate with seeded human melanoma cells (2×10^5 cells) and incubated with virus for 24 h. Afterwards, human melanoma cells were re-infected with the same virus in fresh medium. After 48 h of transduction, the

cells were washed twice with PBS and cultured for 72 h followed by a selection of the transduced cells with 2 µg/ml puromycin.

3.2.6.11 Patients

In this study, 30 patients with melanoma of stages III–IV (AJCC 2018) who were seen at the Skin Cancer Center (University Medical Center Mannheim, Germany) from 2013 to 2018 (ethics approval: 2010-318MMA) were included. Briefly, heparinized blood samples were subjected to the density gradient centrifugation using Biocoll (Biochrom). After removal of plasma, PBMC was collected, aliquoted and stored at -80 °C. For each patient, PBMCs before and post treatment until the 6th treatment cycle was collected and separated into responding and non-responding groups. Patients with complete response (CR) and partial response on ICI therapies were classified as responders, whereas those with stable disease (SD) and progressive disease (PD) were considered as non-responders (Fig. 9).

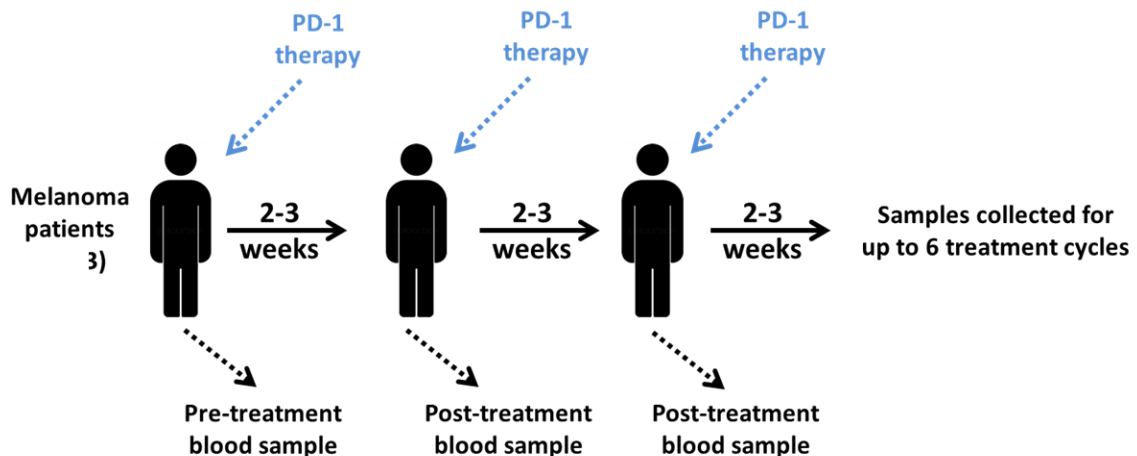


Figure 9: Scheme of study design

3.2.7 Statistical analysis

Statistical analyses were performed using GraphPad Prism software. Results were assessed with one-way ANOVA or an unpaired two-tailed Student's t test. Survival curves were generated using the product limit (Kaplan-Meier) method, and comparisons were conducted using the log-rank (Mantel-Cox) test. A p value below 0.05 was considered statistically significant.

4 RESULTS

4.1 Characterization of EVs

4.1.1 Characterization of EV from melanoma cell lines

An updated guideline “Minimal information for studies of extracellular vesicles 2018 (MISEV2018)” was published in 2018 by the International Society for Extracellular Vesicles (Théry et al., 2018). We performed the steps in accordance with this guideline to quantify and characterize the protein content in our EV preparations.

The concentration and size distribution of purified EVs were measured using nanoparticle tracking analysis (NTA) that uses the properties of Brownian motion and light scattering. A representative histogram of NTA revealed that the particles have the mean size at 118 nm and concentration of $1.5 \times 10^{12} \pm 3.23 \times 10^{11}$ EVs/mL (Fig. 10A). Isolated EVs were also characterized by Western Blot analysis (Fig. 10B). HT-144 EVs are tested for the EV-associated markers such as CD9, CD81 and ALIX, which are involved in the biogenesis of multivesicular bodies (El Andaloussi et al., 2013). Those EVs were negative for the endoplasmic reticulum resident protein calreticulin, confirming that the EV preparations were not contaminated with cellular components (Fig. 11B). Importantly, we also detected the presence of the melanoma-associated antigen gp100 on HT-144 EV that was also detected on HT-144 cells (Fig. 10C). We coupled HT-144 EV with latex-beads and measured the coupled EVs by flow cytometry. The gating strategy is shown in Fig. 11. In parallel, the expression of gp100 on HT-144 EV was also confirmed by Western Blot (Fig.10D).

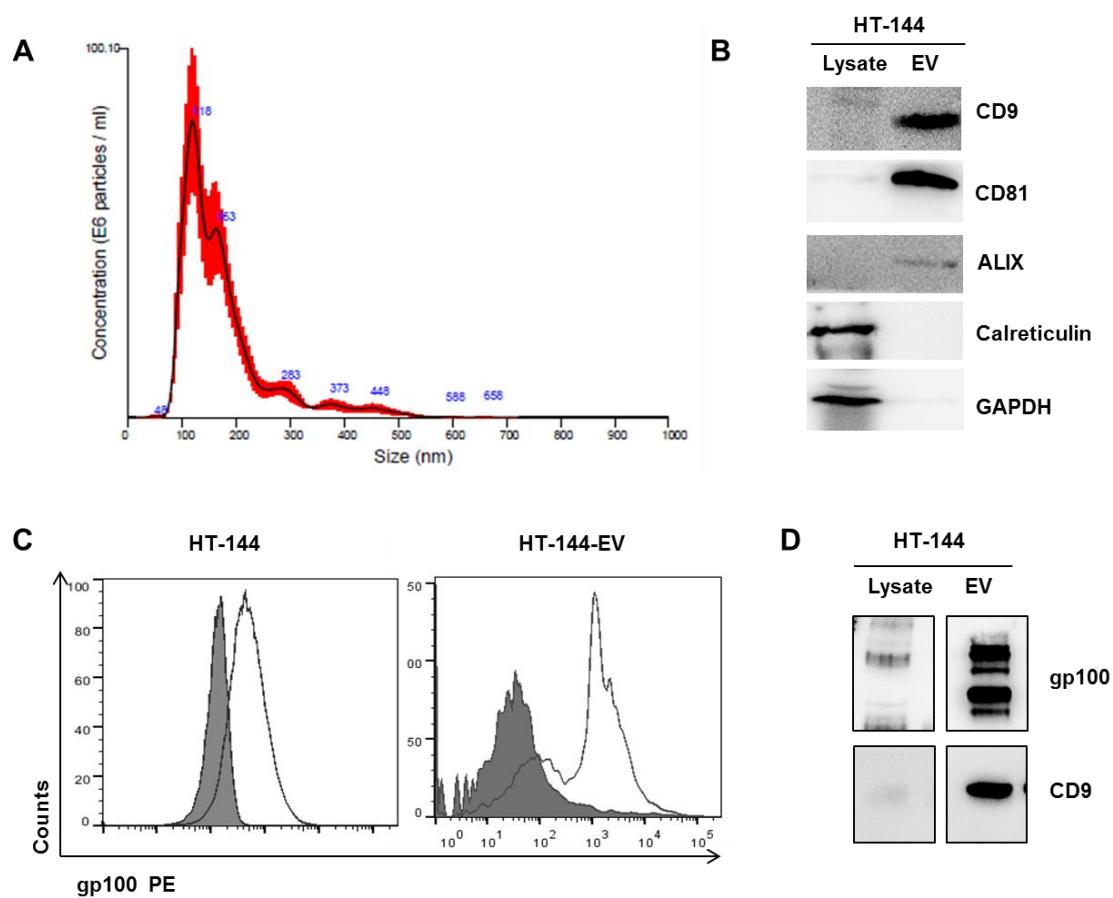


Figure 10: Characteristic of HT-144 EV. A) Representative Nanoparticle Tracking Analysis (NTA) for the size determination of HT-144-EV. B) Western blot analysis of EVs markers (CD9, CD81 and ALIX), loading control (GAPDH) and negative control (calreticulin) in EVs. C) HT144-EV were coupled with latex beads and stained for gp100. The expression level of gp100 was measured via flow cytometry. Solid line without shading indicates the secondary antibody control and Solid line shows the expression of gp100.

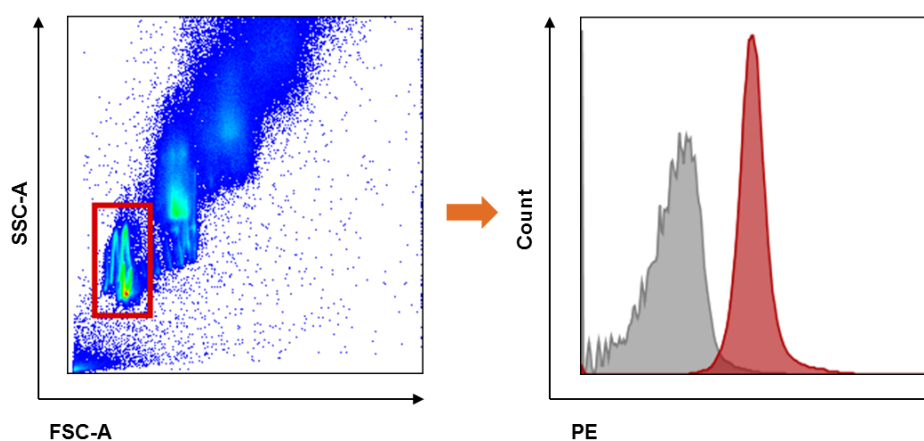


Figure 11: Representative dot plot showing the gating strategy of latex bead-conjugated EVs. Latex beads were gated according to SSC-A and FSC-A in A) and the fluorescence detection of isotype (grey) or CD9 (red) on HT-144 EV shows in B).

4.1.2 Characterization of EV from plasma of melanoma patients

It was described that platelet-derived EV may account for over 50% of EVs in serum (Gemelli et al., 1993). This makes plasma a better source of EVs (Bemis et al., 2013). Based on this, we isolated EVs from plasma of stage IV melanoma patients by differential ultracentrifugation. NTA and Western Blots were also made for the characterization for plasma-EV of melanoma patients (Fig. 12 A and B).

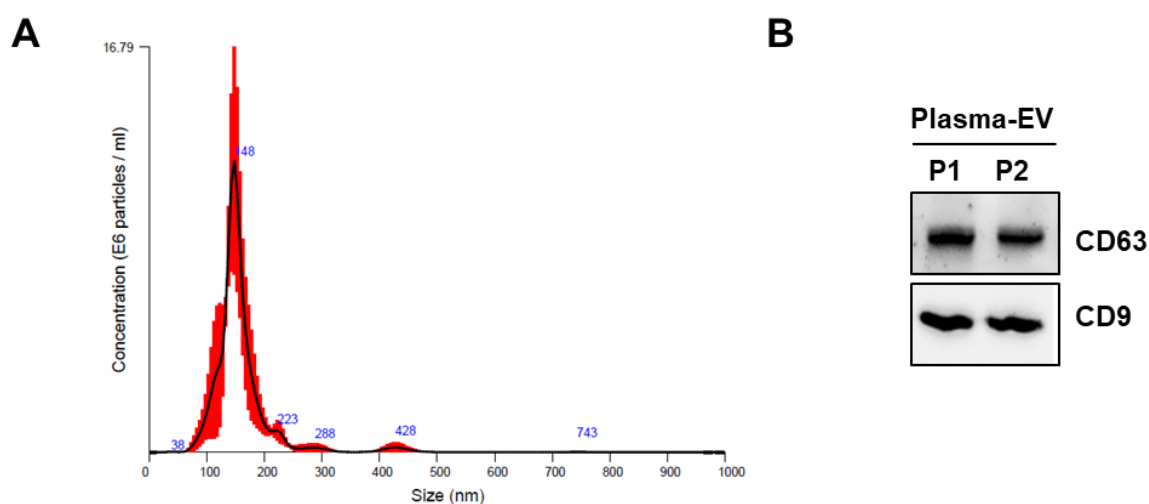


Figure 12: Characteristic of EVs isolated from plasma of melanoma patients. A) Representative Nanoparticle Tracking Analysis (NTA) for the size distribution of EVs from melanoma patients. B) Western blot analysis shows the expression of EV markers (CD9, CD63).

4.2 Effect of HT-144 EV on CD14⁺ monocytes

As mentioned previously, the expansion and activation of MDSC is strongly associated with inflammatory and immunosuppressive factors produced in the tumor microenvironment by tumor cells and stroma cells. We selected a panel of cytokines such as interleukin (IL)-1 β , IL-6, IL-10, and TNF- α as well as chemokine like monocyte chemoattractant protein-1 (MCP-1/CCL2). The gene expression of those cytokines and chemokines was measured in monocytes by RT-PCR. We observed a pronounced upregulation of cytokine and chemokine transcription in monocytes following 16 h exposure to HT-144 EV (Fig. 13 A).

Since CCL-2 was shown to play an important role in the attraction of M-MDSC in the tumor microenvironment (Chang et al., 2016), we examined whether the incubation with HT-144 EV affected the migration of monocytes via Boyden chamber assays. We could see that monocyte migration ability was significantly stimulated by melanoma derived EVs in a dose dependent manner. (Fig. 13B, C)

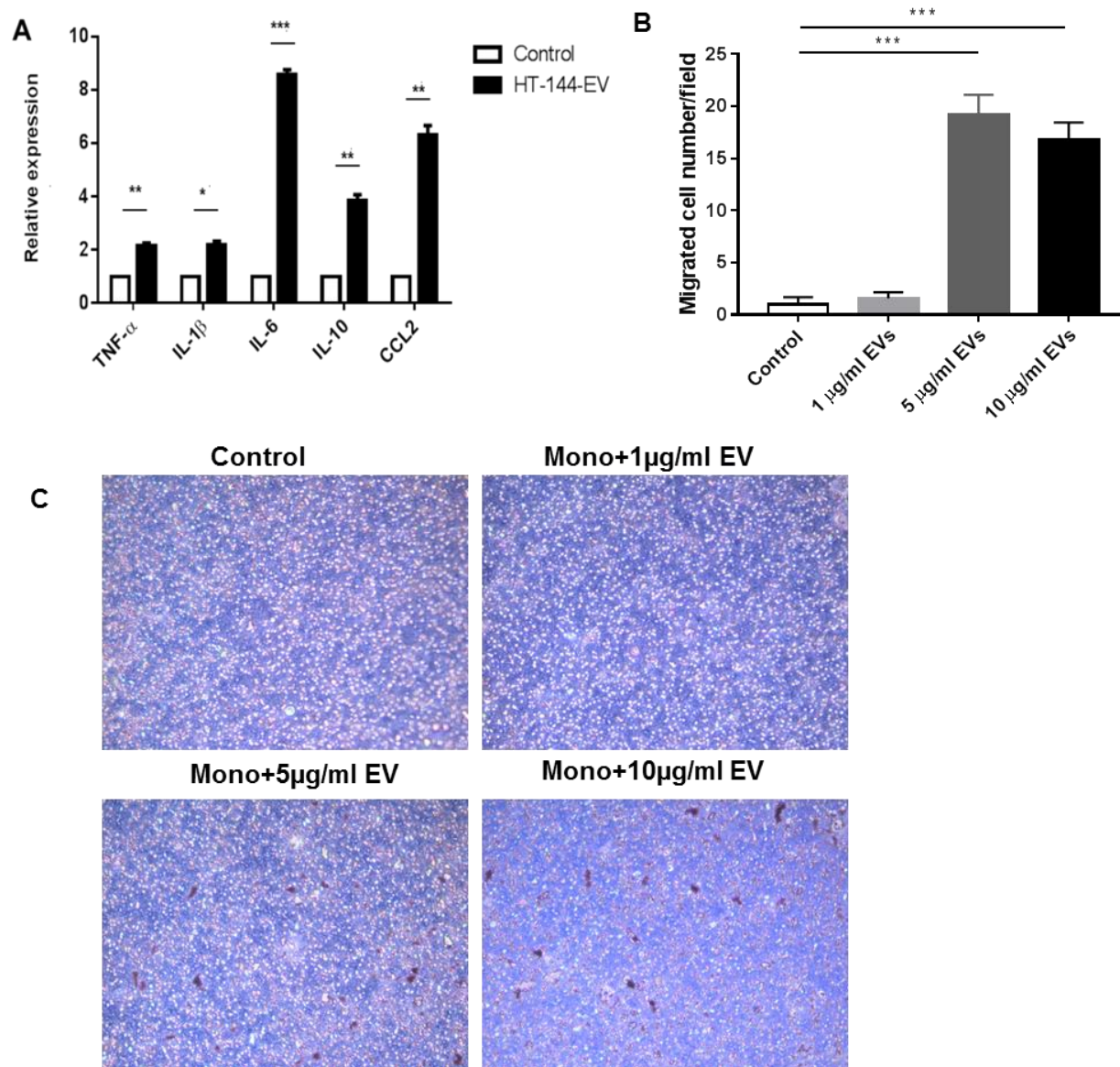


Figure 13: HT-144 EVs induce cytokine gene expression and migration activity of monocytes. A) Expression of cytokines and chemokines in monocytes was measured by RT-PCR normalized to β -actin. B) Monocytes in the transwell migration assay were incubated with HT-144 EVs at the concentration of 1 μ g/mL, 5 μ g/mL and 10 μ g/mL. The migrated cells were stained with Gemsa solution after 3 h and counted manually under microscope. Five representative field in each well were quantified to determine the number of migrated cells (mean \pm SEM; n=3) and representative photos are shown in C. * $p < 0.05$, ** $p < 0.01$, *** $p < 0.001$.

4.3 HT-144 EVs protect CD14⁺ monocytes from spontaneous apoptosis

Previous publications showed that EVs from different cells have different effects on the survival of their target cells (Andreola et al., 2002; Valenti et al., 2006). To this regard, normal human monocytes were evaluated in apoptotic assay following the treatment with HT-144 EV. CD14⁺ monocytes were cultured with or without 15 µg/ml of EVs in 24-well plates (2×10^5 cells/well) in monocyte culture medium. In agreement with previously published finding (Valenti et al., 2006), co-culture with EVs resulted in a decrease in total apoptosis of monocytes (Fig. 14A and B). Besides, we studied the expression of various pro- and anti-apoptotic gene. and found that the expression of anti-apoptotic proteins Bcl-2 and survivin were significantly upregulated at the mRNA level. Finally, the upregulation of Bcl-2 at the protein level in monocytes was also confirmed by Western Blot upon the treatment with HT-144 EV in a time- and dose-dependent manner (Fig. 14D and E). These observations demonstrated the capacity of melanoma EVs to protect monocytes from spontaneous apoptosis via the induction of Bcl-2.

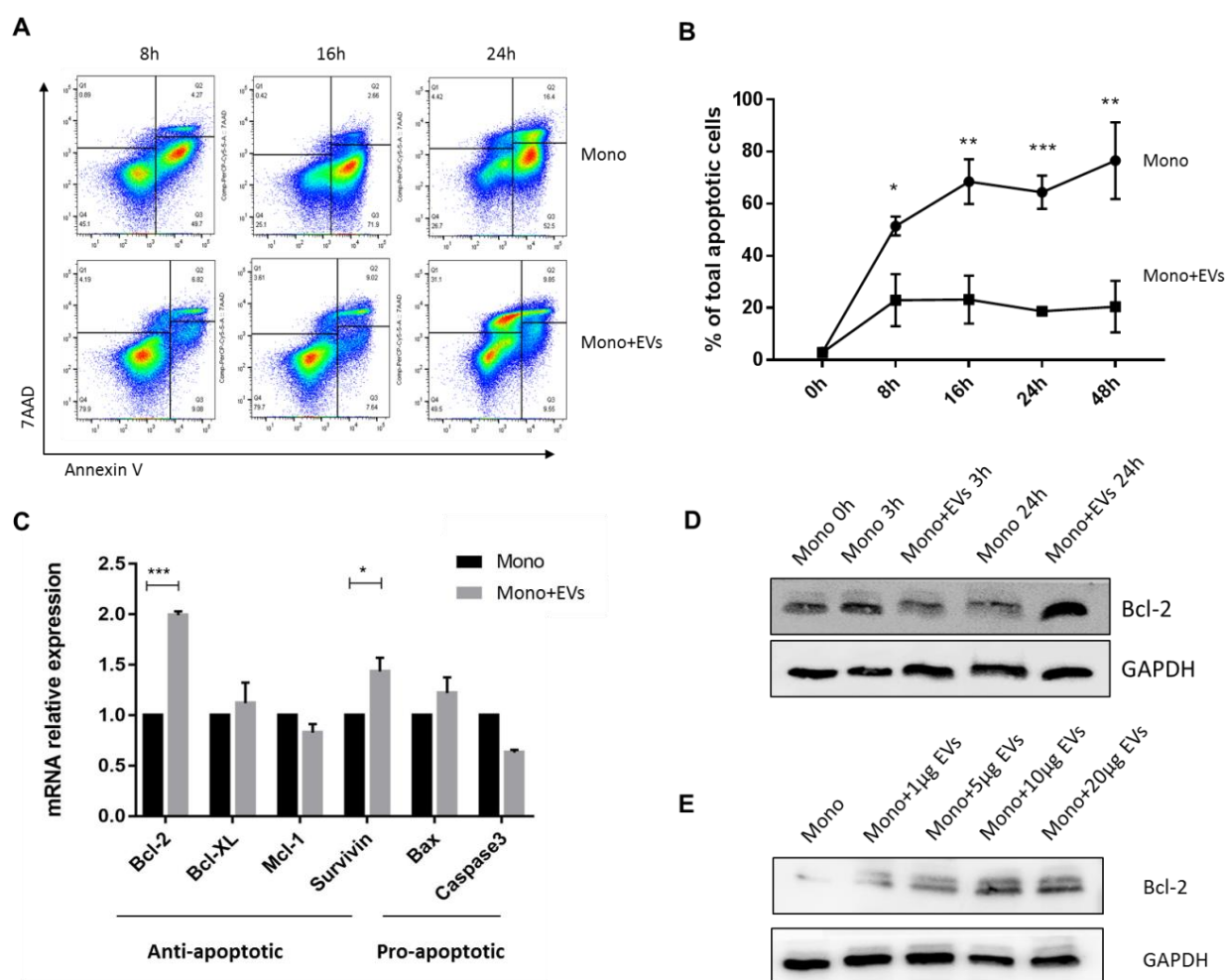


Figure 14: Effect of HT-144 EV on the apoptosis of primary monocytes. A) Representative dot-plots illustrating the apoptotic status of monocytes with or without EV stimulation. B) The percentage of apoptotic monocytes compared to the control group. C) The expression levels of anti-apoptotic genes Bcl-2, Bcl-XL, Mcl-1 and survivin as well as pro-apoptotic genes Bax and Caspase3 in monocytes with or without HT-144 EV stimulation. D) Western Blot for Bcl-2 in monocytes upon 10 μ g HT-144 EV treatment at 0h, 3h and 24h or stimulated with different concentration of HT-144 EV for 24h E). GAPDH was used as a loading control. * $p < 0.05$, ** $p < 0.01$, *** $p < 0.001$.

4.4 CD14⁺ monocytes show immunosuppressive activity upon HT-144 EV treatment

To determine the immunomodulatory effect of HT-144 EVs on circulating monocytes, 2×10^5 cells resuspended in 200 μ l of medium were pre-incubated with 15 μ g HT-144 EV in 96-well plate for 16 h followed by co-culture with T cells for 72 h. Proliferated CD8⁺ T cells were gated according to the cells without activation by CD3/CD28 Dynabeads. Gating strategy was shown in Fig. 15. CD8⁺ T cell co-cultured with monocytes without EV stimulation were used as positive control.

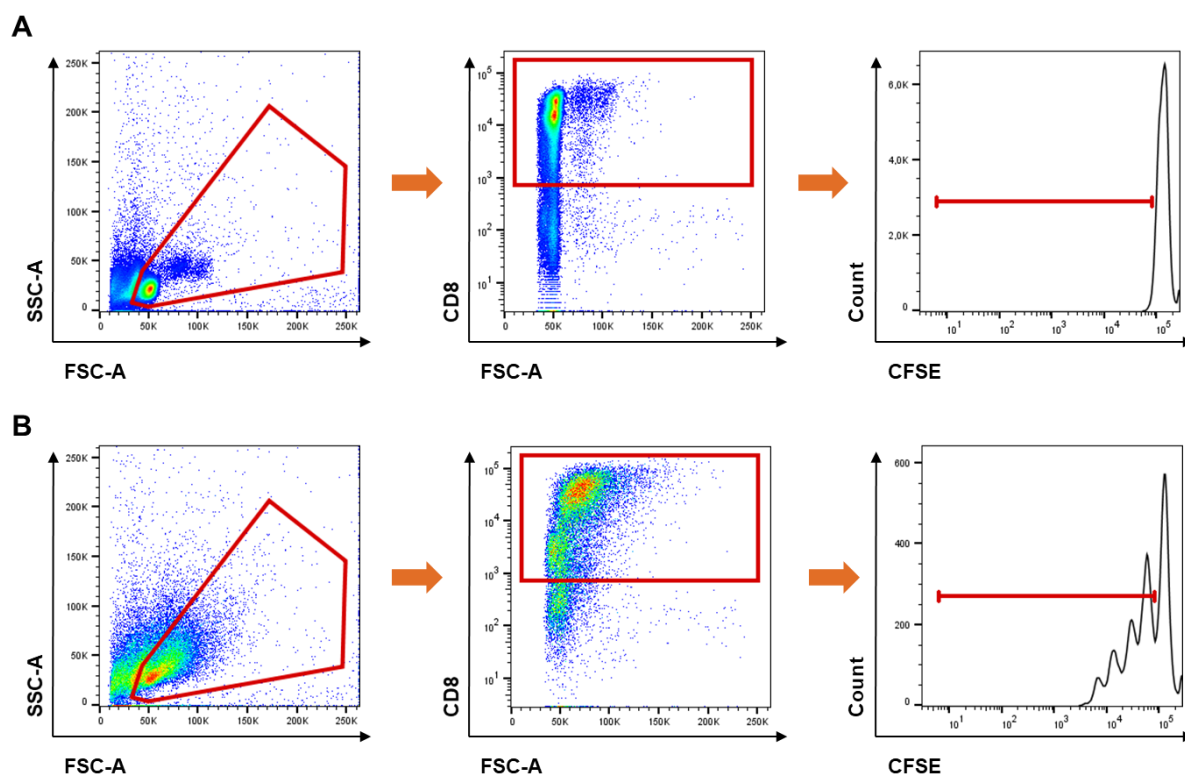


Figure 15: Gating strategy of T cell proliferation assay. Live lymphocytes were gated using the forward and side scatter characteristics to include both resting and dividing cells(left). CD8⁺ T cells were then gated from the lymphocyte gate (middle). The proliferated cells were gated according to the negative control of non-activated T cells A) and CFSE staining in activated CD8⁺ T cells showed the different generation of cells B).

We found that monocytes treated with HT-144 EVs significantly impaired CD8⁺ T cells proliferation (Fig. 16A and B) in a manner dependent on EV concentration. The inhibitory effect was also dependent on the ration between EV-treated monocytes and stimulated T cells. In parallel, the secretion of IFN- γ in the supernatant of proliferating CD8⁺ T cells were tested. The production of IFN- γ was also decreased upon the incubation of T cells with EV-treated monocytes (Fig. 16C).

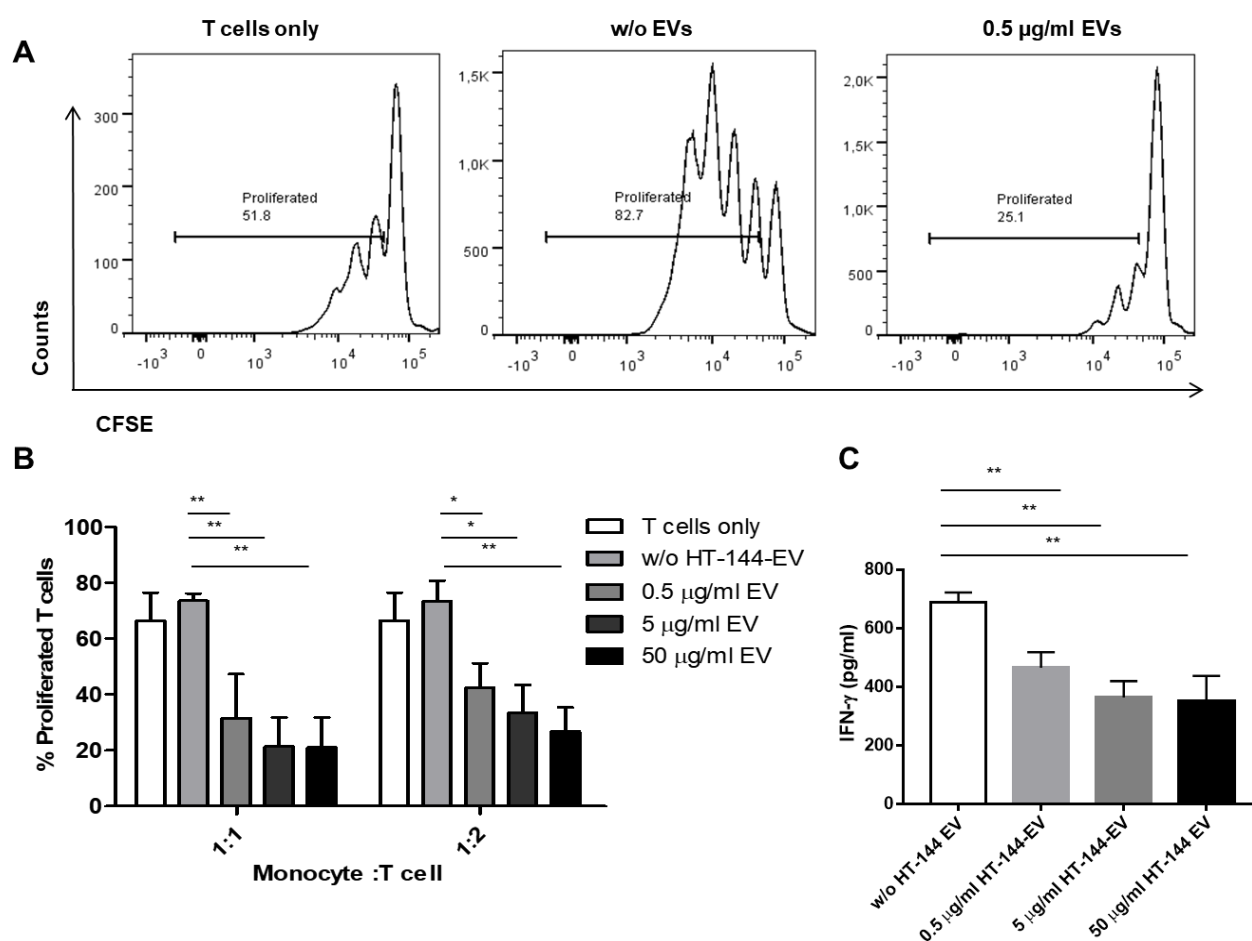


Figure 16: HT-144 EV treated monocytes inhibit CD8⁺ T cell proliferation and modulate IFN- γ production. A) Representative CFSE histograms showing the proliferation of CD8⁺ T cells alone (left), or co-cultured with monocytes (Monocytes: T cells ratio =1:1) stimulated without (middle) or with 0.1 µg HT-144 EV (right). B) Inhibition of CD8⁺ T cell proliferation by EV-treated monocytes at indicated Monocytes: T cells ratio. C) IFN- γ secretion by CD8⁺ T cell were tested by ELISA (Monocytes: T cells ratio =1:1). * $p < 0.05$, ** $p < 0.01$, *** $p < 0.001$.

4.5 HT-144 EVs upregulate PD-L1 on CD14⁺ monocytes

PD-L1 expression on MDSCs has been demonstrated to play a crucial role in mediating the immunosuppressive function on cytotoxic T cells. We thus wanted to know whether the observed mechanism of EV-mediated suppression of T cell activation involved PD-L1. First, we examined the expression of PD-L1 on CD14⁺ monocytes upon the treatment of HT-144 EV by flow cytometry. Compared to the cells treated with PBS, we observed a dramatic increase in the frequency of PD-L1⁺ monocytes and the level of PD-L1 expression measured by median fluorescence intensity (MFI) (Fig. 17 A, B and C). Furthermore, the application of EVs isolated from another melanoma cell line SK-MEL-28 revealed that the same amount of EVs (15 µg) induced a strong upregulation (Fig. 17 A-C).

To address the question whether new synthesis of PD-L1 is induced by melanoma EVs, we studied PD-L1 expression at the mRNA level. We observed more than two times higher PD-L1 mRNA expression in HT-144 EV-treated monocytes compared to cells treated with PBS (Fig. 17 D). In the SK-MEL-28 EV treated samples, the induction of PD-L1 mRNA was observed, although to a lower extent (Fig. 17 D).

To further characterize the phenotype of these immunosuppressive monocytes, we checked the expression of HLA-DR which is important to distinguish MDSCs from monocytes. We found that 6h after the addition of HT-144 EVs, monocytes showed an upregulation of HLA-DR. However, upon a longer time exposure to tumor EVs, the frequency of HLA-DR⁺ monocytes and the intensity of HLA-DR expression (measured as MFI) was decreased as compared to the monocytes treated with PBS (Fig. 17. E and F). Taken together, the upregulation of PD-L1 and down regulation of HLA-DR indicated the conversion of monocytes to MDSCs.

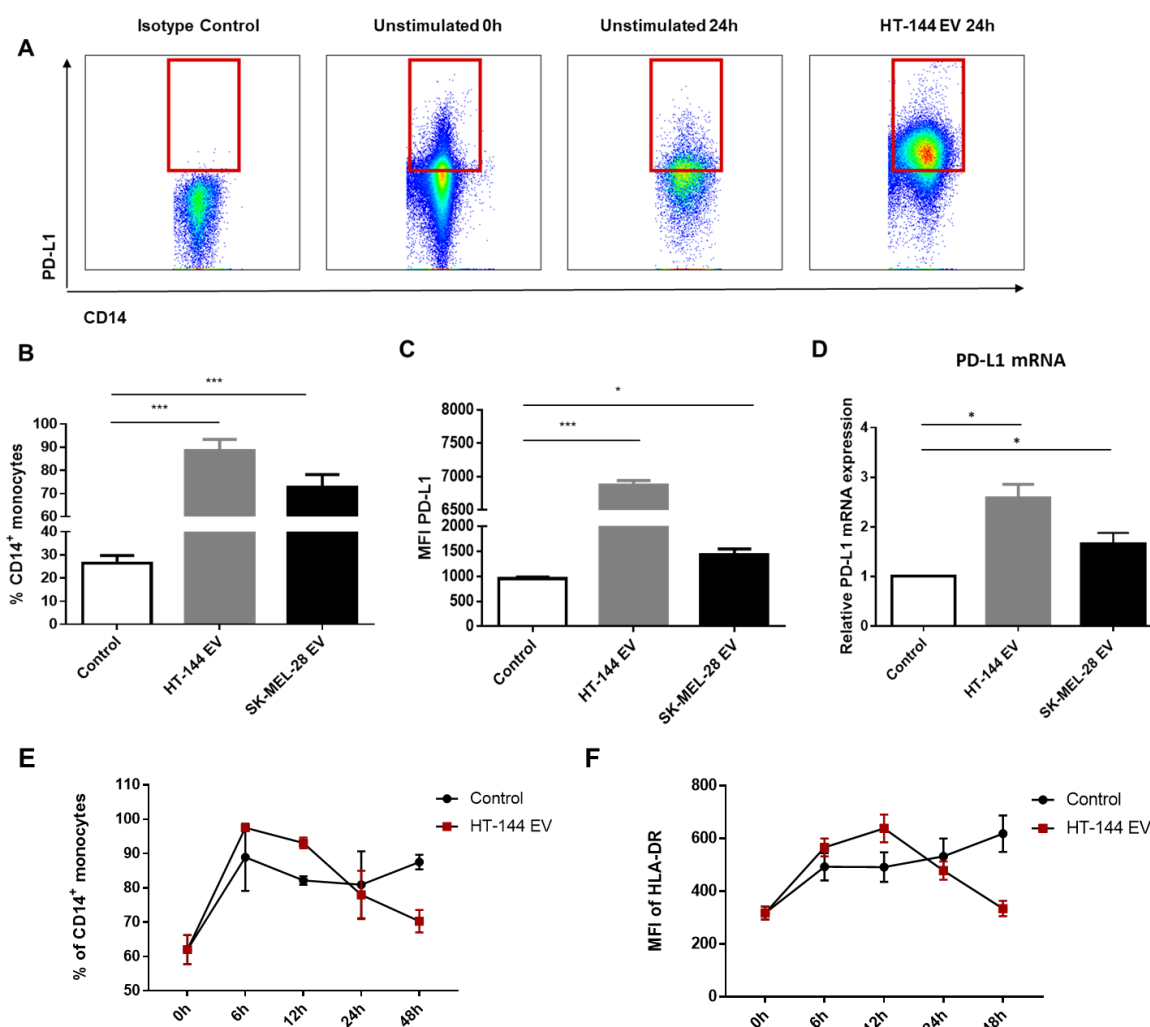


Figure 17: PD-L1 expression on monocytes upon the treatment of melanoma EV. CD14⁺ monocytes isolated from buffy coats of healthy donors were treated with EVs of melanoma cell lines HT-144 and SK-MEL-28 for 16 h. A) Representative dot plots of PD-L1 expression on monocytes with or without HT-144 EV treatment after 16 h incubation (including isotype control and unstimulated monocytes). B) The level of PD-L1 expression measured as frequency of PD-L1⁺ cells and C) median fluorescence intensity (MFI) of PD-L1 on CD14⁺ monocytes. D) The relative PD-L1 mRNA expression levels (normalized to β -actin) after the stimulation of HT-144 EVs and SK-MEL-28 EVs for 16 h in CD14⁺ monocytes were measured by RT-PCR. The level of HLA-DR was measured at different time point (n=2) as frequency (E) and MFI on CD14⁺ monocytes (F). * $p < 0.05$, ** $p < 0.01$, *** $p < 0.001$.

4.6 The involvement of NF- κ B activation in PD-L1 upregulation

As mentioned in the introduction, NF- κ B is a crucial player in regulating the expression of pro-inflammatory genes and play an important role in the anti-apoptotic effect (Lawrence, 2009; Sen and Baltimore, 2013). Therefore, we wanted to study whether tumor-derived EVs could trigger NF- κ B activation. As shown in Figure 15A, NF- κ B phosphorylation was induced by HT-144 EV in purified CD14⁺ monocytes. In order to further characterize the role of NF- κ B in the upregulation of PD-L1, a NF- κ B Activation Inhibitor VI (BOT-64) was added to monocytes prior to the treatment with HT-144 EVs. We observed that the upregulation of PD-L1 on monocytes was strongly abrogated with the application of BOT-64 measured by flow cytometry (Fig. 18B)

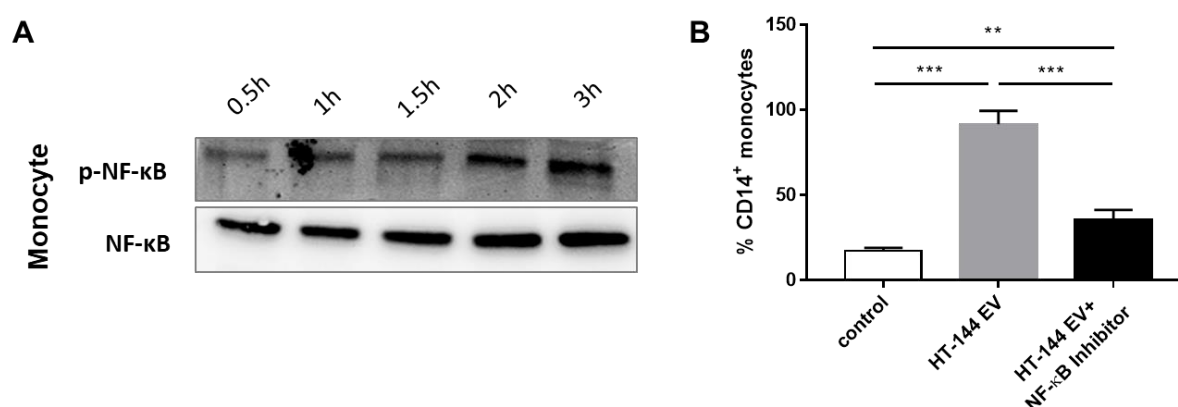


Figure 18: HT-144 EV induces NF- κ B activation in CD14⁺ monocytes. Western blot analysis was performed to assess NF- κ B activation after 0.5, 1, 1.5 and 3 h stimulation with 15 μ g/mL HT-144 EV. Total NF- κ B were used as a loading control (A). Flow cytometry was performed to measure the PD-L1 expression on HT-144 EV treated monocytes with or without prior application of NF- κ B activation inhibitor BOT-64 (B). * $p < 0.05$, ** $p < 0.01$, *** $p < 0.001$.

4.7 The upregulation of PD-L1 via TLR signaling

We then sought to determine the mechanisms triggering NF- κ B activation. Since EVs can interact with target cells through a ligand-receptor interaction and TLRs have been proposed as potential receptors for EVs (Fabbri et al., 2013; Paschon et al., 2016; Seo et al., 2016), we decided to test PD-L1 expression using HT-144 EVs as well as TLR2 agonists Pam3/CSK4 and TLR4 agonists LPS. Interestingly, PD-L1 expression was strongly induced by HT-144 EV, Pam3/CSK4 and LPS (Fig. 19A). Importantly, the effect of tumor derived EVs on monocytes for PD-L1 upregulation was at the similar level as TLR2 and TLR4 agonists. In addition, we examined the PD-L1 expression on HT-144 EV stimulated monocytes in the presence of anti-TLR2, anti-TLR4 blocking antibodies or isotype control antibodies. As shown in Fig. 19B, the treatment with anti-TLR4 blocking antibodies completely abrogated the induction of PD-L1 expression by HT-144 EVs, whereas anti-TLR2 antibodies could inhibit such induction only partially.

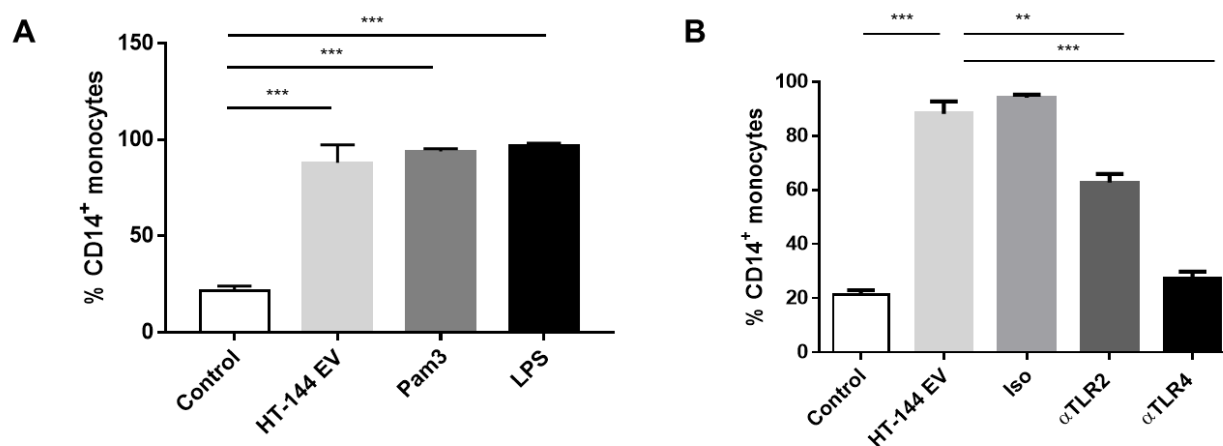


Figure 19: Involvement of TLR in the upregulation of PD-L1 on CD14⁺ monocytes. A) Monocytes were treated with HT-144 EV, TLR2 agonists Pam3/CSK4 and TLR4 agonists LPS for 16 h. PD-L1 expression was detected by flow cytometry. B) Specific blocking anti-TLR2, anti-TLR4 or IgG2a κ isotype control was added 1 h prior to the addition of HT-144 EV. Frequency of CD14⁺PD-L1⁺ cells was measured by flow cytometry. * $p < 0.05$, ** $p < 0.01$, *** $p < 0.001$.

4.8 Melanoma cells release EVs carrying HSP86

HSPs are known as TLR ligands for many years, and are abundantly detected in EVs derived from different cell types (Reddy et al., 2018; Shi et al., 2018; Zhang et al., 2017). Based on this, we decided to check the expression and the possible role of HSP86 (HSP90 α) in our EV preparations. As shown in Fig. 20A, both HT-144 and HT-144 EV strongly expressed HSP86. However, SK-MEL-28 melanoma cells expressed lower level of HSP86 compared to HT-144 cells, and the expression of HSP86 was barely detected on SK-MEL-28 EVs by Western Blot. The expression of HSP86 on EVs of HT-144 and SK-MEL-28 was also confirmed by flow cytometry by coupling of EVs to latex beads. In addition, both melanoma cell lines and EVs derived from them displayed a very low expression of PD-L1 (Fig. 20B). Interestingly, as shown previously in the chapter 4.5, we observed a higher potential of HT-144 EVs to upregulate PD-L1 expression on monocytes than that of SK-MEL-28 EVs, suggesting the importance of the level of HSP86 expression for the upregulation of PD-L1.

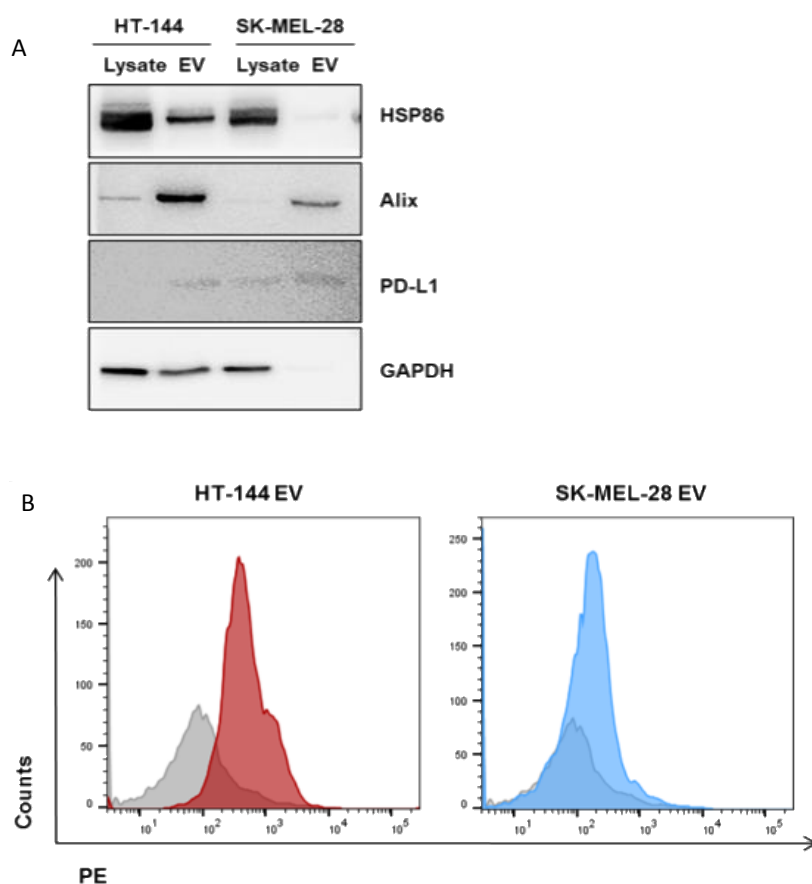


Figure 20: Expression of HSP86 and PD-L1 on EVs from melanoma cell lines. A) Western Blot analysis was performed to measure the expression of HSP86 and PD-L1 on HT-144 and SK-MEL-28 melanoma cell lines as well as on EVs derived from these lines. GAPDH and Alix were used as controls for cells and EVs respectively. B) Flow cytometry was performed to measure the HSP86 expression on HT-144 EV (red) and SK-MEL-28 EV (blue). Grey line indicates the staining with the secondary antibody only (control). * $p < 0.05$, ** $p < 0.01$, *** $p < 0.001$.

4.9 HSP86 knockdown results in the impairment of PD-L1 upregulation

To further analyze the impact of HSP86⁺ melanoma EVs on monocytes and its immunosuppressive activity, a stable knockdown of HSP86 via shRNA targeting HSP90AA1 was used. Two clones were tested, showing HSP86 depletion in HT-144 cells (Fig. 21A). Clone 1 was chosen for the isolation of EVs (shHSP86 HT-144 EV). Expression of HSP86 on EVs isolated from both HT-144 cells transfected with control

shRNA (shSCR HT-144 cells) and shHSP HT-144 cells were measured. A decreased expression of HSP86 on shHSP86 HT-144 EV was observed which indicated the successful knockdown of HSP86 on tumor cells (Fig. 21B). Then, we examined the upregulation of PD-L1 on monocytes treated with shHSP86 HT-144 EV or shSCR HT-144 EV. As expected, the knockdown of HSP86 resulted in a decreased ability of EVs to upregulate the frequency of PD-L1⁺ monocytes and the intensity of PD-L1 expression (Fig. 21A and B).

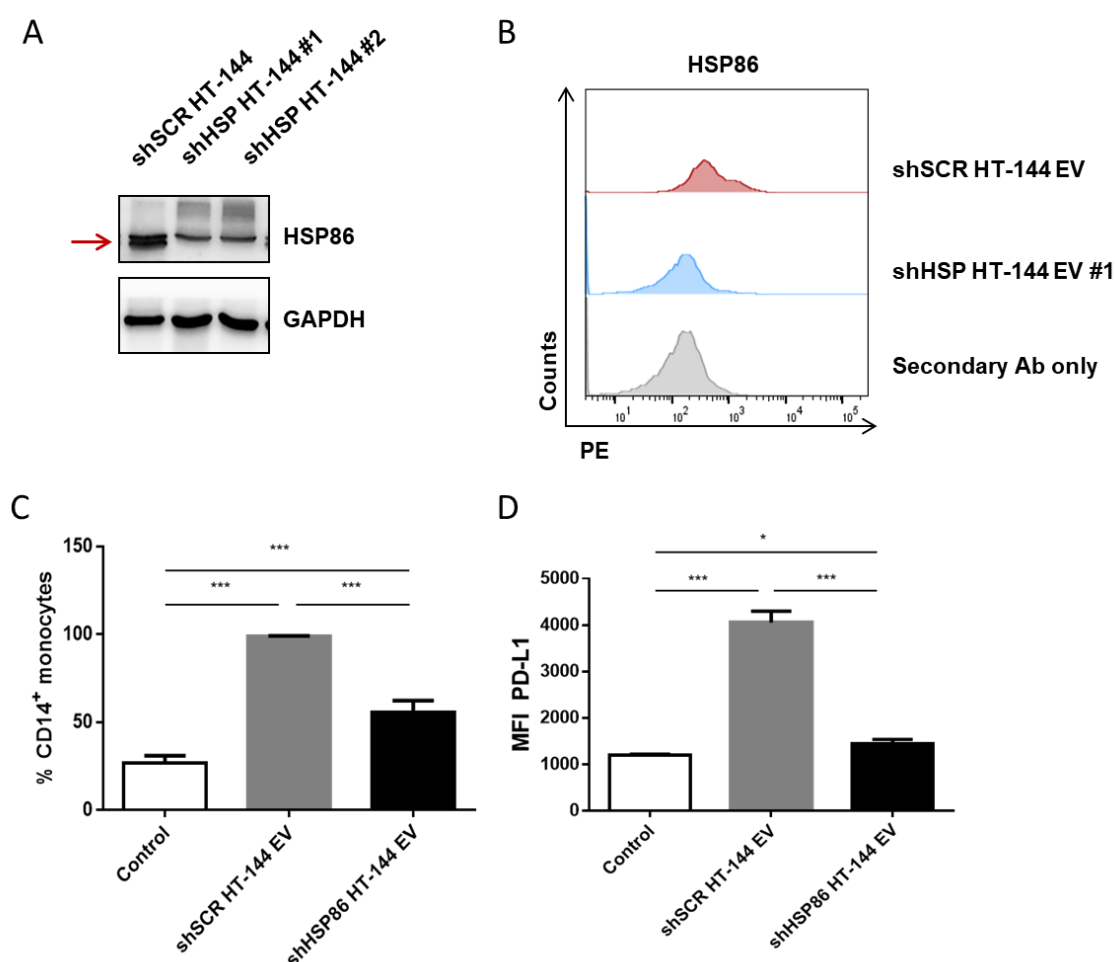


Figure 21: HSP86 is required for PD-L1 upregulation. A) HSP86 expression was measured in HT-144 cells transfected with HSP86 shRNA (shHSP86 HT-144) or control shRNA (shSCR HT-144) by Western Blot. B) Flow cytometry was used to validate the expression of HSP86 in shHSP86 HT-144 EV and shSCR HT-144 EV. Secondary antibody

was used as a control. PD-L1 expression was measured in CD14⁺ monocytes upon the treatment with shHSP86 HT-144 EV, shSCR HT-144 or PBS. PD-L1 expression was shown as the percentage of CD14⁺PD-L1⁺ monocytes among total CD14⁺ monocytes (C) and as the level of PD-1 expression by MFI (D). * $p < 0.05$, ** $p < 0.01$, *** $p < 0.001$.

4.10 Functional inhibition of CD8⁺ T cells by HSP86⁺ melanoma EVs

To evaluate whether the immunosuppressive activity of monocytes stimulated by melanoma EVs was mainly dependent on HSP86, T cell proliferation assay was performed. 2×10^5 CD14⁺ monocytes were pre-incubated with 15 μ g shHSP86 HT-144 EV or shSCR HT-144 EV in 96-well plate for 16 h. After washing out EVs, monocytes were incubated with activated T cells. We observed a significant impairment of CD8⁺ T cells proliferation upon the treatment of monocytes with shSCR HT-144 EV. However, the inhibitory effect was abrogated when the shHSP86 HT-144 EV was applied (Fig. 22A and B). Moreover, decreased production of IFN- γ was detected in CD8⁺T cells cocultured with shSCR HT-144 EV treated monocytes, whereas this decrease was not shown in CD8⁺T cells cocultured with monocytes treated with EVs expressing no HSP86 (Fig. 22C).

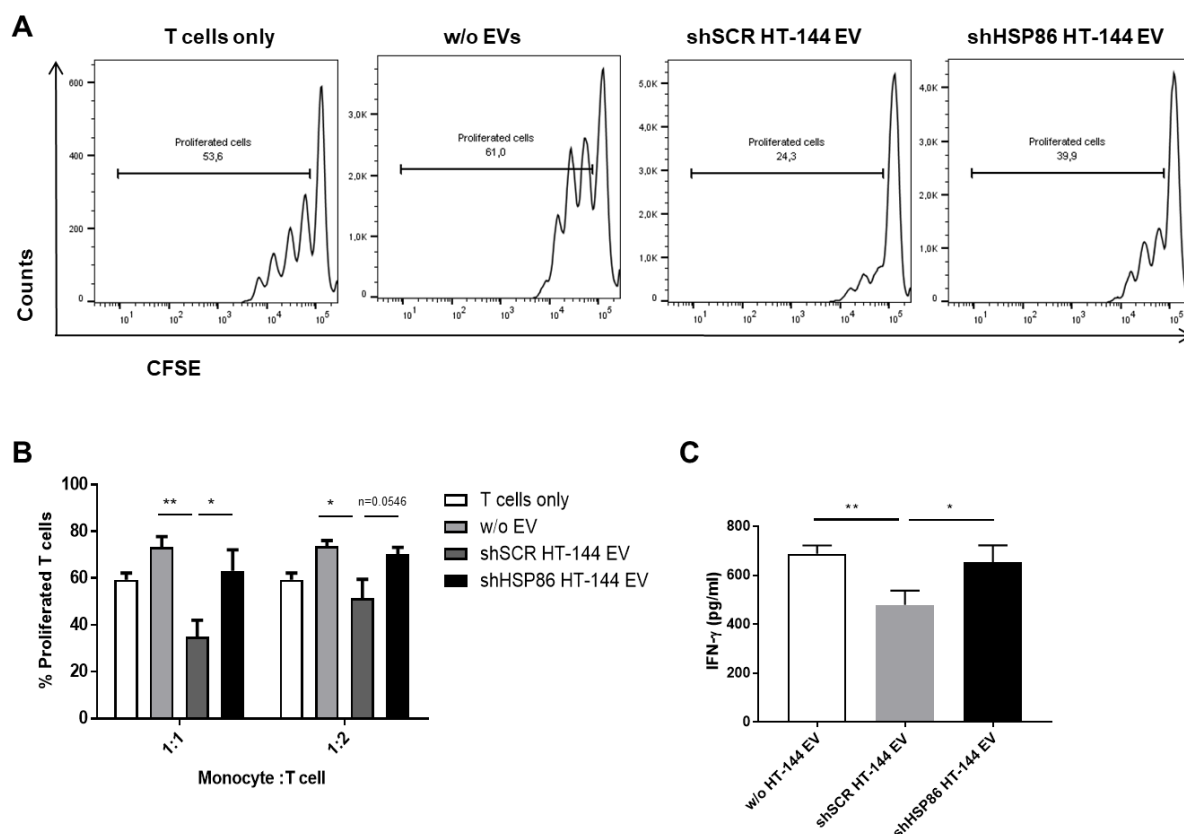


Figure 22: HSP86 on HT-144 EV play a crucial role in acquiring the immunosuppressive activity by monocytes. A) Representative CFSE histograms showing the proliferation of CD8⁺ T cells alone (left), CD8⁺ T cells cocultured with non-treated CD14⁺ monocytes or monocytes treated with shSCR HT-144 EV and shHSP86 HT-144 EV respectively. B) Inhibition of CD8⁺ T cell proliferation by EV-treated monocytes at indicated monocytes: T cells ratio. C) IFN- γ secretion by CD8⁺ T cells was tested by ELISA (monocytes: T cells ratio = 1:1). * $p < 0.05$, ** $p < 0.01$, *** $p < 0.001$.

4.11 Circulating EVs from melanoma patients upregulate PD-L1 and show anti-apoptotic effect on monocytes

To address the question whether EVs circulating in melanoma patients could induce the same effect on normal CD14⁺ monocytes as EVs isolated from melanoma cell lines, we purified the EVs from plasma of stage IV melanoma patients. Apoptotic assay and PD-L1 expression on monocytes were tested after their coculture with

EVs. We found a strong inhibition of monocyte apoptosis upon the treatment with plasma EVs from stage IV melanoma patients as compared to EV-depleted plasma (containing only soluble factors) or PBS treated monocytes (control). In addition, we observed an increase in the frequency of PD-L1⁺ monocytes upon the treatment with plasma EVs as compared to these values in monocytes incubated with EV-depleted plasma or with PBS (Fig. 23B). The level of PD-L1 expression under these conditions was also significantly elevated (Fig. 23C).

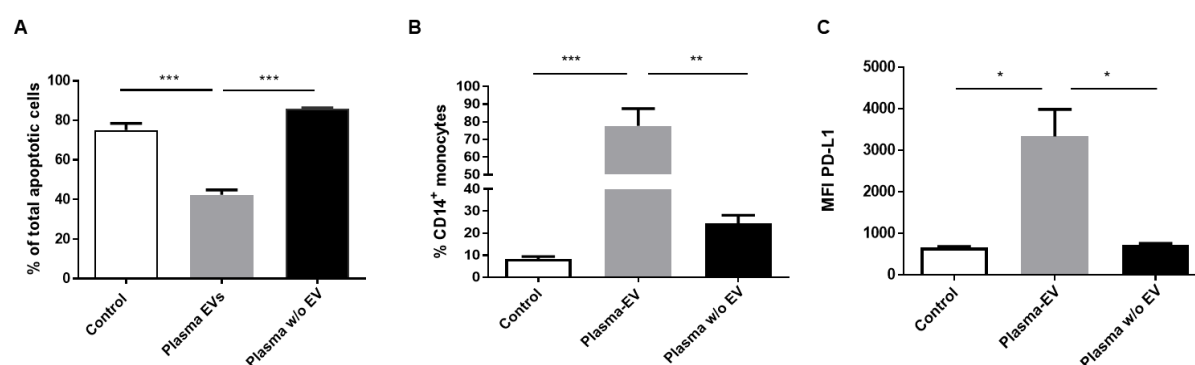


Figure 23: Effects of EV from plasma of melanoma patients on normal monocytes. CD14⁺ monocytes were incubated with EV from plasma of untreated stage IV melanoma patients or with plasma of these patients without EV. 7AAD and Annexin V were used for staining of apoptotic cells (A). PD-L1 protein expression was presented as the percentage of PD-L1⁺CD14⁺ cells within total monocytes (B) and as the MFI of PD-L1 (mean \pm SEM; n=6) (C). * $p < 0.05$, ** $p < 0.01$, *** $p < 0.001$.

4.12 HSP86 expression and monocyte modulation by EVs from melanoma patients undergoing anti-PD-1 therapy

EVs or their content (proteins or miRNAs) in circulation of patients have been found to show promising value for the prediction of clinical response to various therapies of melanoma (Fattore et al., 2015; Huber et al., 2018; Tucci et al., 2018). Here we investigated the content of HSP in EVs from melanoma patients that responded

differently to anti-PD-1 therapy. The level of HSP86 on circulating EVs in non-responders was much higher than that on EVs from responders (Fig.24 A). However, HSP70, which was previously reported to be widely expressed on EVs under various pathological conditions, showed very low expression and no difference in responders and non-responders (Fig. 24A). Moreover, the immunosuppressive capacity of monocytes stimulated by those EVs was tested. A stronger inhibition of CD8⁺ T cell proliferation was observed for monocytes treated with EVs isolated from non-responders as compared to those treated with EVs from responder or with PBS (Fig. 24B). Of note, responder EV-treated monocytes showed no, or only marginal difference as compared to PBS treated control (Fig. 24B).

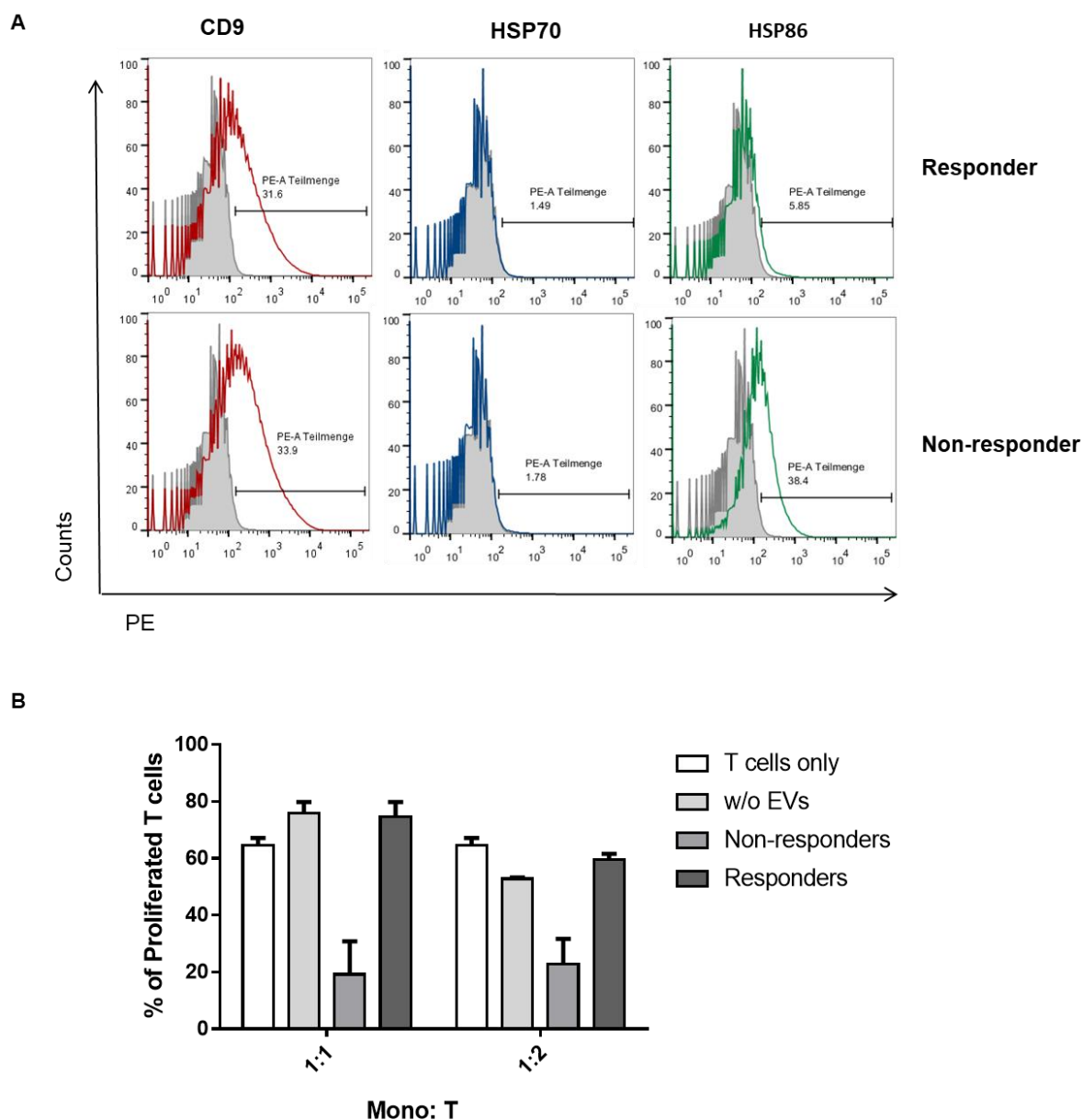


Figure 24: HSP86 expression on EVs and their capacity to stimulate immunosuppressive activity on monocytes. EVs were isolated from responders (n=3) and non-responders (n=2) of melanoma patients undergoing anti-PD-1 therapy. HSP86 expression was tested in those EVs by flow cytometry and representative histograms were shown in (A). Secondary antibody was used as a control. B) CD14⁺ monocytes were incubated with EV from responders and non-responders or with PBS. Inhibition of CD8⁺ T cell proliferation by EV-treated monocytes at indicated monocytes: T cells ratio.

4.13 Effects of EVs from melanoma patients undergoing anti-PD-1 therapy

Based on our previous findings, HT-144 EVs with higher HSP86 expressions had a higher capacity of PD-L1 upregulation. Here, we tested whether EVs from responders and non-responders that differently expressed HSP86 could induce different PD-L1 upregulation on monocytes. Moreover, another marker HLA-DR was also checked in parallel to prove the conversion of monocytes into MDSC-like cells. As expected, EVs from non-responders can dramatically upregulate PD-L1 and showed 20-30% inhibition of HLA-DR on monocytes after 16 h incubation, whereas those from responder failed to induce such changes in the expression of PD-L1 and HLA-DR.

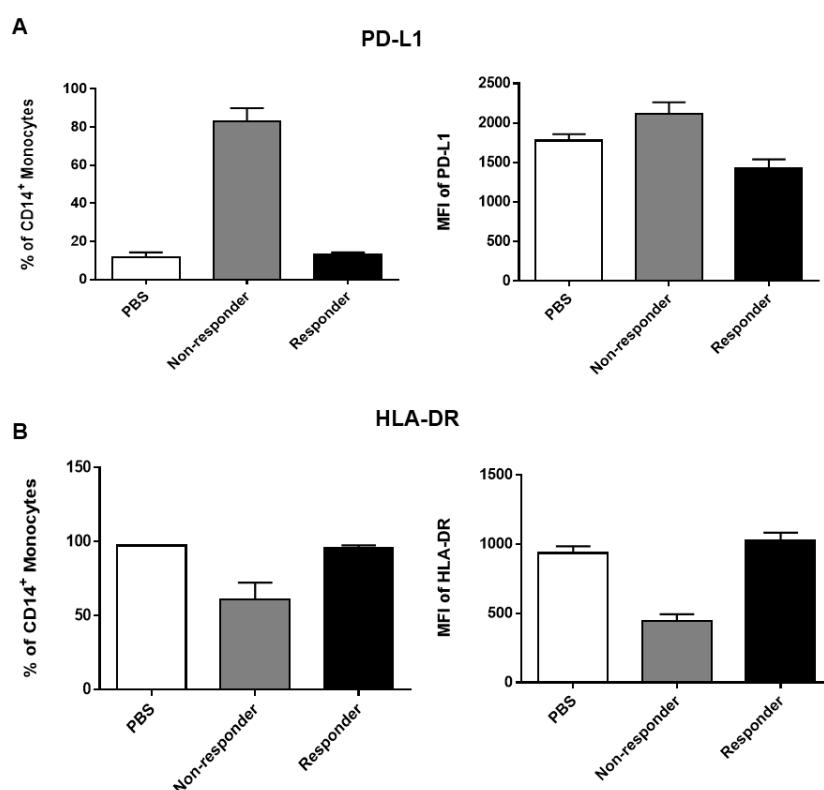


Figure 25: PD-L1 and HLA-DR expression on monocytes upon the treatment of responder and non-responder EVs. CD14⁺ monocytes isolated from buffy coats of healthy donors were treated with EVs from responders (n=3) and non-responders (n=2) for 16 h. A) The level of PD-L1 expression measured as the frequency of PD-L1⁺ cells (left) and MFI of

PD-L1 on CD14⁺ monocytes (right). B) The level of HLA-DR was measured at the same time point as the frequency (left) and MFI (right). * $p < 0.05$, ** $p < 0.01$, *** $p < 0.001$.

4.14 PD-L1 expression on circulating monocytes predicts the response to anti-PD-1 immunotherapy

Next, we used cryopreserved PBMCs isolated from the peripheral blood of 30 patients with metastatic melanoma before and during therapy to check the association of PD-L1 expression on classical CD14⁺ monocytes with responsiveness to anti-PD-1 immunotherapy.

4.14.1 Clinical characteristics of melanoma patients

The patients' mean age was 66.53 years, and 63.3% were female. 22 patients (73.33%) were treated with pembrolizumab and 8 patients (26.67%) with Nivolumab or Ipilimumab (Table 3). More than half of the patients had lymph node (80.0%) and lung (53.33%) metastasis. 10% were classified as stage III by the American Joint Committee on Cancer (AJCC) staging system and 90% were AJCC IV. None of the patients had received immune checkpoint inhibition immunotherapy before. Table 4 provides information on the clinical responses. Patients showing complete (3.03%) and partial responses (24.24%) were defined as responders, whereas those with stable (9.09%) and progressive disease (54.55%) were defined as non-responders.

Table 3. Baseline characteristic	
Characteristics	Values
Total number of patients	30
Age, years, mean (min–max)	66.53 (15–82)
Gender, n (%)	
Female	19(63.33)
Male	11(36.67)
AJCC stage, n (%)	
IIIB+C	3(10.00)
IV	27 (90.00)
Treatment, n (%)	
Pembro	22(73.33)
Nivo/Ipi	8(26.67)
Previous treatment, n (%)	
target therapy	11(36,67)
immune therapy	11(36,67)
Other therapy	12(40.00)
Metastasis,, n (%)	
lymph nodes	24(80.00)
lung	16(53.33)
Liver	11(36,67)
Brain	10(33.33)

Table 4. Overall response	
CR	1(3.03)
PR	8(24.24)
SD	3(9.09)
PD	18(54.55)

4.14.2 PD-L1 expression on circulating monocytes is associated with anti-PD-1 response

Classical monocyte markers CD14, CD11b, HLA-DR were used to define monocytes by flow cytometry (Fig 26).

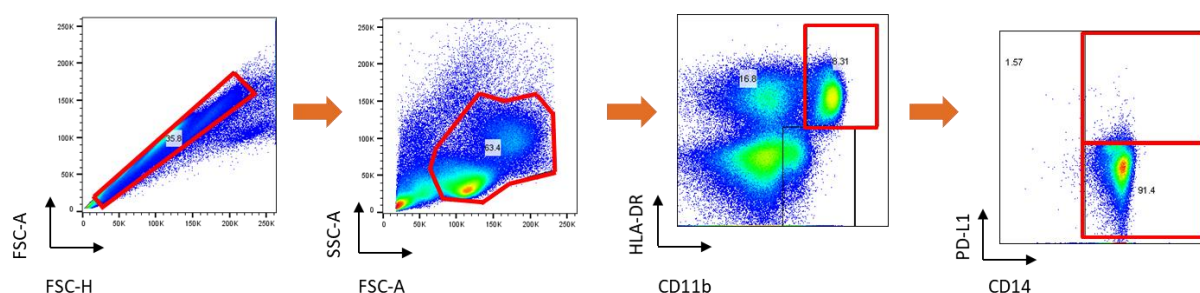


Figure 26: Gating strategy of PD-L1 on classical monocytes. Cell gated for live singlets using FSC-A and -H, live singlets gated for lymphocytes using FSC and SSC. Classical monocytes were further gated as CD11b⁺, HLA-DR⁺ and CD14⁺. PD-L1 expression was gated according to FMO control.

In responders, the frequency of PD-L1⁺ classical monocytes were significantly decreased after the first injection of anti-PD-1 antibodies as compared to the basal level. In contrast, the percentage of these cells in non-responders showed no changes (Fig. 27A). Of note, the frequency of PD-L1⁺ monocytes after the first injection in non-responders was significantly higher than in responders. However, we did not observe any difference before the start of the therapy (Fig. 27A). Interestingly the intensity of PD-L1 expression measured as MFI displayed no differences (Fig. 27B). Moreover, to assess the influence of the frequency of PD-L1⁺ classical monocytes after the first injection of anti-PD-1 antibodies on the survival, we calculated the optimal cutoff point (17.495%), which discriminated between high and low PD-L1 expression. It was found that patients with low frequency of these monocytes showed significantly better overall as well as progression free survival

(Fig. 27 C and D), indicating a role of this marker in predicting response to such therapy.

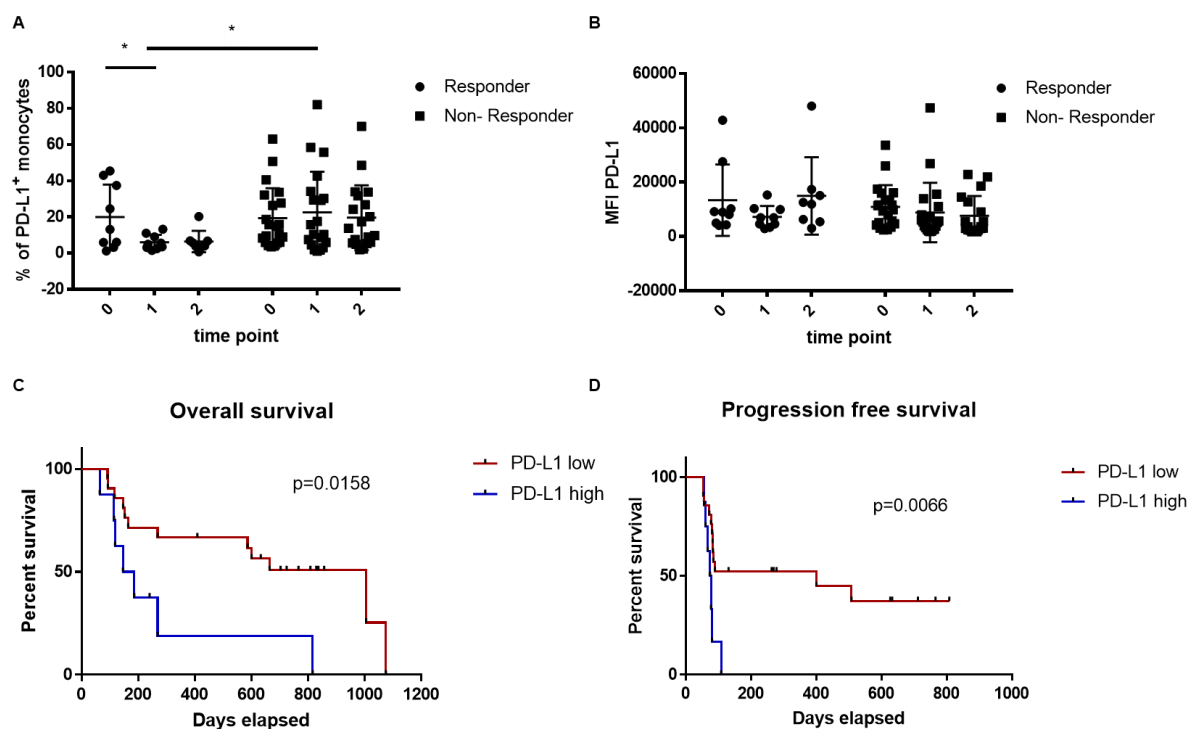


Figure 27: PD-L1 expression on classical monocytes from patients treated with anti-PD-1 antibodies and its effect on their overall and progression-free survival. PBMCs obtained from the peripheral blood of 30 melanoma patients (point 0 - prior the treatment; point 1 - after the first infusion of anti-PD1 antibodies; point 2 - after the second infusion) were assessed by flow cytometry. The frequency of PD-L1⁺ classical monocytes (A) and MFI of PD-L1 (B) in patients responding or not responding to the treatment Cs. Overall (C) and progression-free (D) survival of melanoma patients displaying high or low expression of PD-L1 on monocytes after the first infusion of anti-PD-1 antibodies. * $p < 0.05$, ** $p < 0.01$, *** $p < 0.001$.

5 DISCUSSION

EVs secreted by tumor cells are emerging as critical mediators in tumor progression and metastasis. They are shown to express oncogenic molecules and to interact with cancer cells (Al-Nedawi et al., 2008; Keller et al., 2009). Moreover, they were found to modulate the immune system and promote the formation of immunosuppressive microenvironment via the interaction with myeloid cells and lymphocytes (Clayton et al., 2008; Gross et al., 2012; Peinado et al., 2012; Wilcox and Hirshkowitz, 2009). Malignant melanoma is known as a highly immunogenic tumor, and the unsatisfactory results of the immunotherapeutic strategies are often due to the enrichment of immunosuppressive regulatory leukocytes, especially of MDSCs (Holmgaard et al., 2015; Mandruzzato et al., 2009; Meyer et al., 2011, 2014; Nelson and Guyer, 2013; Umansky et al., 2014). PD-L1 expression on MDSCs has been characterized to be an important mediator of their immunosuppressive activity to T cells (Noman et al., 2014; Youn Je-In, Nagaraj Srinivas, Collazo Michelle, 2009). To date, the underlying molecular mechanism of the link between tumor-derived EVs and PD-L1 upregulation on M-MDSC remains poorly understood.

5.1 EVs from melanoma cell lines and plasma of patients show typical EV characterization

Various techniques have been used for EV isolation, for example differential (ultra) centrifugation, density gradients, polymer-based precipitation, microfiltration and size-exclusion-based methods (Gardiner et al., 2016). To date, standardized purification methods for EV subsets isolation are not well established because EVs are heterogeneous in size, origin and molecular constituents. Moreover, subsets of EVs are overlapping in phenotype and size (Théry et al., 2018). Purification of EVs

from body fluids is more difficult since lipoproteins, DNA, RNA and protein aggregates are potential factors to contaminate EV fraction (Zaborowski et al., 2015). Besides, anticoagulants, temperature during isolation, freeze–thaw cycles, storage conditions and so on have been shown to influence the usability, vesicle purity, yield and components of the isolated EVs (Szatanek et al., 2015). In our study, we isolated EVs from melanoma cell lines HT-144 and SK-MEL-28 as well as human plasma. Using the established protocol (Lobb et al., 2015), we could show that our EV preparations fulfill the minimal requirements for EV as characterized by NTA and Western Blot. NTA analysis indicated that purified EVs from cell supernatants were mainly small particles with a diameter of approximately 100-120 nm and plasma EVs with peaks showed up at 140-160 nm. Besides, Western Blot analysis showed the expression of EV surface marker CD9, CD81 as well as the intraluminal marker ALIX. By checking the negative expression of calreticulin, a specific marker of the endoplasmic reticulum, the purity of isolated EV fraction was confirmed since the proteins of intracellular compartments and cell debris were excluded as possible contamination factors (Van Deun et al., 2014). Of note, the marker of parental cells gp100 was also detected in cell line-derived EVs. However, it was undetectable in plasma EVs from melanoma patients by Western Blot. This could be to the insufficient sensitivity of the detection methods, or to the low quantity of tumor-derived EVs in the mixed EV population in circulation. Similar observation has been recently reported, showing that a minor portion of plasma EVs (less than 1%) derives directly from melanoma tissue; melanoma markers could be clearly detected on melanoma EVs isolated from primary melanoma cell culture but not from plasma of patients (Koliha et al., 2016).

5.2 Melanoma EVs promote survival and migration ability of monocytes

Apoptosis is a physiological form of cell suicide, and extracellular microenvironment plays a crucial role in regulating apoptosis (Mangan et al., 1993). Our data provide evidence that CD14⁺ monocytes had a diminished apoptosis upon EV stimulation, which is in accordance with the previous findings (Valenti et al., 2006). In addition, we found that anti-apoptotic genes such as Bcl-2 and survivin are upregulated. Importantly, the expression of Bcl-2 protein was enhanced by HT-144 EVs in a time- and dose-dependent manner. Interestingly, previous publications showed that EVs purified from melanoma and colorectal carcinoma can induce FasL- or TRAIL-mediated apoptosis in activated anti-tumor cytotoxic T and NK cells (Andreola et al., 2002; Huber et al., 2005). It seems that tumor-derived EVs have different effect on apoptosis depending on the type of their target cells.

Migration of monocytes from the bloodstream to the tumor lesion is required for routine immunological surveillance of tissues and their entry into inflamed sites (Parihar et al., 2010) (ref.). We, therefore, evaluated the migration ability of monocytes 3 h after the exposure to EVs. CD14⁺ monocytes showed enhanced migration in Boyden chamber assays in a dose-dependent manner. It has been reported that tumor-derived EVs could enhance also the migration of fibroblasts and further promote pre-metastatic niche formation (Becker et al., 2016). In addition, an enhanced migratory capacity was observed for normal human astrocytes stimulated with glioblastoma multiforme-derived EVs leading to enhanced cytokine production, which promote tumor growth (Oushy et al., 2018). Taken together, tumor derived EVs are able to induce the migratory behavior of immune cells or stroma cells promoting thereby their pro-tumor activity.

5.3 The change of phenotype and induction of immunosuppressive activity of monocytes by tumor-derived EVs

Minimal phenotypic and functional criteria for classifying MDSCs have been recently suggested (Bronte et al., 2016). Although the activity of different effector cells like B cells (Lelis et al., 2017; Wang et al., 2018) and NK cells (Lindau et al., 2013) can be influenced by immune suppressor cells, inhibition of T cells is the current 'gold' standard to evaluate immunosuppressive function. We asked whether HT-144 EVs could convert monocytes into immunosuppressive cells and inhibit CD8⁺ T cells activated with CD3/CD28 antibodies. A significant decrease of proliferating CD8⁺ T cells and IFN- γ secretion was observed when T cells were co-cultured with monocytes previously stimulated with HT-144 EVs. Monocytes without EV stimulation showed no inhibition of T cells as well as the production of IFN- γ . Previous publications have shown that tumor-derived EVs could have a direct influence on T cells, for example inducing apoptosis of activated CD8⁺ effector T cells in vitro (Wilcox and Hirshkowitz, 2009). To get rid of the direct effect of EVs on T cells, we washed out the EVs from the cultured monocytes after overnight incubation. These findings demonstrate that melanoma EVs suppress T proliferation and activity.

Moreover, the phenotype of stimulated monocytes was also tested. As one of the most important inhibitory checkpoint molecules, PD-L1 has been supposed to play a crucial role in suppressing the immune system, especially T cells under pathological conditions. A dramatic increase of PD-L1 protein on the surface of monocytes was observed. Interestingly, new PD-L1 mRNA synthesis was also seen in monocytes stimulated with EVs derived from two different melanoma cell lines. For further characterizing the conversion of monocytes into M-MDSCs, the expression of another important molecule, HLA-DR, was evaluated. We observed a slight

upregulation of HLA-DR on monocyte after 24 h followed by its downregulation after a longer exposure (48 h). Treatment with plasma-derived EVs also triggered similar alterations in PD-L1 and HLA-DR expression, resulting in CD14⁺PD-L1⁺HLA-DR^{low} cells, a phenotype typical for M-MDSCs.

5.4 PD-L1 upregulation on monocytes by tumor-derived EVs is dependent on Toll-like receptor signaling pathway

Next, we wanted to investigate the signaling pathway involved in PD-L1 upregulation. Various factors have been previously studied that regulated PD-L1 expression on immune and stroma cells (Sun et al., 2018). Among them, interferons were shown to stimulate the expression of PD-L1. Alternatively, LPS or miRNA that bind to the 3' UTR of the PD-L1 mRNA were also reported to control PD-L1 expression (Gong et al., 2009, 2010; Hawn and Underhill, 2005; Lu et al., 2008; Sun et al., 2018) . Importantly, inflammatory signaling has been shown to be involved in the upregulation of PD-L1 gene (Sun et al., 2018). In our study, we observed that PD-L1 can be highly upregulated on the surface of normal monocytes upon the stimulation of the TLR2 agonist Pam3/CSK4 and the TLR4 agonist LPS. Surprisingly, the effect of tumor-derived EVs on PD-L1 upregulation on monocytes was almost as strong as those agonists. Using TLR blocking antibodies, we could confirm the involvement of TLR signaling, especially TLR4, in controlling PD-L1 expression by tumor-derived EVs. Previous study showed that bone marrow progenitor cells from mice could be induced by LPS to develop into MDSC cells, both in vivo and in vitro, which also strongly proved the importance of TLR4 signaling in the MDSC induction (Tu et al., 2008).

Huber et al. (2018) have recently described that the conversion of monocyte into MDSCs was mediated by tumor-derived miRNAs. It was further indicated that the miR signature (miR-146a, miR-100, miR-125b, and miR-155) carried by melanoma EVs was associated with resistance to immune checkpoint inhibitors in melanoma patients (Huber et al., 2018). However, miRNA-155 was also shown to be strongly upregulated upon IFN- γ and TNF- α treatment in endothelial cells and fibroblasts (Yee et al., 2017). miRNA-155 could bind to PD-L1 3'-UTR and suppress the expression of PD-L1 miRNA-155 induction via TNF- α and IFN- γ suppresses expression of PD-L1 in human primary cells (Yee et al., 2017). Moreover, noncoding Y RNA hY4 may serve as a driver for PD-L1 upregulation upon the treatment with exosomes from plasma of CLL patients which involves the TLR (Haderk et al., 2017). Our finding represented one of the likely mechanisms involved in immunosuppression mediated by EV. However, more TLR signaling pathways should be further investigated.

5.5 Inflammatory pathway is induced in circulation monocytes by tumor-derived EV

Monocyte activation is controlled by different transcription factors. Among them, NF- κ B was shown to be crucial in regulating inflammatory gene expression as well as the accumulation and function of MDSC, mainly M-MDSC (Condamine and Gabrilovich, 2011). Moreover, TLR family plays a prominent role in NF- κ B activation (Condamine and Gabrilovich, 2011). In our study, an increase of NF- κ B activity was observed upon tumor-derived EV stimulation. Besides, the observed upregulation of pro-inflammatory (like IL-6, IL-1 β , TNF- α and CCL-2) and anti-inflammatory factors IL-10 was in line with the induction of NF- κ B. Moreover, the application of NF- κ B inhibitor led to partial abrogation of the PD-L1 upregulation.

In addition, NF- κ B is also known to be a key regulator of apoptosis (Fan et al., 2008). It was found that the pro- or anti-apoptotic function of NF- κ B was determined by the nature of the apoptotic stimulus (Kaltschmidt et al., 2000). Here, we provided evidences that HT-144 EVs could deliver an anti-apoptotic stimulus on circulating monocytes that involved NF- κ B activation.

5.6 HSP86 as major player on EVs from melanoma cell lines and patients for PD-L1 upregulation and immunosuppression

Given the results showing that TLR signaling especially TLR4 was highly involved in the upregulation of PD-L1 on monocytes by HT-144 EVs, we addressed the question about the possible ligand for TLR4 signaling activation. It is well known that HSP families are widely expressed on EVs (Maas et al., 2016). Moreover, HSPs like HSP27, HSP70, HSP90, HSP110 can interact with TLRs (Asea A, 2008; Higashikuni et al., 2013; Hutchinson et al., 2009; Jin et al., 2014). Interestingly, it has been recently demonstrated that HSP90 inhibitors are promising candidates for combined immunotherapy of melanoma (Mbofung et al., 2017). Through a screen of 850 bioactive compounds, HSP90 inhibitors 17-DMAG, BIIB021 and 17-AAG showed increased sensitivity of human melanoma cells to T cell-mediated killing. Moreover, in vivo experiments also indicated that response to anti-CTLA4 or anti-PD1 therapy was enhanced with the application of HSP inhibitor ganetespib (Mbofung et al., 2017). On the other hand, in the study of Chalmin et al. (2010), HSP72 on tumor-derived exosomes was demonstrated as the main driver of the suppressive activity of MDSCs via the activation of the TLR2/STAT3 pathway. Furthermore, a reduced phosphorylation of Stat3 in MDSC, leading to the inhibition of their function, was observed in patients with colorectal metastatic cancer 3 weeks after the application of

dimethylamiloride (Chalmin et al., 2010) which is known to reduce the release of exosome (Iero et al., 2008; Savina et al., 2003). Our data provided evidences that HSP86 on tumor-derived EVs may represent a crucial molecule to regulate PD-L1 expression on monocytes. More importantly, the acquisition of monocyte immunosuppressive functions was found to be dependent on HSP86 concentration. Taken together, these data indicated the role of HSPs in mediating an immunosuppressive TME and converting monocytes into MDSCs.

5.7 EVs from plasma of responders and non-responders undergoing anti-PD1 treatment show different activity on monocytes

It has recently been reported that PD-L1 expression on EVs isolated from plasma of head and neck cancer patients could induce T cell dysfunction directly (Theodoraki et al., 2018). In our study, we raised the question if EVs from plasma of melanoma patients with different responsiveness to the treatment with negative check point inhibitors could display different effects on normal monocytes. We purified circulating EVs from responders and non-responders and cultured them with monocytes isolated from healthy donors. Interestingly, non-responder EVs showed a strong upregulation of PD-L1 and a moderate downregulation of HLA-DR expression. Moreover, monocytes stimulated with those EVs were able to inhibit the proliferation of CD8⁺ T cells and IFN- γ production of these cells. In contrast, EVs from responders failed to induce PD-L1 upregulation and the acquisition of immunosuppressive properties by monocytes. Furthermore, non-responder EVs showed higher expression of HSP86 compared to responder EVs. These results are consistent with our previous finding of monocyte-mediated immunosuppression upon the treatment with EVs from HT-144 melanoma cells. However, due to the limited patient numbers,

a definitive conclusion cannot be made. A larger cohort of melanoma patients under an anti-PD-1 therapy should be tested, and the expression of HSP86 on EVs of patients from responders and non-responders should be monitored before and after therapy.

Of note, although tumor cells may not be the only source of EVs collected from patients' plasma, the detrimental effect on differentiating monocytes into M-MDSC was exclusively induced by EVs purified from non-responders and not from responders.

5.8 PD-L1 on monocytes as potential predictive marker for responsiveness of anti-PD1 therapy in melanoma patients

Next, we tested the PD-L1 expression on circulating monocytes from responders and non-responders, considering that those monocytes were consistently under the influence of circulation EVs in plasma. PBMCs from 30 melanoma patients under anti-PD-1 therapy were collected. A significant decrease of PD-L1 on monocytes was observed in responders after the first infusion of anti-PD-1 antibodies as compared to the basal levels. In contrast, no changes were seen in non-responders. Moreover, melanoma patients with low PD-L1 expression on monocytes had a significantly better overall and progression free survivals. It has previously been demonstrated that PD-L1 expression on tumor cells plays an important role in preventing T cell-mediated anti-tumor activity and could be used for prediction of the efficiency of anti-PD-1 therapy (Blank et al., 2005; Iwai et al., 2002). In a randomized, phase 3 study where 834 patients with advanced melanoma were recruited for pembrolizumab therapy, a clinical benefit of pembrolizumab over ipilimumab was observed in both PD-L1–positive and PD-L1–negative subgroups (Robert et al.,

2015). Moreover, accumulating data from preclinical and clinical studies demonstrated the importance of PD-L1 on myeloid cells for PD-1/PD-L1 blockade-mediated tumor regression (Tang et al., 2018). In clinical study, it was shown that the frequency of CD14⁺CD16⁻HLA-DR^{hi} monocytes was a strong predictor of progression free and overall survival upon anti-PD-1 immunotherapy (Krieg et al., 2018). Our data suggest that the change of PD-L1 expression on monocytes after first application of anti-PD1 therapy could predict the responsiveness of melanoma patients to this therapy.

5.9 Conclusion

Taken together, our results demonstrate the importance of tumor-derived EVs in the induction of immunosuppression by converting normal monocytes into M-MDSCs resulting in inhibition of T cell-mediated antitumor immunity. HSP86 was shown to be the main driver for this conversion. Moreover, EVs isolated from non-responding melanoma patients treated with anti-PD-1 antibodies displayed higher HSP86 expression and showed similar immunosuppressive effects on monocytes as those mediated by EVs purified from melanoma cell lines. Furthermore, our study offers a rationale for using the measurement of PD-L1 expression on circulating monocytes as a predictive marker for the clinical outcome of anti-PD-1 therapy. Further studies with larger patient cohorts involving pre/post therapy assessments of HSP86 on EVs are needed to further validate their potential role as a reliable predictive marker.

6 SUMMARY

The aim of the study was to investigate the role of extracellular vesicles (EVs) derived from human melanoma cell lines as well as from plasma of melanoma patients in conversion of circulating CD14⁺ monocytes into monocytic myeloid-derived suppresser cells (M-MDSCs). We demonstrated that EVs purified from melanoma cell line HT-144 (HT-144 EVs) showed an anti-apoptotic effect on CD14⁺ monocytes via the upregulation of Bcl-2 at the mRNA and protein level. Moreover, CD14⁺ monocytes showed a modulation in inflammatory gene expression as well as an enhanced migration activity upon HT-144 EV stimulation. Furthermore, upregulation of PD-L1 and downregulation of HLA-DR was observed in monocytes upon the treatment with EVs from HT-144 and another melanoma cell line SK-MEL-28, which confirmed the change of phenotype from classical monocytes to M-MDSCs. Importantly, the stimulated monocytes showed a strong immunosuppressive activity by inhibiting CD8⁺ T cell proliferation and the production of IFN- γ . The upregulation of PD-L1 was induced via Toll-like receptor (TLR) signaling pathway, including TLR2 and TLR4, where TLR4 showed a prominent role. NF- κ B was activated, which led to the upregulation of PD-L1. The blockage of TLR4 with anti-TLR4 blocking antibody or NF- κ B with an NF- κ B inhibitor significantly diminished PD-L1 upregulation. We also found that HSP86 was expressed on EVs from melanoma cell lines. By comparing monocytes stimulated with HSP86⁺ EVs with those from HSP86^{low/-} EVs of HT-144 cells, we observed an abrogation of PD-L1 upregulation and immunosuppressive activity. Besides, we tested the expression of HSP86 on plasma EVs from melanoma patients responding and non-responding to anti-PD-1 therapy. We demonstrated that EVs from non-responders upregulated PD-L1 expression and induced immunosuppressive activity of circulating monocytes,

converting them into M-MDSCs. In addition, those EVs displayed higher HSP86 expression as compared to non-responder EVs. Finally, we studied PBMCs from 30 melanoma patients before and after anti-PD-1 therapy and found a significant decrease of PD-L1 expression in circulating monocytes from responders as compared to the level before therapy. Moreover, patients with lower PD-L1 expression on circulating monocytes showed better overall and progression free survival. Taken together, our finding demonstrated a crucial role of tumor-derived EVs in converting circulating monocytes into M-MDSCs and the importance of PD-L1 expression on monocytes in melanoma patients undergoing anti-PD-1 therapy for the prediction of therapy responsiveness.

7 ZUSAMMENFASSUNG

Das Ziel dieser Studie war es die Rolle von extrazellulären Vesikeln (EVs) bei der Umwandlung von zirkulierenden CD14⁺ Monozyten in monozytäre myeloide suppressor Zellen (M-MDSCs) zu untersuchen. Dabei wurden EVs aus humanen Melanomzelllinien, sowie Plasma von Melanompatienten isoliert. Wir haben gezeigt, dass EVs von HT-144 Zellen (HT-144 EVs) Bcl-2 in CD14⁺ Monozyten hochregulierten (auf mRNA -und Proteinebene) und dieses eine anti-apoptotische Wirkung hatten. Darüber hinaus zeigten CD14⁺ Monozyten ein verstärktes Entzündungsprofil, sowie eine verstärkte Migration nach der Stimulation mit HT-144 EVs. Nach der Behandlung der Monozyten mit EVs aus HT-144 und SK-MEL-28 Zellen, wurde ein Hochregulation von PD-L1 und eine herunter Regulierung von HLA-DR auf Monozyten beobachtet. Dieser Phänotyp bestätigte die Konversion von klassischen Monozyten zu M-MDSCs. Die stimulierten Monozyten zeigten eine stark immunsuppressive Aktivität, da diese die Proliferation von CD8⁺ T Zellen, sowie deren Produktion von IFN- γ unterdrückten. Die Hochregulation von PD-L1 wurde über den Toll-like-Rezeptor (TLR)2 und TLR4 Signalweg induziert, wobei TLR4 eine dominantere Rolle spielte. Der Signalweg aktivierte NF- κ B, was zur Hochregulation von PD-L1 führte. Die Blockade von TLR4 mittels TLR4-blockierenden Antikörpern, sowie NF- κ B mit NF- κ B Inhibitoren verringerte die PD-L1 Expression signifikant. Des Weiteren fanden wir, dass auf EVs von Melanomzelllinien HSP86 exprimiert wurde. Der Vergleich von HSP86⁺ EVs mit HSP86^{low/-} EVs verdeutlichte die Bedeutung von der HSP86 vermittelten PD-L1 Expression und der immunsuppressiven Aktivität. Zudem haben wir die Expression von HSP86 in Plasma EVs von Melanompatienten getestet, welche eine Anti-PD-1 Therapie erhielten. Wir haben gezeigt, dass EVs von Nicht-Respondern die PD-L1 Expression hochregulierten und eine

immunsuppressive Aktivität in zirkulierenden Monozyten induzierten. Diese EVs zeigten zusätzlich eine deutlich höhere Expression von HSP86 im Vergleich zu EVs von Respondern. Schließlich untersuchten wir PBMCs von 30 Melanompatienten vor und nach einer Anti-PD-1 Behandlung. Wir fanden eine signifikante Abnahme der PD-L1-Expression in zirkulierenden Monozyten von Respondern im Vergleich zum Beginn der Therapie. Darüber hinaus zeigten Patienten mit niedrigerer PD-L1 Expression auf zirkulierenden Monozyten besseres progressionsfreies Überleben. Zusammengefasst demonstrieren unsere Ergebnisse eine bedeutende Rolle von Tumor-EVs bei der Umwandlung von zirkulierender Monozyten in M-MDSCs. Des Weiteren konnten wir zeigen, dass die PD-L1 Expression auf Monozyten bei Melanompatienten, welche sich einer Anti-PD-1 Therapie unterziehen, eine entscheidende Rolle bei der Vorhersage des Therapieerfolgs hat.

8 REFERENCES

- Akbani, R., Akdemir, K., Aksoy, B., Albert, M., Ally, A., Amin, S., Arachchi, H., and Arora, A. (2015). HHS Public Access. *Cell* 161, 1681–1696.
- Al-Nedawi, K., Meehan, B., Micallef, J., Lhotak, V., May, L., Guha, A., and Rak, J. (2008). Intercellular transfer of the oncogenic receptor EGFRvIII by microvesicles derived from tumour cells. *Nature Cell Biology* 10, 619–624.
- El Andaloussi, S., Mägerr, I., Breakefield, X.O., and Matthew J. A. Wood (2013). Extracellular vesicles: biology and emerging therapeutic opportunities. *Nature Reviews Drug Discovery* 12, 347–357.
- Andreola, G., Rivoltini, L., Castelli, C., Huber, V., Perego, P., Deho, P., Squarcina, P., Accornero, P., Lozupone, F., Lugini, L., et al. (2002). Induction of Lymphocyte Apoptosis by Tumor Cell Secretion of FasL-bearing Microvesicles. 195.
- Anfossi, N., André, P., Guia, S., Falk, C.S., Roetyncck, S., Stewart, C.A., Bresó, V., Frassati, C., Reviron, D., Middleton, D., et al. (2006). Human NK Cell Education by Inhibitory Receptors for MHC Class I. *Immunity* 25, 331–342.
- Antonov, N.S., and Stulova, O.Y. (2013). Extracellular vesicles: Exosomes, microvesicles, and friends. *The Journal of Cell Biology* 200, 373–383.
- Asea A (2008). Heat Shock Proteins and Toll-Like Receptors. In: Bauer S., Hartmann G. (eds) Toll-Like Receptors (TLRs) and Innate Immunity. *Handbook of Experimental Pharmacology* 183.
- Baba, H., Kuwabara, K., Ishiguro, T., Kumamoto, K., Kumagai, Y., Ishibashi, K., Haga, N., and Ishida, H. (2013). Prognostic factors for stage IV gastric cancer. *International Surgery* 98, 181–187.
- Barry, M., and Bleackley, R.C. (2002). Cytotoxic T lymphocytes: all roads lead to death. *Nature Reviews Immunology* 2, 401–409.
- Barton, G.M., Medzhitov, R., Barton, G.M., and Medzhitov, R. (2014). Toll-Like Receptor Signaling Pathways. 1524, 36–38.
- Beatty, G.L., and Gladney, W.L. (2015). Immune escape mechanisms as a guide for cancer immunotherapy. *Clinical Cancer Research* 21, 687–692.
- Becker, A., Thakur, B.K., Weiss, J.M., Kim, H.S., Peinado, H., and Lyden, D. (2016). Extracellular Vesicles in Cancer: Cell-to-Cell Mediators of Metastasis. *Cancer Cell* 30, 836–848.
- Bemis, L.T., Witwer, K.W., Buza, E.I., Lo, J., Nolte, E.N., Bora, A., La, C., Piper, M.G., Sivaraman, S., The, C., et al. (2013). Standardization of sample collection, isolation and analysis methods in

extracellular vesicle research . 1, 1–25.

Blank, C., and Mackensen, A. (2007). Contribution of the PD-L1/PD-1 pathway to T-cell exhaustion: An update on implications for chronic infections and tumor evasion. *Cancer Immunology, Immunotherapy* 56, 739–745.

Blank, C., Gajewski, T.F., and Mackensen, A. (2005). Interaction of PD-L1 on tumor cells with PD-1 on tumor-specific T cells as a mechanism of immune evasion: Implications for tumor immunotherapy. *Cancer Immunology, Immunotherapy* 54, 307–314.

Boes, M., and Meyer-Wentrup, F. (2015). TLR3 triggering regulates PD-L1 (CD274) expression in human neuroblastoma cells. *Cancer Letters* 361, 49–56.

Bonilla, F.A., and Oettgen, H.C. (2010). Adaptive immunity. *Journal of Allergy and Clinical Immunology* 125, S33–S40.

Bronte, V., Brandau, S., Chen, S., Colombo, M.P., Frey, A.B., Greten, T.F., Mandruzzato, S., Murray, P.J., Ochoa, A., Ostrand-Rosenberg, S., et al. (2016). Recommendations for myeloid-derived suppressor cell nomenclature and characterization standards. *Nature Communications* 7, 12150.

Brown, J.A., Dorfman, D.M., Ma, F.-R., Sullivan, E.L., Munoz, O., Wood, C.R., Greenfield, E.A., and Freeman, G.J. (2003). Blockade of Programmed Death-1 Ligands on Dendritic Cells Enhances T Cell Activation and Cytokine Production. *The Journal of Immunology* 170, 1257–1266.

Burnet, M. (1957). *Cancer—A BIOLOGICAL APPROACH. I THE PROCESSES OF CONTROL.* *British Medical Journal* 780–786.

Catlett-Falcone, R., Landowski, T.H., Oshiro, M.M., Turkson, J., Levitzki, A., Savino, R., Ciliberto, G., Moscinski, L., Fernández-Luna, J.L., Nuñez, G., et al. (1999). Constitutive activation of Stat3 signaling confers resistance to apoptosis in human U266 myeloma cells. *Immunity* 10, 105–115.

Chalmin, F., Ladoire, S., Mignot, G., Vincent, J., Bruchard, M., Boireau, W., Rouleau, A., Simon, B., Lanneau, D., Thonel, A. De, et al. (2010). Membrane associated Hsp72 from tumor derived exosomes mediates STAT3 dependent immunosuppressive function of mouse and human myeloid derived suppressor cells. *J. Clin. Invest.* 120, 467–471.

Chang, A.L., Miska, J., Wainwright, D.A., Dey, M., Rivetta, C. V., Yu, D., Kanojia, D., Pituch, K.C., Qiao, J., Pytel, P., et al. (2016). CCL2 produced by the glioma microenvironment is essential for the recruitment of regulatory t cells and myeloid-derived suppressor cells. *Cancer Research* 76, 5671–5682.

Chen, L., and Flies, D.B. (2013). Molecular mechanisms of T cell co-stimulation and co-inhibition. *Nat*

Rev Immunol 13, 227–242.

Chen, B., Zhong, D., and Monteiro, A. (2006). Comparative genomics and evolution of the HSP90 family of genes across all kingdoms of organisms. *BMC Genomics* 7, 1–19.

Ciocca, D.R., and Calderwood, S.K. (2005). Heat shock proteins in cancer: diagnostic, prognostic, predictive, and treatment implications. *Cell Stress & Chaperones* 10, 86–103.

Clayton, A., Mitchell, J.P., Court, J., Linnane, S., Mason, M.D., and Tabi, Z. (2008). Human Tumor-Derived Exosomes Down-Modulate NKG2D Expression. *The Journal of Immunology* 180, 7249–7258.

Colaco, C.A., Bailey, C.R., Walker, K.B., and Keeble, J. (2013). Heat shock proteins: Stimulators of innate and acquired immunity. *BioMed Research International* 2013.

Condamine, T., and Gabrilovich, D.I. (2011). Molecular mechanisms regulating myeloid-derived suppressor cell differentiation and function. *Trends in Immunology* 32, 19–25.

Croce, C.M. (2008). Oncogenes and cancer. *N. Engl. J. Med.* 267, 502–511.

Van Deun, J., Mestdagh, P., Sormunen, R., Cocquyt, V., Vermaelen, K., Vandesompele, J., Bracke, M., De Wever, O., and Hendrix, A. (2014). The impact of disparate isolation methods for extracellular vesicles on downstream RNA profiling. *Journal of Extracellular Vesicles* 3, 1–14.

Dong, H., Strome, S.E., Salomao, D.R., Tamura, H., Hirano, F., Flies, D.B., Roche, P.C., Lu, J., Zhu, G., Tamada, K., et al. (2002). Tumor-associated B7-H1 promotes T-cell apoptosis: A potential mechanism of immune evasion. *Nature Medicine* 8, 793–800.

Dunn, G.P., Bruce, A.T., Ikeda, H., Old, L.J., and Schreiber, R.D. (2002). Cancer immunoediting: from immunosurveillance and to tumor escape. *Nature Immunology* 3, 991–998.

Dunn, G.P., Old, L.J., and Schreiber, R.D. (2004). The Three Es of Cancer Immunoediting. *Annual Review of Immunology* 22, 329–360.

Dunn, G.P., Koebel, C.M., and Schreiber, R.D. (2006). Interferons, immunity and cancer immunoediting. *Nature Reviews Immunology* 6, 836–848.

Eroglu, Z., Ann Chen, Y., Gibney, G.T., Weber, J.S., Kudchadkar, R.R., Khushalani, N.I., Markowitz, J., Brohl, A.S., Tetteh, L.F., Ramadan, H., et al. (2018). Combined BRAF and HSP90 inhibition in patients with unresectable BRAFV600E-mutant melanoma. *Clinical Cancer Research* 24, 5516–5524.

Fabrizi, M., Paone, A., Calore, F., Galli, R., Croce, C.M., and Mediators, C.C. (2013). A new role for microRNAs, as ligands of Toll-like receptors. *RNA Biology* 10:2, 10, 169–174.

Fan Y., Dutta J., Gupta N., Fan G., G.C. (2008). Regulation of Programmed Cell Death by NF- κ B and its Role in Tumorigenesis and Therapy. In: *Programmed Cell Death in Cancer Progression and*

Therapy. *Advances in Experimental Medicine and Biology* 615.

Fattore, L., Costantini, S., Malpicci, D., Ruggiero, C.F., Ascierto, P.A., Croce, C.M., Mancini, R., and Ciliberto, G. (2015). MicroRNAs in melanoma development and resistance to target therapy. *Oncotarget*.

Gajewski, T.F., Schreiber, H., and Fu, Y.-X. (2013). Innate and adaptive immune cells in the tumor microenvironment. *Nat Immunol* 14, 1014–1022.

Galley, H.F., and Webster, N.R. (1996). The immuno-inflammatory cascade. *British Journal of Anaesthesia* 77, 11–16.

Garcia-Carbonero, R., Carnero, A., and Paz-Ares, L. (2013). Inhibition of HSP90 molecular chaperones: Moving into the clinic. *The Lancet Oncology* 14, e358–e369.

Gardiner, C., Vizio, D. Di, Sahoo, S., Théry, C., Witwer, K.W., Wauben, M., and Hill, A.F. (2016). Techniques used for the isolation and characterization of extracellular vesicles: Results of a worldwide survey. *Journal of Extracellular Vesicles* 5, 1–6.

Ge, R., Tan, E., Sharghi-Namini, S., and Asada, H.H. (2012). Exosomes in cancer microenvironment and beyond: Have we overlooked these extracellular messengers? *Cancer Microenvironment* 5, 323–332.

Gemelli, C.H., Seftoni, M. V, and Yeol, E.L. (1993). Platelet-derived Microparticle formation Involves Glycoprotein IIb-IIIa. *The Journal of Biological Chemistry* 268, 14586–14589.

Ghansah, T. (2012). A novel strategy for modulation of MDSC to enhance cancer immunotherapy. *OncolImmunology* 1, 984–985.

Goldszmid, R.S., and Trinchieri, G. (2012). The price of immunity. *Nature Immunology* 13, 932–938.

Gong, A., Zhou, R., Hu, G., Li, X., Splinter, P.L., O'Hara, S.P., LaRusso, N.F., Soukup, G.A., Dong, H., and Chen, X.-M. (2009). MicroRNA-513 Regulates B7-H1 Translation and Is Involved in IFN- γ -Induced B7-H1 Expression in Cholangiocytes. *The Journal of Immunology* 182, 1325–1333.

Gong, A., Zhou, R., Hu, G., Liu, J., Sosnowska, D., Drescher, K.M., Dong, H., and Chen, X. (2010). *Cryptosporidium parvum* Induces B7-H1 Expression in Cholangiocytes by Down-Regulating MicroRNA-513. *The Journal of Infectious Diseases* 201, 160–169.

Gordon, S., and Taylor, P.R. (2005). Monocyte and macrophage heterogeneity. *Nature Reviews Immunology* 5, 953–964.

Gross, J.C., Chaudhary, V., Bartscherer, K., and Boutros, M. (2012). Active Wnt proteins are secreted on exosomes. *Nature Cell Biology* 14, 1036–1045.

- Haderk, F., Schulz, R., Iskar, M., Cid, L.L., Worst, T., Willmund, K. V, Schulz, A., Warnken, U., Seiler, J., Benner, A., et al. (2017). Tumor-derived exosomes modulate PD-L1 expression in monocytes. *Science Immunology* 2, eaah5509.
- Hahn, W.C., and Weinberg, R.A. (2002). Rules for making human tumor cells. *N Engl J Med* 347, 1593–1603.
- Hawn, T.R., and Underhill, D.M. (2005). Toll-like Receptors in Innate Immunity. *Measuring Immunity: Basic Biology and Clinical Assessment* 17, 80–90.
- He, Y.-F., Zhang, G.-M., Wang, X.-H., Zhang, H., Yuan, Y., Li, D., and Feng, Z.-H. (2004). Blocking Programmed Death-1 Ligand-PD-1 Interactions by Local Gene Therapy Results in Enhancement of Antitumor Effect of Secondary Lymphoid Tissue Chemokine. *The Journal of Immunology* 173, 4919–4928.
- Helen Saibil (2013). Chaperone machines for protein folding, unfolding and disaggregation. *Nat Rev Mol Cell Biol* 14, 630–642.
- Higashikuni, Y., Tanaka, K., Kato, M., Nureki, O., Hirata, Y., Nagai, R., Komuro, I., and Sata, M. (2013). Toll-like receptor-2 mediates adaptive cardiac hypertrophy in response to pressure overload through interleukin-1 β upregulation via nuclear factor κ B activation. *Journal of the American Heart Association* 2, 1–28.
- Holmgaard, R.B., Zamarin, D., Li, Y., Gasmi, B., Munn, D.H., Allison, J.P., Merghoub, T., and Wolchok, J.D. (2015). Tumor-Expressed IDO Recruits and Activates MDSCs in a Treg-Dependent Manner. *Cell Reports* 13, 412–424.
- Huber, V., Fais, S., Iero, M., Lugini, L., Canese, P., Squarcina, P., Zaccheddu, A., Colone, M., Arancia, G., Gentile, M., et al. (2005). Human colorectal cancer cells induce T-cell death through release of proapoptotic microvesicles: Role in immune escape. *Gastroenterology* 128, 1796–1804.
- Huber, V., Rodolfo, M., Rivoltini, L., Huber, V., Vallacchi, V., Fleming, V., Hu, X., Cova, A., Dugo, M., Shahaj, E., et al. (2018). Tumor-derived microRNAs induce myeloid suppressor cells and predict immunotherapy resistance in melanoma Graphical abstract Find the latest version : Tumor-derived microRNAs induce myeloid suppressor cells and predict immunotherapy resistance in melanoma. 128, 5505–5516.
- Hutchinson, M.R., Ramos, K.M., Loram, L.C., Wieseler, J., Paige, W., Kearney, J.J., Lewis, M.T., Crysdale, N.Y., Zhang, Y., Harrison, J.A., et al. (2009). Evidence for a role of heat shock protein-90 (HSP90) in TLR4 mediated pain enhancement in rats. *Neuroscience*. 164, 1821–1832.

- Iero, M., Valenti, R., Huber, V., Filipazzi, P., Parmiani, G., Fais, S., and Rivoltini, L. (2008). Tumour-released exosomes and their implications in cancer immunity. *Cell Death and Differentiation* 15, 80–88.
- Iwai, Y., Ishida, M., Tanaka, Y., Okazaki, T., Honjo, T., and Minato, N. (2002). Involvement of PD-L1 on tumor cells in the escape from host immune system and tumor immunotherapy by PD-L1 blockade. *Proc Natl Acad Sci U S A* 99, 12293–12297.
- Jin, C., Cleveland, J., Ao, L., Li, J., Zeng, Q., Fullerton, D.A., and Meng, X. (2014). Human Myocardium Releases Heat Shock Protein 27 (HSP27) after Global Ischemia: The Proinflammatory Effect of Extracellular HSP27 through Toll-like Receptor (TLR)-2 and TLR4. *Molecular Medicine* 20, 280–289.
- Kaltschmidt, B., Kaltschmidt, C., Hofmann, T.G., Hehner, S.P., Dröge, W., and Schmitz, M.L. (2000). The pro- or anti-apoptotic function of NF- κ B is determined by the nature of the apoptotic stimulus. *European Journal of Biochemistry* 267, 3828–3835.
- Kaur, J., Das, S.N., Srivastava, A., and Ralhan, R. (1998). Cell surface expression of 70 kDa heat shock protein in human oral dysplasia and squamous cell carcinoma: Correlation with clinicopathological features. *Oral Oncology* 34, 93–98.
- Kawai, T., and Akira, S. (2010). The role of pattern-recognition receptors in innate immunity: update on Toll-like receptors. *Nature Publishing Group* 11, 373–384.
- Kawai, T., and Akira, S. (2011). Toll-like Receptors and Their Crosstalk with Other Innate Receptors in Infection and Immunity. *Immunity* 34, 637–650.
- Kawasaki, T., and Kawai, T. (2014). Toll-like receptor signaling pathways. *5*, 1–8.
- Keir, M.E., Butte, M.J., Freeman, G.J., and Sharpe, A.H. (2008). PD-1 and Its Ligands in Tolerance and Immunity. *Annual Review of Immunology* 26, 677–704.
- Keller, S., König, A.K., Marmé, F., Runz, S., Wolterink, S., Koensgen, D., Mustea, A., Sehoul, J., and Altevogt, P. (2009). Systemic presence and tumor-growth promoting effect of ovarian carcinoma released exosomes. *Cancer Letters* 278, 73–81.
- Koebel, C.M., Vermi, W., Swann, J.B., Zerafa, N., Rodig, S.J., Old, L.J., Smyth, M.J., and Schreiber, R.D. (2007). Adaptive immunity maintains occult cancer in an equilibrium state. *Nature* 450, 903–907.
- Koliha, N., Heider, U., Ozimkowski, T., Wiemann, M., Bosio, A., and Wild, S. (2016). Melanoma affects the composition of blood cell-derived extracellular vesicles. *Frontiers in Immunology* 7, 1–12.
- Komatsu, T. (1996). Expression of Heat Shock Proteins HSP70 and HSP90 in Endometrial

Carcinomas. 330–338.

Krieg, C., Nowicka, M., Guglietta, S., Schindler, S., Hartmann, F.J., Weber, L.M., Dummer, R., Robinson, M.D., Levesque, M.P., and Becher, B. (2018). High-dimensional single-cell analysis predicts response to anti-PD-1 immunotherapy. *Nature Medicine* 24, 144–153.

Kumar, B. V., Connors, T.J., and Farber, D.L. (2018). Human T Cell Development, Localization, and Function throughout Life. *Immunity* 48, 202–213.

Kumar, V., Patel, S., Tcyganov, E., and Gabrilovich, D.I. (2016). The Nature of Myeloid-Derived Suppressor Cells in the Tumor Microenvironment. *Trends in Immunology* 37, 208–220.

Lawrence, T. (2009). The nuclear factor NF-kappaB pathway in inflammation. *Cold Spring Harbor Perspectives in Biology* 1, 1–10.

Lelis, F.J.N., Jaufmann, J., Singh, A., Fromm, K., Teschner, A.C., Pöschel, S., Schäfer, I., Beer-Hammer, S., Rieber, N., and Hartl, D. (2017). Myeloid-derived suppressor cells modulate B-cell responses. *Immunology Letters* 188, 108–115.

Lindau, D., Gielen, P., Kroesen, M., Wesseling, P., and Adema, G.J. (2013). The immunosuppressive tumour network: Myeloid-derived suppressor cells, regulatory T cells and natural killer T cells. *Immunology* 138, 105–115.

Liu, X., and Zhang, G. (2008). HSP90 as a marker of progression in melanoma. *Annals of Oncology* 19, 590–594.

Liu, Y., Gu, Y., and Cao, X. (2015). The exosomes in tumor immunity. *Oncolmmunology* 4, e1027472.

Lobb, R.J., Becker, M., Wen, S.W., Wong, C.S.F., Wiegmans, A.P., Leimgruber, A., and Möller, A. (2015). Optimized exosome isolation protocol for cell culture supernatant and human plasma. *Journal of Extracellular Vesicles* 4, 1–11.

Lu, Y.C., Yeh, W.C., and Ohashi, P.S. (2008). LPS/TLR4 signal transduction pathway. *Cytokine* 42, 145–151.

Maas, S.L.N., Breake, X.O., and Weaver, A.M. (2016). Extracellular Vesicles: Unique Intercellular Delivery Vehicles. *xx*, 1–17.

Maas, S.L.N., Breakefield, X.O., and Weaver, A.M. (2017). Extracellular Vesicles: Unique Intercellular Delivery Vehicles. *Trends in Cell Biology* 27, 172–188.

Mandal, A., and Viswanathan, C. (2015). Natural killer cells: In health and disease. *Hematology/Oncology and Stem Cell Therapy* 8, 47–55.

Mandruzzato, S., Solito, S., Falisi, E., Francescato, S., Chiarion-Sileni, V., Mocellin, S., Zanon, A.,

- Rossi, C.R., Nitti, D., Bronte, V., et al. (2009). IL4R α + Myeloid-Derived Suppressor Cell Expansion in Cancer Patients. *The Journal of Immunology* 182, 6562–6568.
- Mangan, D. F., Mergenhagen, S. E., & Wahl, S.M. (1993). Apoptosis in human monocytes: possible role in chronic inflammatory diseases. *Journal of Periodontology* 64, 461–466.
- Mbofung, R.M., McKenzie, J.A., Malu, S., Zhang, M., Peng, W., Liu, C., Kuitse, I., Tieu, T., Williams, L., Devi, S., et al. (2017). HSP90 inhibition enhances cancer immunotherapy by upregulating interferon response genes. *Nature Communications* 8.
- Meng, S., Tripathy, D., Frenkel, E.P., Shete, S., Naftalis, E.Z., Huth, J.F., Beitsch, P.D., Leitch, M., Hoover, S., and Euhus, D. (2004). Circulating Tumor Cells in Patients with Breast Cancer Dormancy. *Clinical Cancer Research* 10, 8152–8162.
- Merle, N.S., Noe, R., Halbwachs-Mecarelli, L., Fremeaux-Bacchi, V., and Roumenina, L.T. (2015). Complement system part II: Role in immunity. *Frontiers in Immunology* 6, 1–26.
- Meyer, C., Sevko, A., Ramacher, M., Bazhin, A. V, Falk, C.S., Osen, W., Borrello, I., Kato, M., Schadendorf, D., Baniyash, M., et al. (2011). Chronic inflammation promotes myeloid-derived suppressor cell activation blocking antitumor immunity in transgenic mouse melanoma model. *Proceedings of the National Academy of Sciences of the United States of America* 108, 17111–17116.
- Meyer, C., Cagnon, L., Costa-Nunes, C.M., Baumgaertner, P., Montandon, N., Leyvraz, L., Michielin, O., Romano, E., and Speiser, D.E. (2014). Frequencies of circulating MDSC correlate with clinical outcome of melanoma patients treated with ipilimumab. *Cancer Immunology, Immunotherapy* 63, 247–257.
- Mittal, D., Gubin, M.M., Schreiber, R.D., and Smyth, M.J. (2014). New insights into cancer immunoediting and its three component phases — elimination, equilibrium and escape Deepak. *Current Opinion in Immunology* 27, 16–25.
- Modi, S., Stopeck, A., Linden, H., Solit, D., Chandarlapaty, S., Rosen, N., D'Andrea, G., Dickler, M., Moynahan, M.E., Sugarman, S., et al. (2011). HSP90 inhibition is effective in breast cancer: A phase II trial of tanespimycin (17-AAG) plus trastuzumab in patients with HER2-positive metastatic breast cancer progressing on trastuzumab. *Clinical Cancer Research* 17, 5132–5139.
- Mogensen, T.H. (2009). Pathogen recognition and inflammatory signaling in innate immune defenses. *Clinical Microbiology Reviews* 22, 240–273.
- Murphy, K.M., Travers, P., Walport, M., and Ehrenstein, M. (2009). (2009). *Janeway-Immunologie*, 7.Aufl.edn Heidelberg: Spektrum, Akad. Verl.

- Nelson, E.E., and Guyer, A.E. (2013). Myeloid-derived suppressor cells are associated with disease progression and decreased overall survival in advanced-stage melanoma patients. *Cancer Immunol Immunother.* 62, 1711–1722.
- Van Niel, G., D'Angelo, G., and Raposo, G. (2018). Shedding light on the cell biology of extracellular vesicles. *Nature Reviews Molecular Cell Biology* 19, 213–228.
- Noman, M.Z., Desantis, G., Janji, B., Hasmim, M., Karray, S., Dessen, P., Bronte, V., and Chouaib, S. (2014). PD-L1 is a novel direct target of HIF-1 α , and its blockade under hypoxia enhanced MDSC-mediated T cell activation. *The Journal of Experimental Medicine* 211, 781–790.
- O'Neill, L.A.J., Golenbock, D., and Bowie, A.G. (2013). The history of Toll-like receptors-redefining innate immunity. *Nature Reviews Immunology* 13, 453–460.
- Oh, S., and Hwang, E.S. (2014). The role of protein modifications of T-bet in cytokine production and differentiation of T helper cells. *Journal of Immunology Research* 2014, 1–7.
- Oushy, S., Hellwinkel, J.E., Wang, M., Nguyen, G.J., Gunaydin, D., Harland, T.A., Anchordoquy, T.J., and Graner, M.W. (2018). Glioblastoma multiforme-derived extracellular vesicles drive normal astrocytes towards a tumour-enhancing phenotype. *Philosophical Transactions of the Royal Society B: Biological Sciences* 373.
- Parihar, A., Eubank, T.D., and Doseff, A.I. (2010). Monocytes and macrophages regulate immunity through dynamic networks of survival and cell death. *Journal of Innate Immunity* 2, 204–215.
- Paschon, V., Takada, S.H., Ikebara, J.M., Sousa, E., Raeisossadati, R., Ulrich, H., and Kihara, A.H. (2016). Interplay Between Exosomes, microRNAs and Toll-Like Receptors in Brain Disorders. *Molecular Neurobiology* 53, 2016–2028.
- Patricia, M., Sana, O., Lisa, K., and Frank, C.R. (2000). Overexpression of the glucose-regulated stress gene GRP78 in ... *Breast Cancer Research and Treatment* 59, 15–26.
- Peinado, H., Alec, M., Lavotshkin, S., Matei, I., Costa-silva, B., Moreno-bueno, G., Hergueta-redondo, M., Williams, C., García-santos, G., Ghajar, C.M., et al. (2012). articles Melanoma exosomes educate bone marrow progenitor cells toward a pro-metastatic phenotype through MET. 18.
- Pol, J., Kroemer, G., and Galluzzi, L. (2016). First oncolytic virus approved for melanoma immunotherapy. *Oncolimmunology* 5, e1115641.
- Prohaszka, Z. (2003). Heat shock proteins as regulators of the immune response. *The Lancet* 469–476.
- Qian, Y., Deng, J., Geng, L., Xie, H., Jiang, G., Zhou, L., Wang, Y., Yin, S., Feng, X., Liu, J., et al.

- (2008). TLR4 signaling induces B7-H1 expression through MAPK pathways in bladder cancer cells. *Cancer Investigation* 26, 816–821.
- Qu, L., Ding, J., Chen, C., Sun, Y., Wang, H., and Wang, L. (2016). Exosome-Transmitted IncARSR Promotes Sunitinib Resistance in Renal Cancer by Acting as a Competing Endogenous RNA. *Cancer Cell* 29, 653–668.
- Reddy, V.S., Madala, S.K., Trinath, J., and Reddy, G.B. (2018). Extracellular small heat shock proteins: exosomal biogenesis and function. *Cell Stress and Chaperones* 23, 441–454.
- Reynolds, T.Y., Rockwell, S., and Glazer, P.M. (1996). Genetic instability induced by the tumor microenvironment. *Cancer Research* 56, 5754–5757.
- Robbins, P.D., and Morelli, A.E. (2014). Regulation of immune responses by extracellular vesicles. *Nature Reviews Immunology* 14, 195–208.
- Robert, C., Schachter, J., Long, G. V., Arance, A., Grob, J.J., Mortier, L., Daud, A., Carlino, M.S., McNeil, C., Lotem, M., et al. (2015). Pembrolizumab versus Ipilimumab in Advanced Melanoma. *New England Journal of Medicine* 372, 2521–2532.
- Ruslan Medzhitov (2001). TOLL-LIKE RECEPTORS AND INNATE IMMUNITY. *Nature Reviews Immunology* 135–145.
- Savina, A., Furlán, M., Vidal, M., and Colombo, M.I. (2003). Exosome release is regulated by a calcium-dependent mechanism in K562 cells. *Journal of Biological Chemistry* 278, 20083–20090.
- Schadendorf, D., van Akkooi, A.C.J., Berking, C., Griewank, K.G., Gutzmer, R., Hauschild, A., Stang, A., Roesch, A., and Ugurel, S. (2018). Melanoma. *The Lancet* 392, 971–984.
- Schreiber, R.D. (2011). Cancer Immunoediting : Integrating Suppression and Promotion. *Science* 331, 1565–1571.
- Schreiber, R.D., Old, L.J., and Smyth, M.J. (2011). Cancer Immunoediting : Integrating Suppression and Promotion. *Science* 331, 1565–1571.
- Sen, R., and Baltimore, D. (2013). The complexity of NF- κ B signaling in inflammation and cancer. *Molecular Cancer* 12.
- Seo, W., Eun, H.S., Kim, S.Y., Yi, H.S., Lee, Y.S., Park, S.H., Jang, M.J., Jo, E., Kim, S.C., Han, Y.M., et al. (2016). Exosome-mediated activation of toll-like receptor 3 in stellate cells stimulates interleukin-17 production by $\gamma\delta$ T cells in liver fibrosis. *Hepatology* 64, 616–631.
- Sheikh, S.Z., Matsuoka, K., Kobayashi, T., Li, F., Rubinas, T., and Plevy, S.E. (2010). Cutting Edge:

- IFN- γ Is a Negative Regulator of IL-23 in Murine Macrophages and Experimental Colitis. *J Immunol* 184, 4069–4073.
- Shi, Y. (2018). Regulatory mechanisms of PD-L1 expression in cancer cells. *Cancer Immunology, Immunotherapy* 67, 1481–1489.
- Shi, C., Ulke-Lemée, A., Deng, J., Batulan, Z., and O'Brien, E.R. (2018). Characterization of heat shock protein 27 in extracellular vesicles: a potential anti-inflammatory therapy. *The FASEB Journal* fj.201800987R.
- Srivastava, P.K., Udono, H., Blachere, N.E., and Li, Z. (1994). Heat shock proteins transfer peptides during antigen processing and CTL priming. *Immunogenetics* 39, 93–98.
- Sun, C., Mezzadra, R., and Schumacher, T.N. (2018). Regulation and Function of the PD-L1 Checkpoint. *Immunity* 48, 434–452.
- Szatanek, R., Baran, J., Siedlar, M., and Baj-Krzyworzeka, M. (2015). Isolation of extracellular vesicles: Determining the correct approach (review). *International Journal of Molecular Medicine* 36, 11–17.
- Talmadge, J.E., and Gabrilovich, D.I. (2013). History of myeloid-derived suppressor cells. *Nat Rev Cancer* 13, 739–752.
- Tang, H., Peng, H., Fu, Y., Tang, H., Liang, Y., Anders, R.A., Taube, J.M., Qiu, X., Mulgaonkar, A., Liu, X., et al. (2018). PD-L1 on host cells is essential for PD-L1 blockade – mediated tumor regression
Find the latest version: PD-L1 on host cells is essential for PD-L1 blockade – mediated tumor regression. *Journal of Clinical Investigation* 128, 580–588.
- Tang D, Kang R, Coyne CB, Zeh HJ, L.M. (2012). PAMPs and DAMPs: Signal 0s that Spur Autophagy and Immunity Daolin. *Immunol Rev* 249, 158–175.
- Theodoraki, M.N., Yerneni, S.S., Hoffmann, T.K., Gooding, W.E., and Whiteside, T.L. (2018). Clinical significance of PD-L1⁺ exosomes in plasma of head and neck cancer patients. *Clinical Cancer Research* 24, 896–905.
- Théry, C., Amigorena, S., Raposo, G., and Clayton, A. (2006). Isolation and Characterization of Exosomes from Cell Culture Supernatants and Biological Fluids. *Current Protocols in Cell Biology* 1–29.
- Théry, C., Witwer, K.W., Aikawa, E., Alcaraz, M.J., Anderson, J.D., Andriantsitohaina, R., Antoniou, A., Arab, T., Archer, F., Atkin-Smith, G.K., et al. (2018). Minimal information for studies of extracellular vesicles 2018 (MISEV2018): a position statement of the International Society for Extracellular Vesicles

- and update of the MISEV2014 guidelines. *Journal of Extracellular Vesicles* 8, 1535750.
- Trepel, J., Mollapour, M., Giaccone, G., and Neckers, L. (2010). Targeting the dynamic HSP90 complex in cancer. *Nature Reviews Cancer* 10, 537–549.
- Tu, S., Bhagat, G., Cui, G., Takaishi, S., Kurt-jones, E.A., Rickman, B., Betz, K.S., Penz, M., Bjorkdhl, O., Fox, J.G., et al. (2008). Overexpression of interleukin-1beta induces gastric inflammation and cancer and mobilizes myeloid-derived suppressor cells in mice. *Cancer Cell* 14, 408–419.
- Tucci, M., Passarelli, A., Mannavola, F., Stucci, L.S., Ascierio, P.A., Capone, M., Madonna, G., Lopalco, P., and Silvestris, F. (2018). Serum exosomes as predictors of clinical response to ipilimumab in metastatic melanoma. *Oncolmmunology* 7.
- Umansky, V., Sevko, A., Gebhardt, C., and Utikal, J. (2014). Myeloid-derived suppressor cells in malignant melanoma. *Journal of the German Society of Dermatology* 12, 1–7.
- Umansky, V., Blattner, C., Gebhardt, C., and Utikal, J. (2016). The Role of Myeloid-Derived Suppressor Cells (MDSC) in Cancer Progression. *Vaccines* 4, 36.
- Van Der Vaart, M., Spaik, H.P., and Meijer, A.H. (2012). Pathogen recognition and activation of the innate immune response in zebrafish. *Advances in Hematology* 2012, 159807.
- Valenti, R., Huber, V., Filipazzi, P., Pilla, L., Sovena, G., Villa, A., Corbelli, A., Fais, S., Parmiani, G., and Rivoltini, L. (2006). Human Tumor-Released Microvesicles Promote the Differentiation of Myeloid Cells with Transforming Growth Factor- B – Mediated Suppressive Activity on T Lymphocytes. 9290–9299.
- Vicencio, J.M., Yellon, D.M., Sivaraman, V., Das, D., Boi-Doku, C., Arjun, S., Zheng, Y., Riquelme, J.A., Kearney, J., Sharma, V., et al. (2015). Plasma exosomes protect the myocardium from ischemia-reperfusion injury. *Journal of the American College of Cardiology* 65, 1525–1536.
- Wang, Y., Schafer, C.C., Hough, K.P., Tousif, S., Duncan, S.R., Kearney, J.F., Ponnazhagan, S., Hsu, H.-C., and Deshane, J.S. (2018). Myeloid-Derived Suppressor Cells Impair B Cell Responses in Lung Cancer through IL-7 and STAT5. *The Journal of Immunology* 201, 278–295.
- Whiteside, T. (2016). Tumor-Derived Exosomes and Their Role in Tumor-Induced Immune Suppression. *Vaccines* 4, 35.
- Wilcox, T., and Hirshkowitz, A. (2009). Tumor-Derived Microvesicles Promote Regulatory T Cell Expansion and Induce Apoptosis in Tumor-Reactive Activated CD8+T Lymphocytes. *J Immunol.* 183, 3720–3730.
- Wu, J., Liu, T., Rios, Z., Mei, Q., Lin, X., and Cao, S. (2017). Heat Shock Proteins and Cancer. *Trends*

in *Pharmacological Sciences* 38, 226–256.

Yang, J., Zhang, L., Yu, C., Yang, X.F., and Wang, H. (2014). Monocyte and macrophage differentiation: Circulation inflammatory monocyte as biomarker for inflammatory diseases. *Biomarker Research* 2, 1–9.

Yano, M., Naito, Z., Yokoyama, M., Shiraki, Y., Ishiwata, T., Inokuchi, M., and Asano, G. (1999). Expression of hsp90 and cyclin D1 in human breast cancer. *Cancer Letters* 137, 45–51.

Yasumasa Ishida, Yasutoshi Agata, Keiichi Shibahara, T.H. (1992). Induced expression of PD-1, a novel member of the immunoglobulin gene superfamily, upon programmed cell death. *The EMBO Journal* 11, 3887–3895.

Yee, D., Shah, K.M., Coles, M.C., Sharp, T. V., and Lagos, D. (2017). MicroRNA-155 induction via TNF- α and IFN- γ suppresses expression of programmed death ligand-1 (PD-L1) in human primary cells. *Journal of Biological Chemistry* 292, 20683–20693.

Youn Je-In, Nagaraj Srinivas, Collazo Michelle, G.D.I. (2009). Subsets of Myeloid- derived Suppressor Cells in Tumor Bearing Mice. *Journal of Immunology* 181, 5791–5802.

Zaborowski, M.P., Balaj, L., Breakefield, X.O., and Lai, C.P. (2015). Extracellular Vesicles: Composition, Biological Relevance, and Methods of Study. *BioScience* 65, 783–797.

Zhang, G., Liu, Z., Ding, H., Zhou, Y., Doan, H.A., Sin, K.W.T., Zhu, Z.J., Flores, R., Wen, Y., Gong, X., et al. (2017). Tumor induces muscle wasting in mice through releasing extracellular Hsp70 and Hsp90. *Nature Communications* 8.

Ziegler-Heitbrock, L. (2015). Blood monocytes and their subsets: Established features and open questions. *Frontiers in Immunology* 6, 1–5.

9 CURRICULUM VITAE

Personal details:

Name: Xiaoying Hu
 Date of Birth: 26th January 1990
 Gender: Female
 Nationality: China
 Marital Status: Single
 Father: Yanzheng Hu
 Mother: Ruiling Zhou
 Sister: Xiaocong Hu

Education:

2015 - present PhD student in Clinical Cooperation Unit Dermato-Oncology,
 German Cancer Research Center (DKFZ) and University
 Medical Center Mannheim of Heidelberg University, Germany
 2013 - 2015 Master in Plastic and Reconstructive Surgery,
 University of Zhengzhou, China
 2008 - 2013 Bachelor's in clinical medicine, University of Zhengzhou, China
 2005 – 2008 Pingdingshan No.1 High School , Henan, China

Professional Experience :

2013 - 2015 Residency at the Plastic and Reconstructive Surgery
 Department of University Hospital Zhengzhou
 Clinical Internship in Internal Medicine, Surgery, Gynecology,
 2012 - 2013 Pediatrics , Neurology , Dermatology and Emergency
 department at University Hospital Zhengzhou

10 ACKNOWLEDGEMENTS

There are so many people without whom this thesis might not have been written and to whom I am greatly indebted.

I would like to express the deepest appreciation to **Prof. Dr. Viktor Umansky** who gave me the opportunity to work on this project in his lab and for his expertise, guidance, patience and persistent help. He taught me a great deal about both scientific research and life in general.

I want to thank **Prof. Dr. Hans-Peter Altevogt** for insightful discussion, and his immense knowledge. His teaching style and enthusiasm for the topic left a strong impression on me and I have always carried positive memories of his classes.

I want to thank **Prof. Dr. Jochen Utikal** for his clinical input and constructive comments during my work as well as the precious suggestion for my career in future.

I want to thank **Prof. Dr. Adelheid Cerwenka** and **Prof. Dr. Jonathan P. Sleeman** for being a part of my thesis advisory committee. Their insightful comments and encouragement, but also the hard questions pushed me to widen my research from various perspectives.

A big thank you also to all the former and actual lab members for their feedback, cooperation and all the fun we have had together in the last few years: **Carolin Blattner, Mareike Grees, Loreen Kloss, Sonja Simon, Daniel Thomas, Christos Evangelou, Rebakka Webber, Christopher Groth, Céline Weller, Zeno Riester, Vera Petrova**. They are such great colleagues and friends that were always so helpful to me. My heartfelt appreciation goes to **Viktor Fleming**. I would never explore the depths of this project without his help and dedicated involvement in every step.

I would like to thank **Sophie Kopetschke** for her great help with my project and being my Bachelor student. It was such a special and great experience.

I would also like to show gratitude to my friends out there in Mannheim, Heidelberg, Germany, China and around the world. I owe a very important debt to **Jiedong Qiu**, who was always there, listening to my problems when experiments drove me crazy, putting me on solid ground times and times again when I was down.

Moreover, I would also like to acknowledge the fund of **Chinese Government Scholarship**. This work would not have been possible without the financial support from my country.

Most importantly, none of this could have happened without **my family**. To my parents and sister who support me in overcoming numerous obstacles throughout my life. 感谢我的**爸爸, 妈妈和姐姐**！是你们，永远支持着我的选择，给我自由闯荡的勇气和空间，让我变成了更好的自己。